The Abdus Salam
International Centre
for Theoretical Physics

United Nations
Educational, Scientific and
Cultural Organization

IAEA
International Atomic Energy Agency

Radio Occultation for Ionospheric Studies

Bruno Nava
ICTP, Trieste, Italy

International Colloquium on Equatorial and Low Latitude Ionosphere
Abuja, 18-23 September 2022

Outline

- The importance of RO data
  - The Onion Peeling algorithm
    - TEC calibration
- Simulation results
- Test cases

The importance of the RO data

RO derived Ne

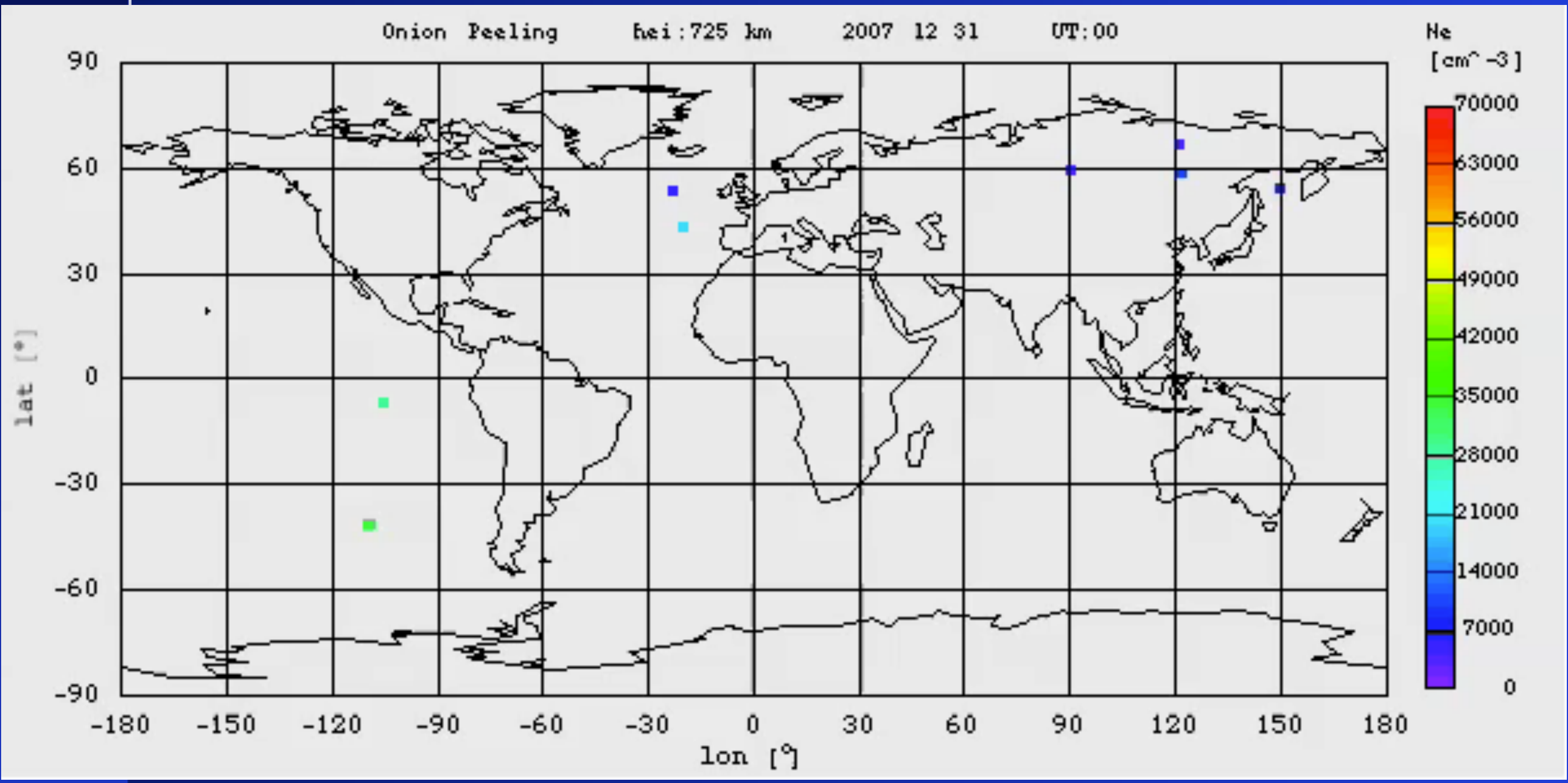

One hour RO data per frame

RO derived Ne

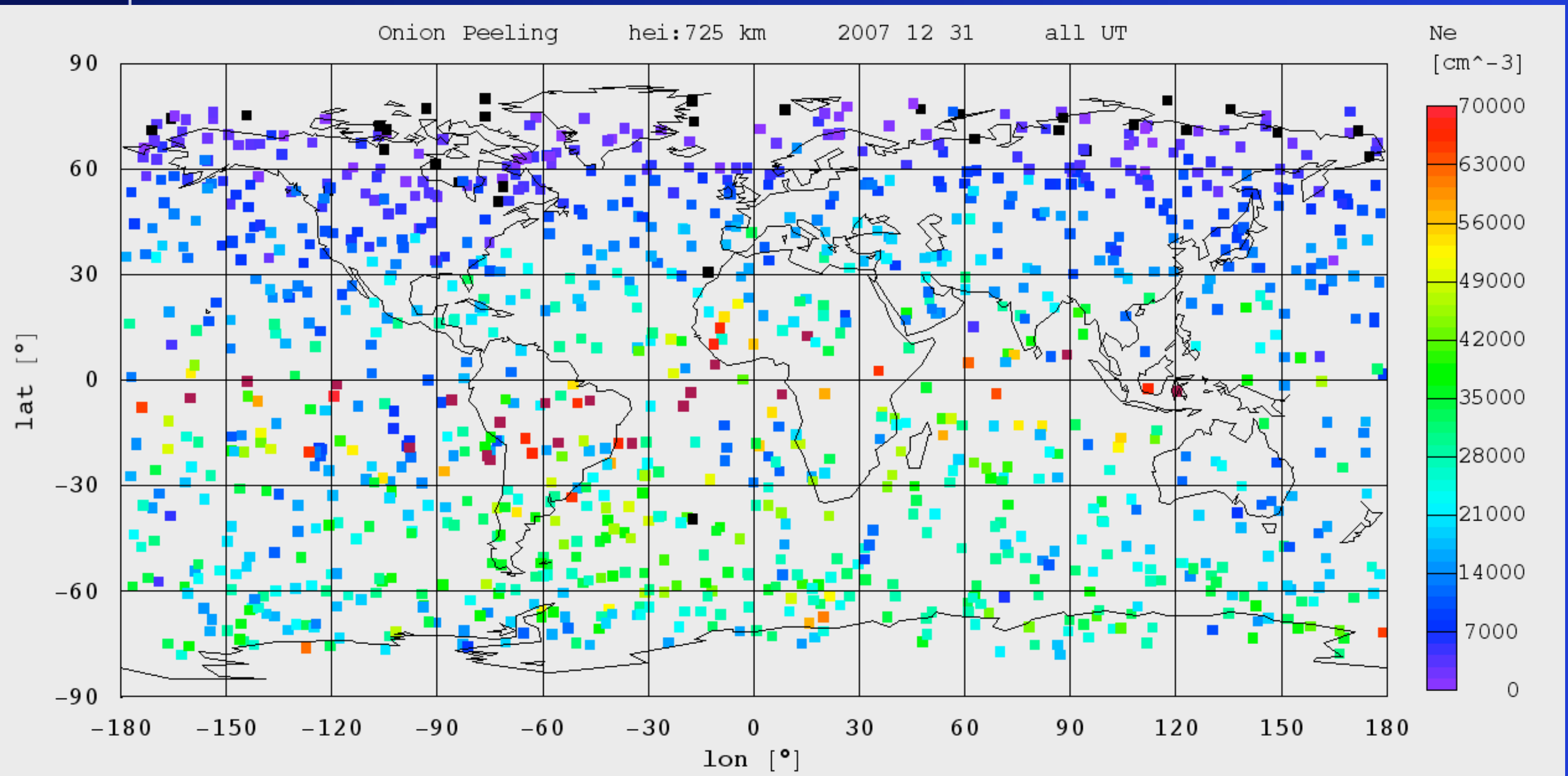

One day RO data (Onion Peeling)

RO derived Ne

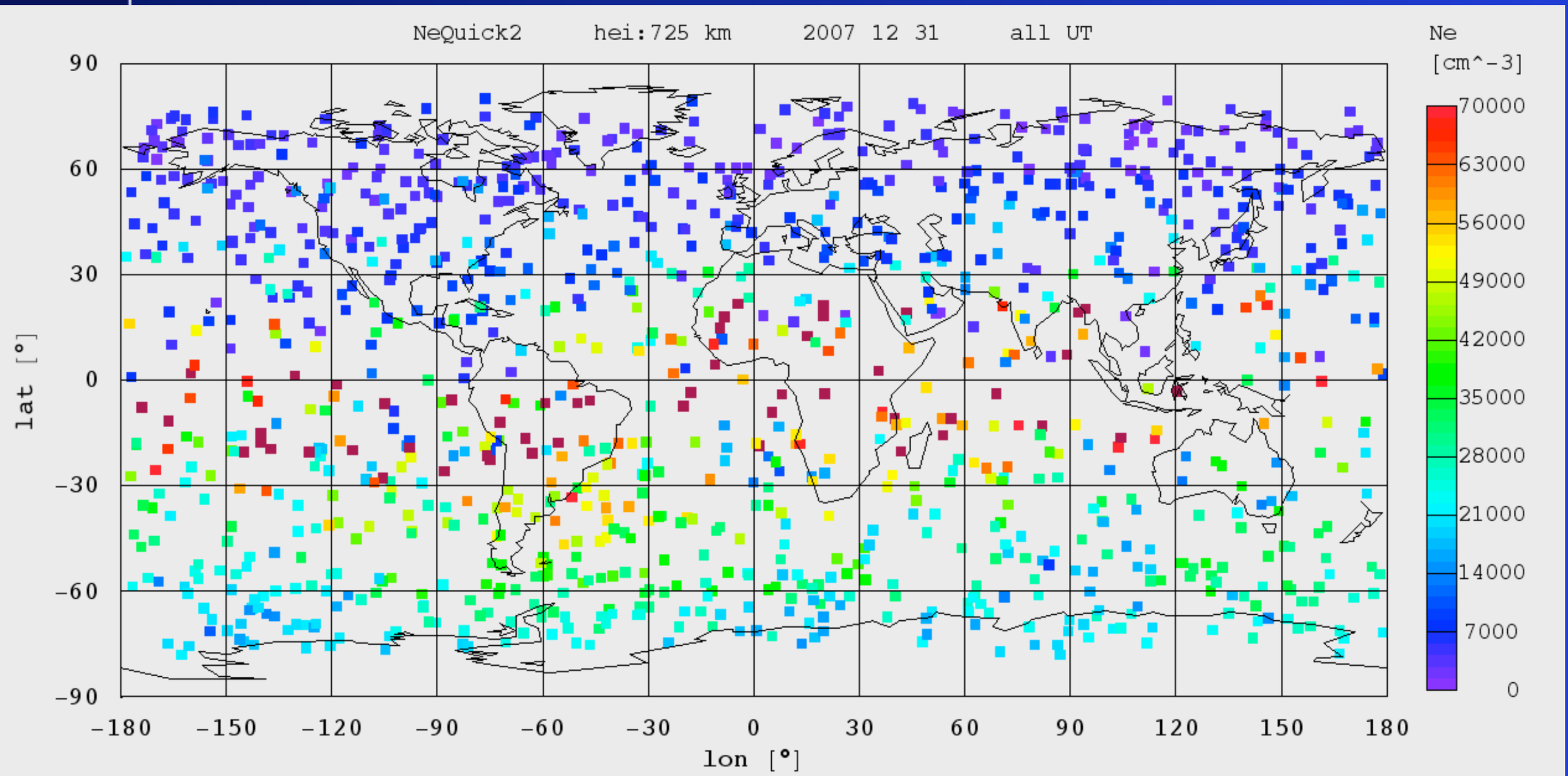

One day RO data (NeQuick)

RO derived Ne difference

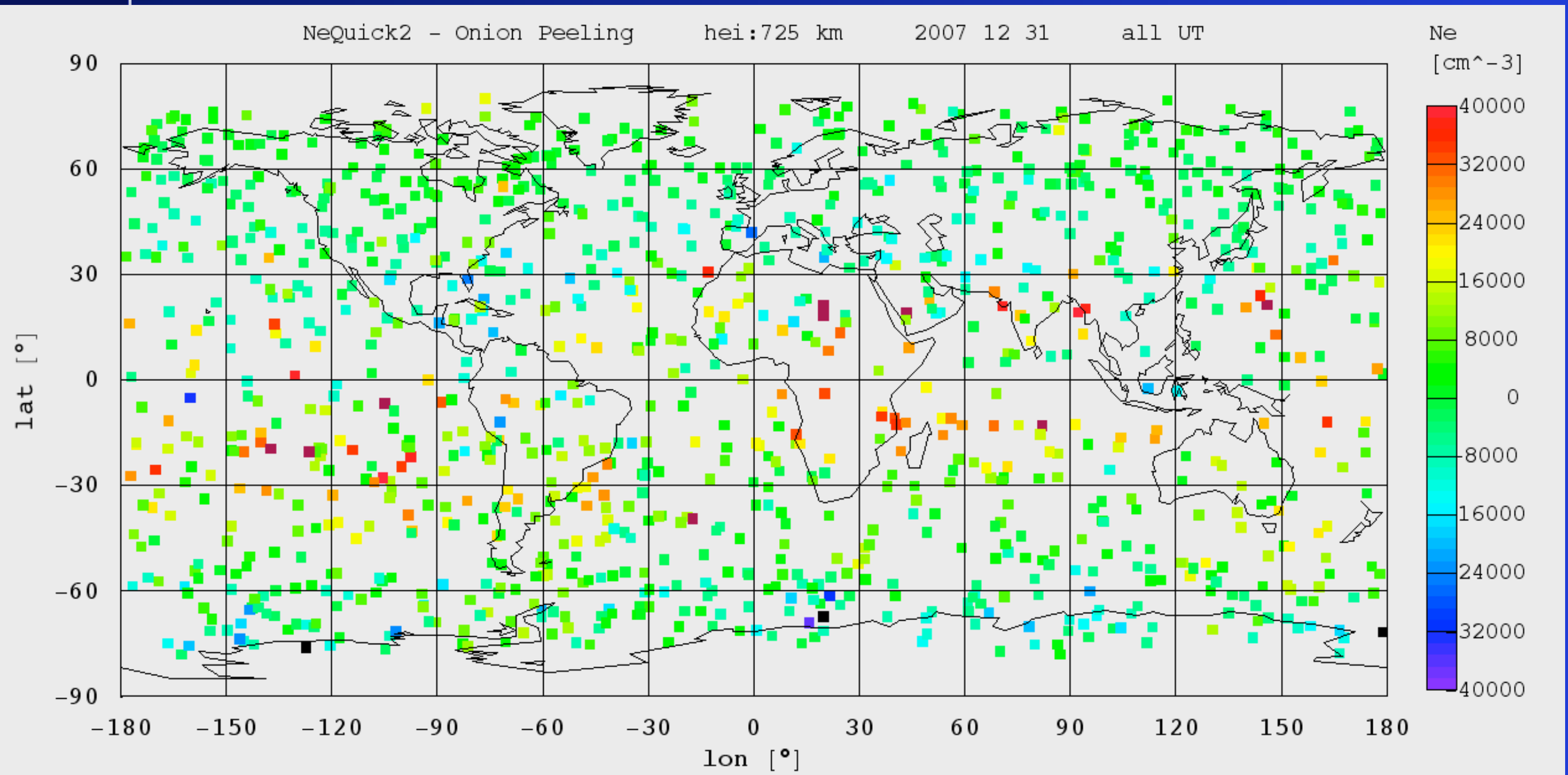

One day RO data (NeQuick - Onion Peeling)

Global constant LT NmF2 maps

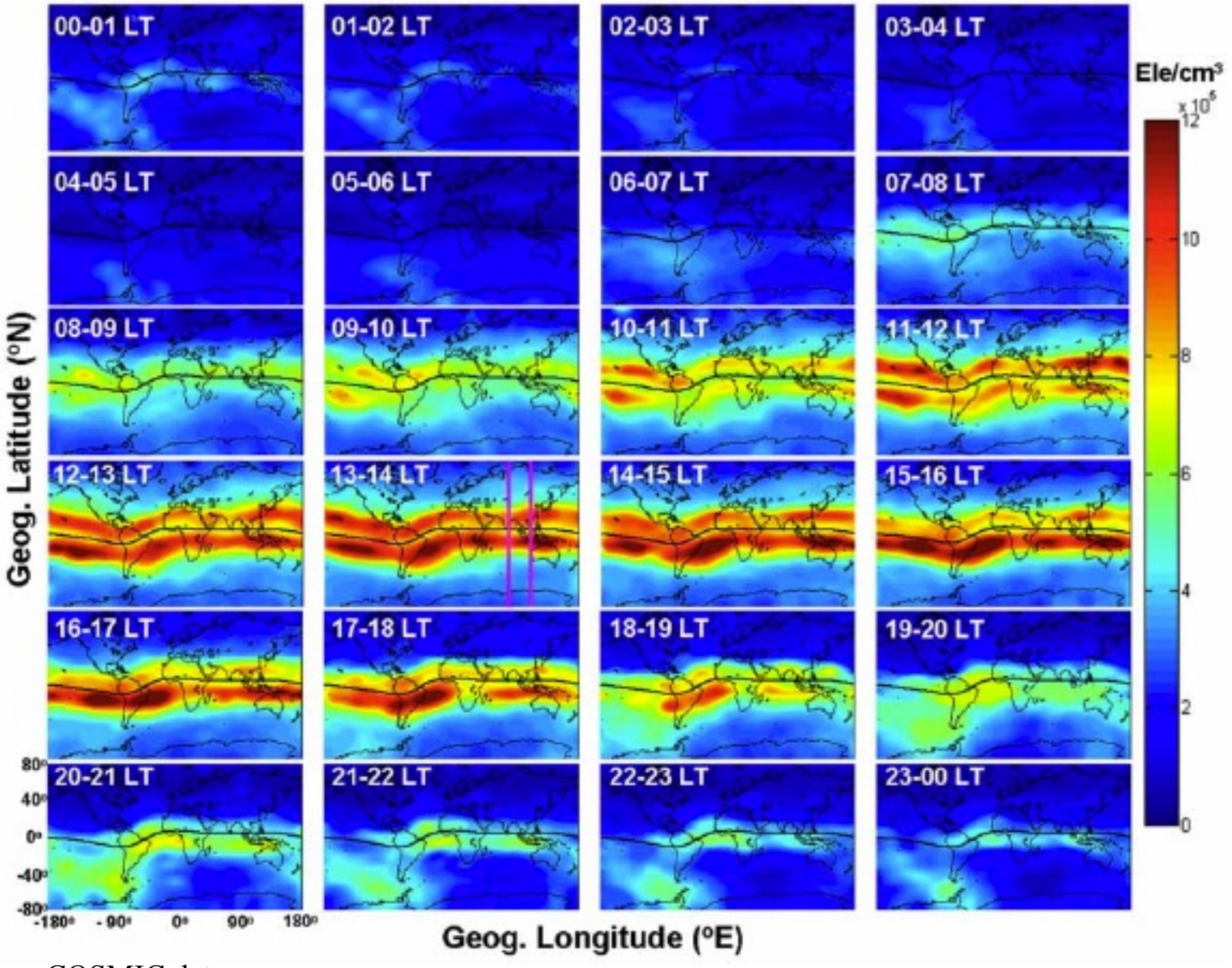

COSMIC data

from: Tulasi Ram, et al.; J. Geophys. Res., 2009

Global hmF2 maps

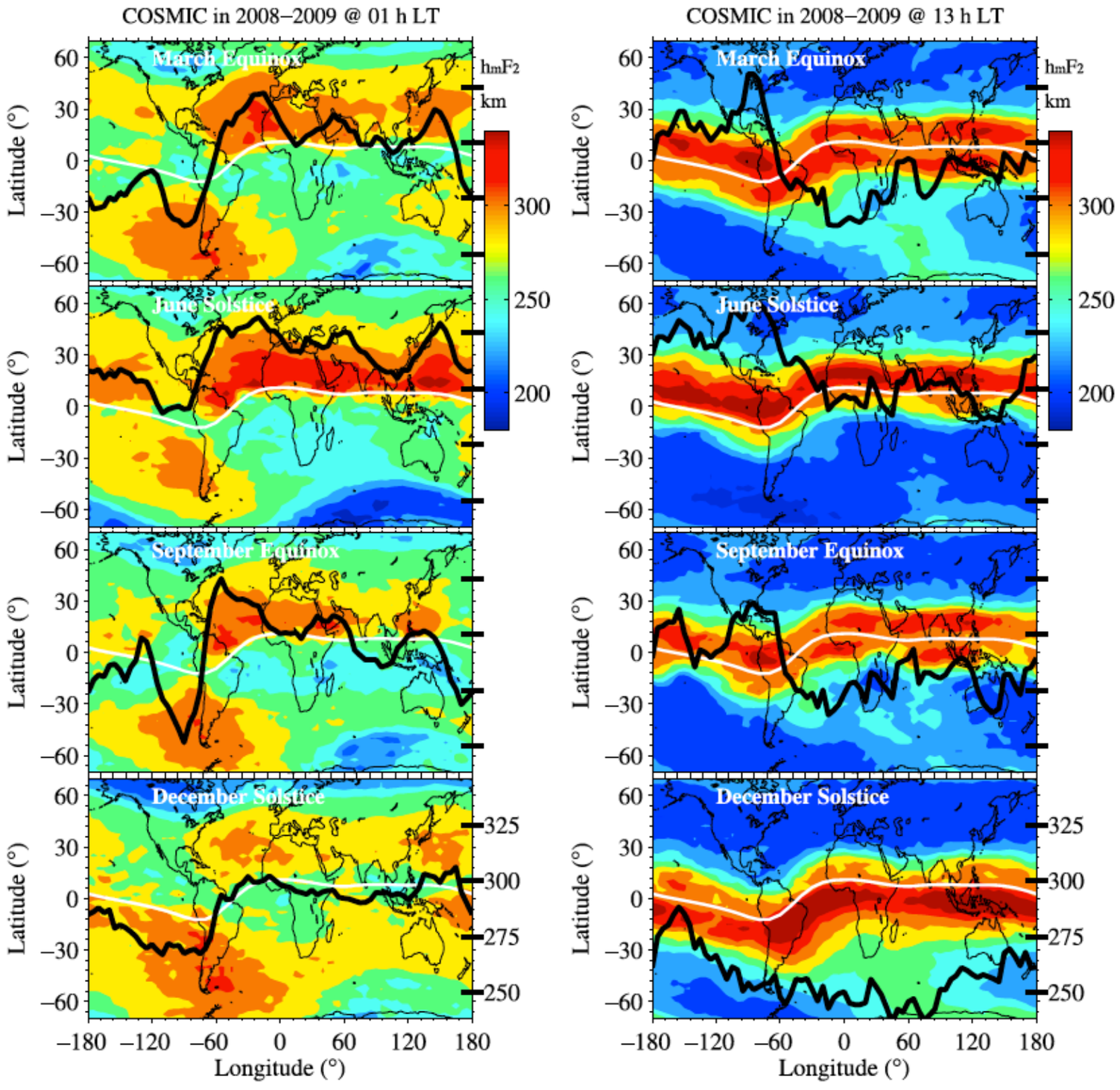

from: Liu et al.; JGR, 2011

Midlatitude trough

The ionospheric midlatitude trough observed by FORMOSAT-3/ COSMIC during solar minimum

I. T. Lee,[1,2] W. Wang,[2] J. Y. Liu,[1,2] C. Y. Chen,[1] and C. H. Lin[3]

JOURNAL OF GEOPHYSICAL RESEARCH, VOL. 116, A06311, doi:10.1029/2010JA015544, 2011

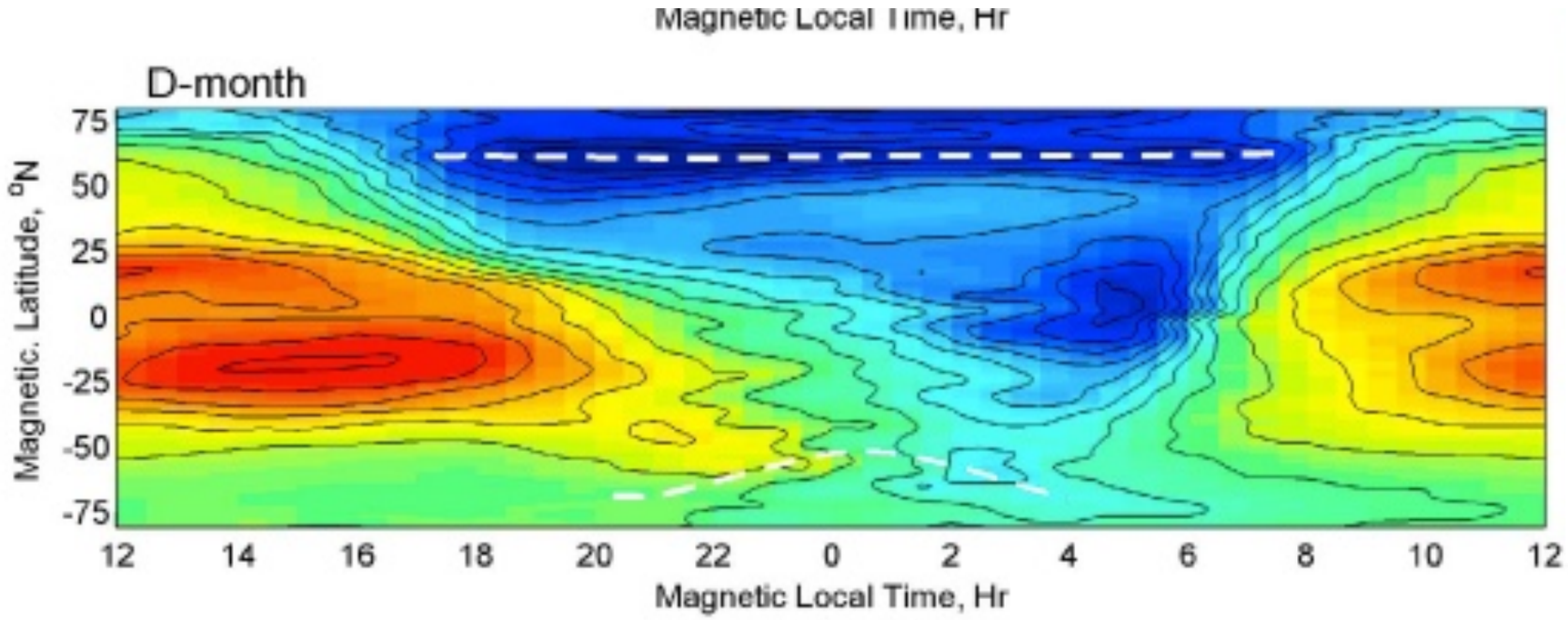

The NmF2 on MLAT versus MLT

Peak parameter reconstruction

Limberger et al., "Long-term comparison of the ionospheric F2 layer electron density peak derived from ionosonde data and Formosat-3/COSMIC occultations", J. Space Weather Space Clim., 5, A21 (2015). DOI: 10.1051/swsc/2015023

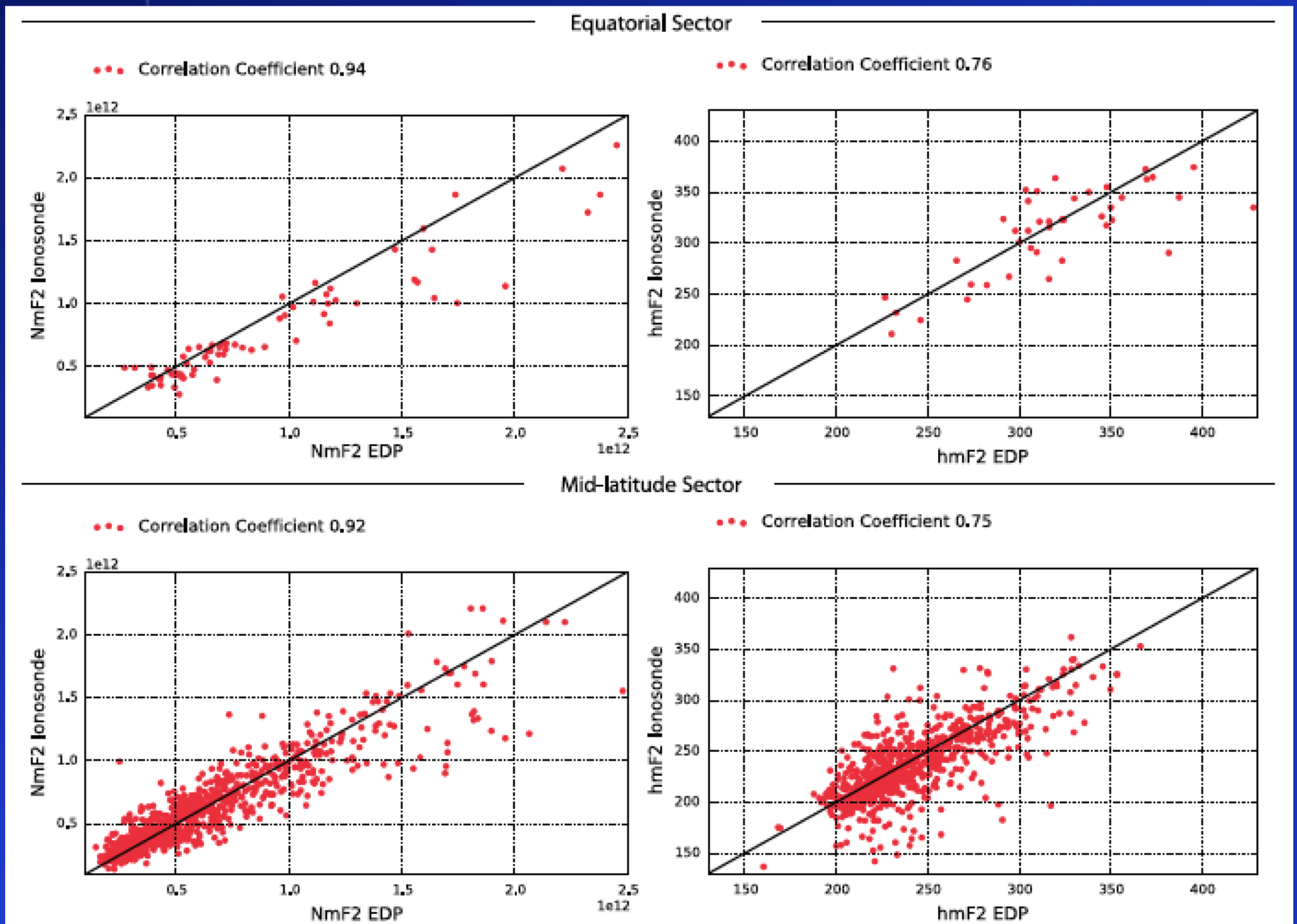

Data correspond to years 2006 - 2014

Separability hypothesis (Hernández-Pajares et al., 2000) has been used to invert RO data

Peak parameters reconstruction

American sector

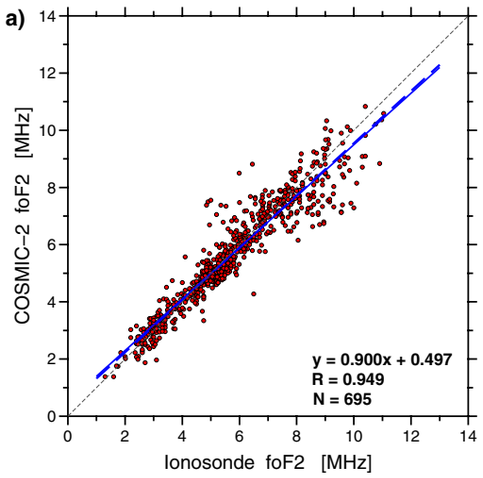

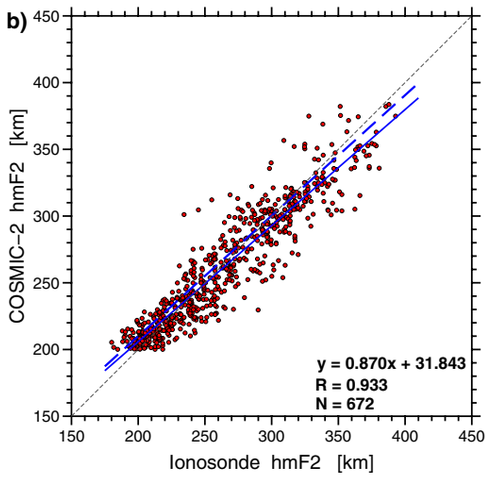

Europe–African sector

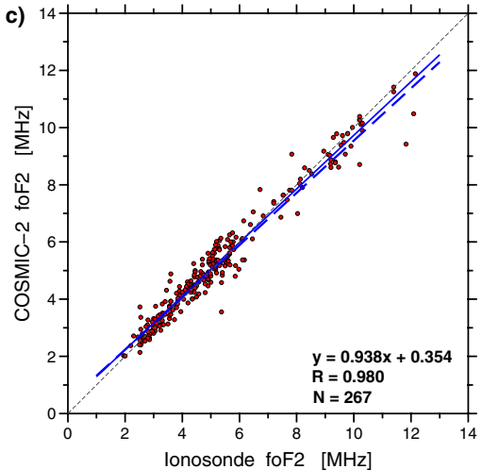

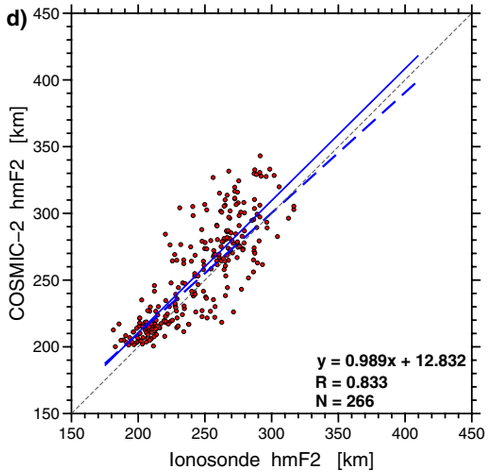

Asia–Pacific sector

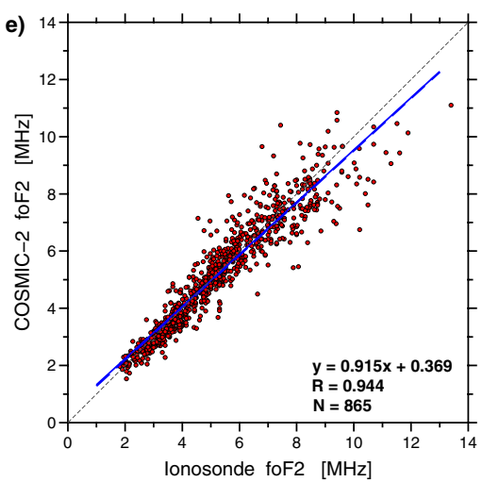

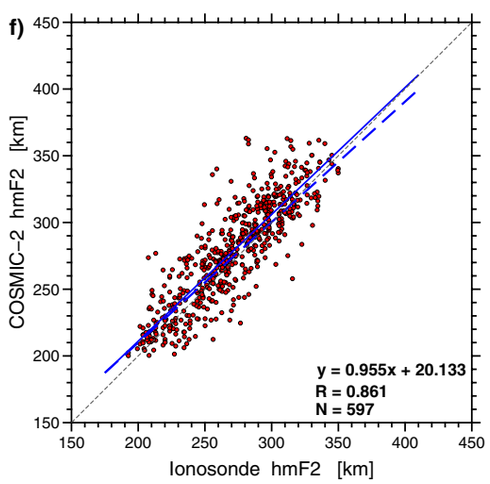

Scatter plots of the COSMIC-2 RO-based foF2 and hmF2 values against the corresponding ionosonde-derived ones with a separation to American, Europe-African, and Asia-Pacific longitudinal sectors. The solid blue lines show the best fit line, while the dashed blue lines show the best fit lines without zone separation.

from: Accuracy assessment of the quiet-time ionospheric F2 peak parameters as derived from COSMIC-2 multi-GNSS radio occultation measurements Iurii Cherniak, Irina Zakharenkova, John Braun, Qian Wu, Nicholas Pedatella, William Schreiner, Jan-Peter Weiss, Douglas Hunt J. Space Weather Space Clim. 11 18 (2021) DOI: 10.1051/swsc/2020080

COSMIC-2 footprint

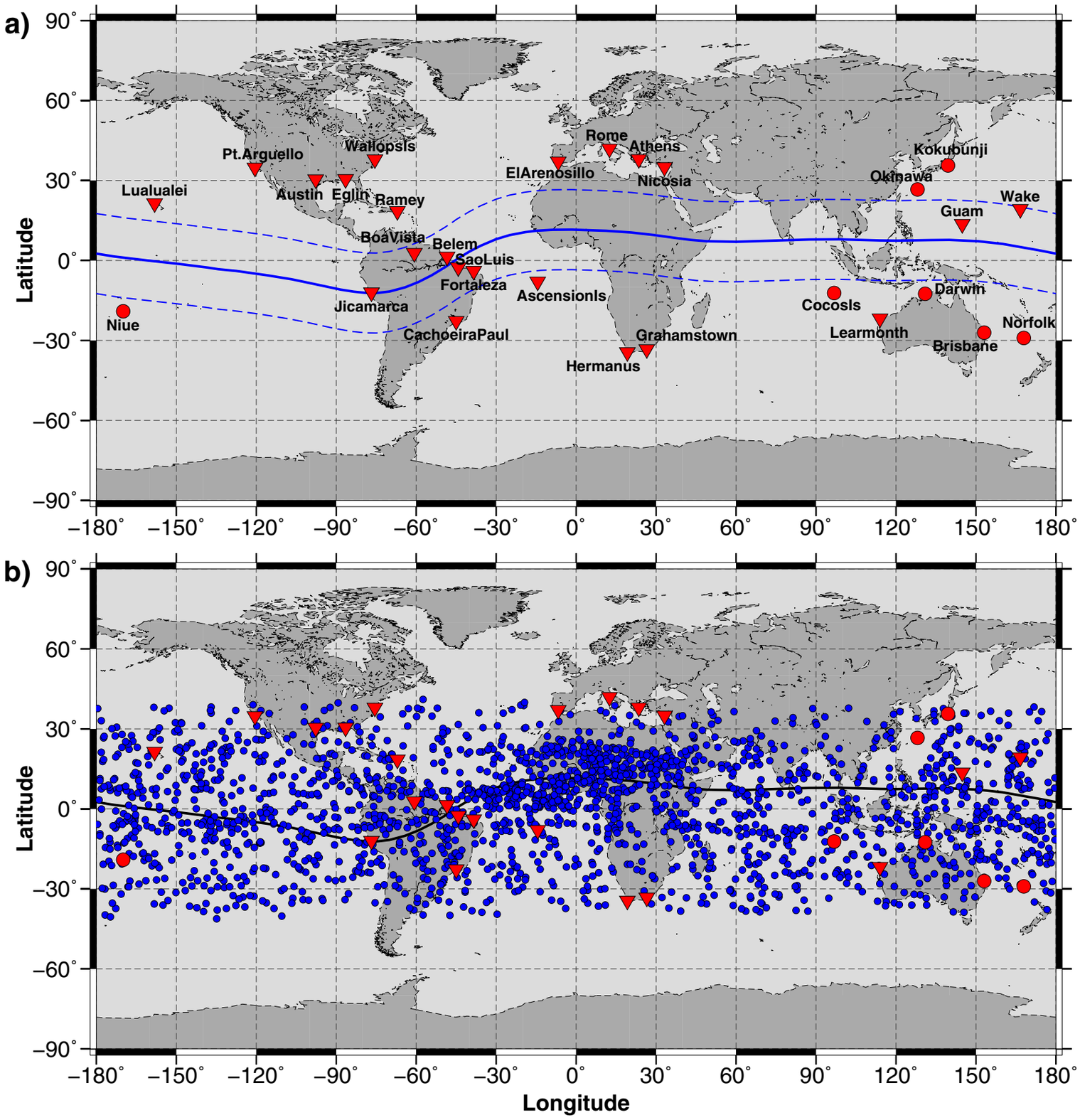

(a) Geographical map with Digisondes (red triangle) and ionosondes (red circles) locations used in this study; lines show the magnetic equator and ±15°MLAT.

(b) Example of global distribution of the F2 peak points as derived from COSMIC-2 RO observations during 24 hr (25 January 2020).

from: Cherniak et al., 2021

Sporadic E

Effect of sporadic E clouds on GPS radio occultation signals

Z. Zeng[1] and S. Sokolovskiy[1]

GEOPHYSICAL RESEARCH LETTERS, VOL. 37, L18817, doi:10.1029/2010GL044561, 2010

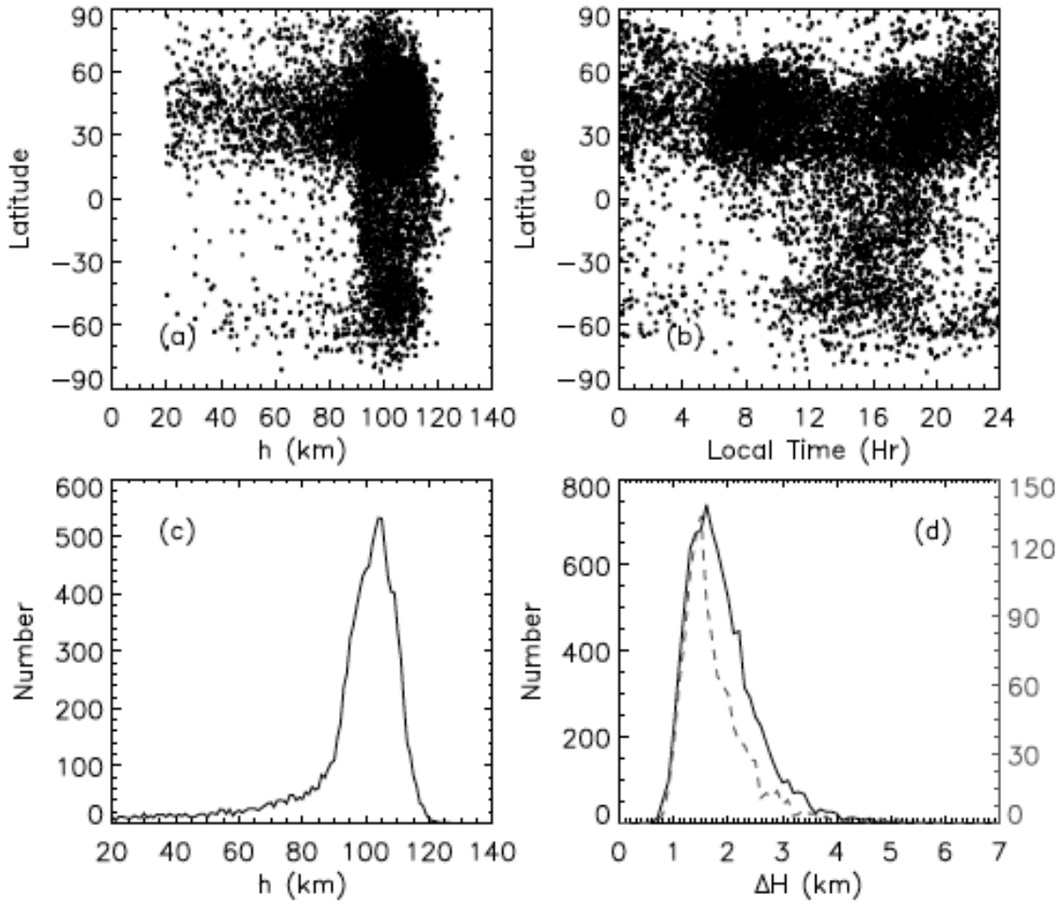

Distributions of the Es cloud events in COSMIC data from July 2009

Sporadic E

The occurrence rate of sporadic E as derived from COSMIC-2 radio occultation data at 90–120 km during June–August 2020 (upper left), September–November 2020 (upper right), December 2020–February 2021 (lower left), and March–May 2021 (lower right).

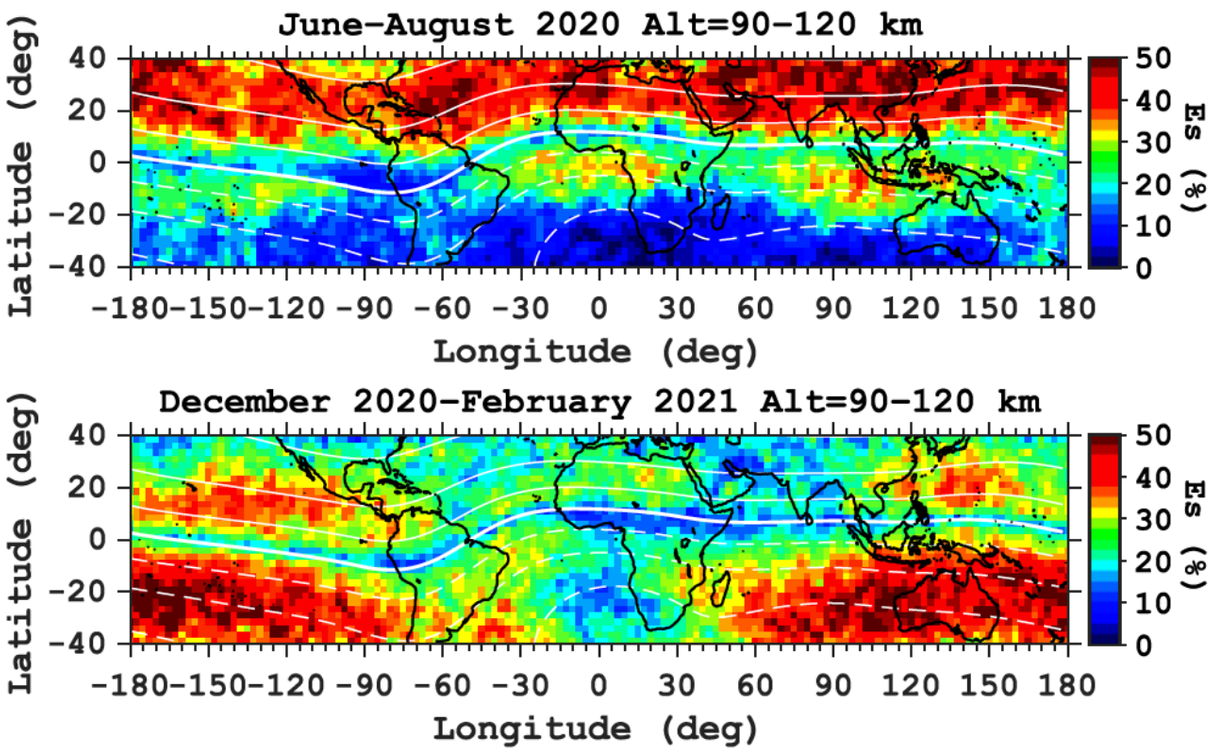

from: Yamazaki, Y., Arras, C., Andoh, S., Miyoshi, Y., Shinagawa, H., Harding, B. J., et al. (2022). Examining the wind shear theory of sporadic E with ICON/MIGHTI winds and COSMIC-2 Radio 2 occultation data. Geophysical Research Letters, 49, e2021GL096202. https://doi. org/10.1029/2021GL096202

Scintillations (COSMIC-2)

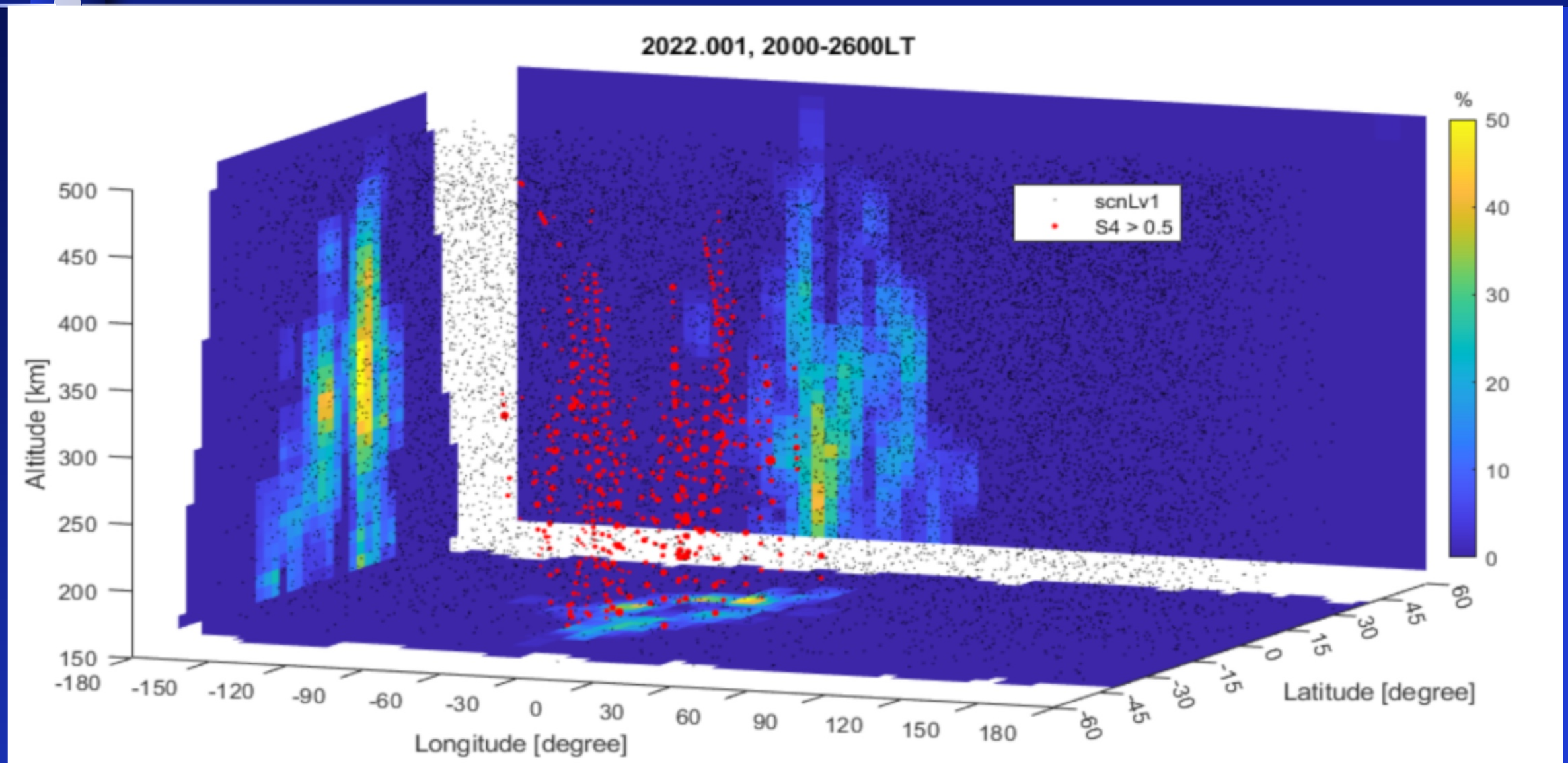

Distribution of nighttime intense scintillation (S4-index > 0.5). The color maps indicate the occurrence of intense S4 (red solid dots) in latitudinal (rear diagram), longitudinal (side diagram), and altitudinal intersections (bottom diagram) during 2000 LT to 0200 LT of 2022.001 to 2022.002 (from Liu et al., 2022).

Spire Constellation

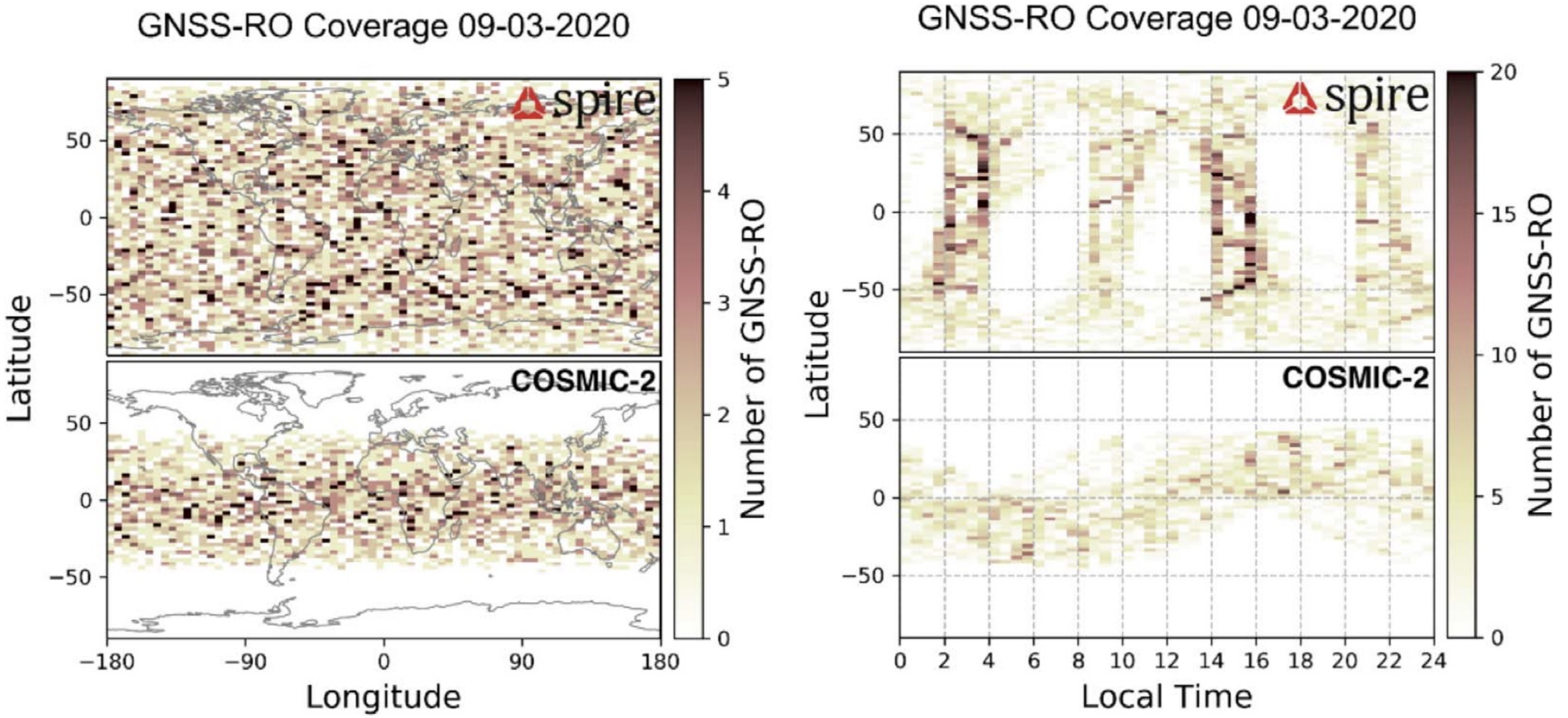

One day of RO coverage for the Spire constellation and COSMIC-2 for 9 March 2020. The left panel shows the geographic distribution over the day, while the right panel shows the distribution with local time. Gaps are apparent in the local time distribution due to the limited number of orbital planes (from Angling et al., 2021).

GNSS RO data inversion

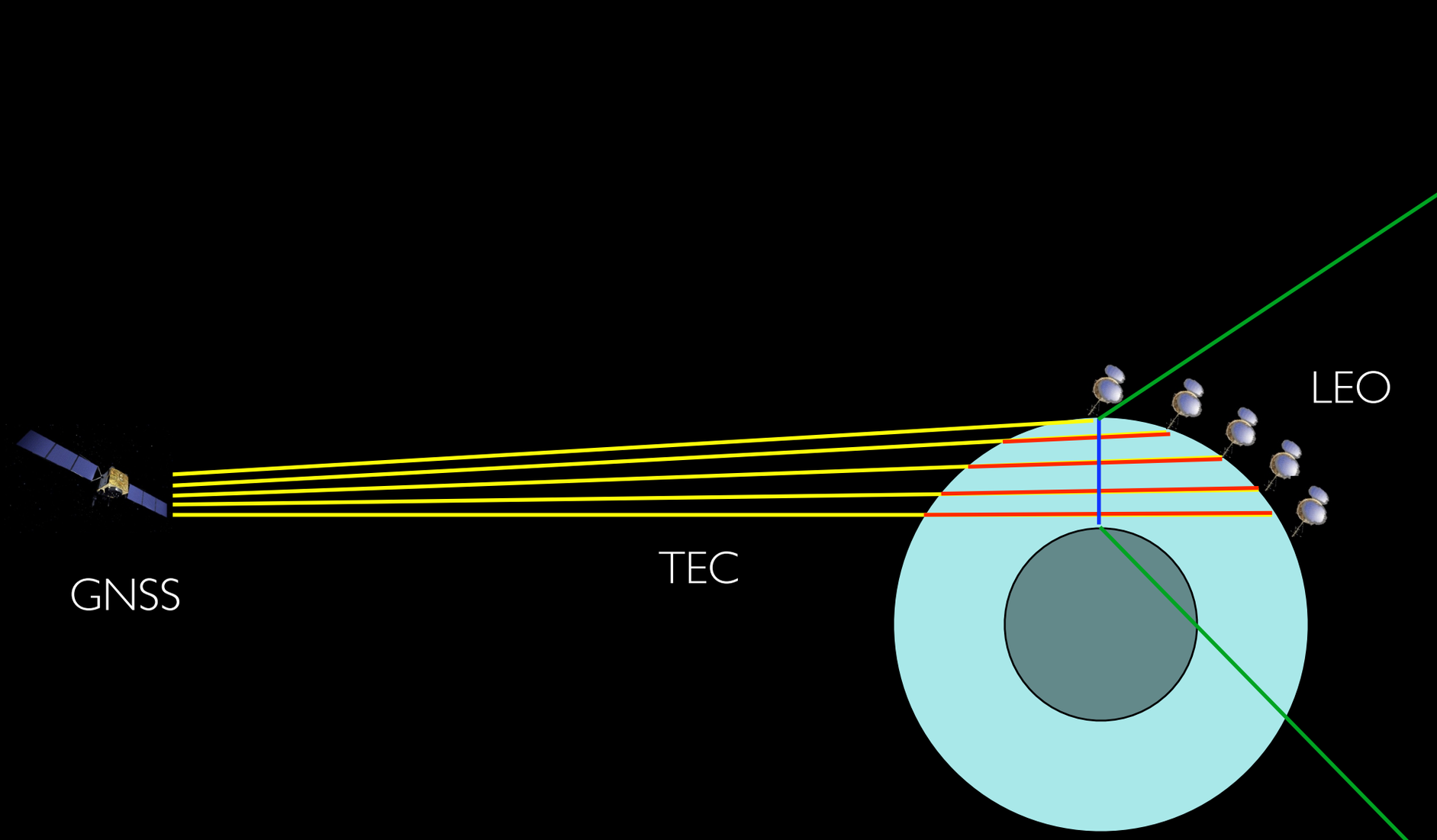

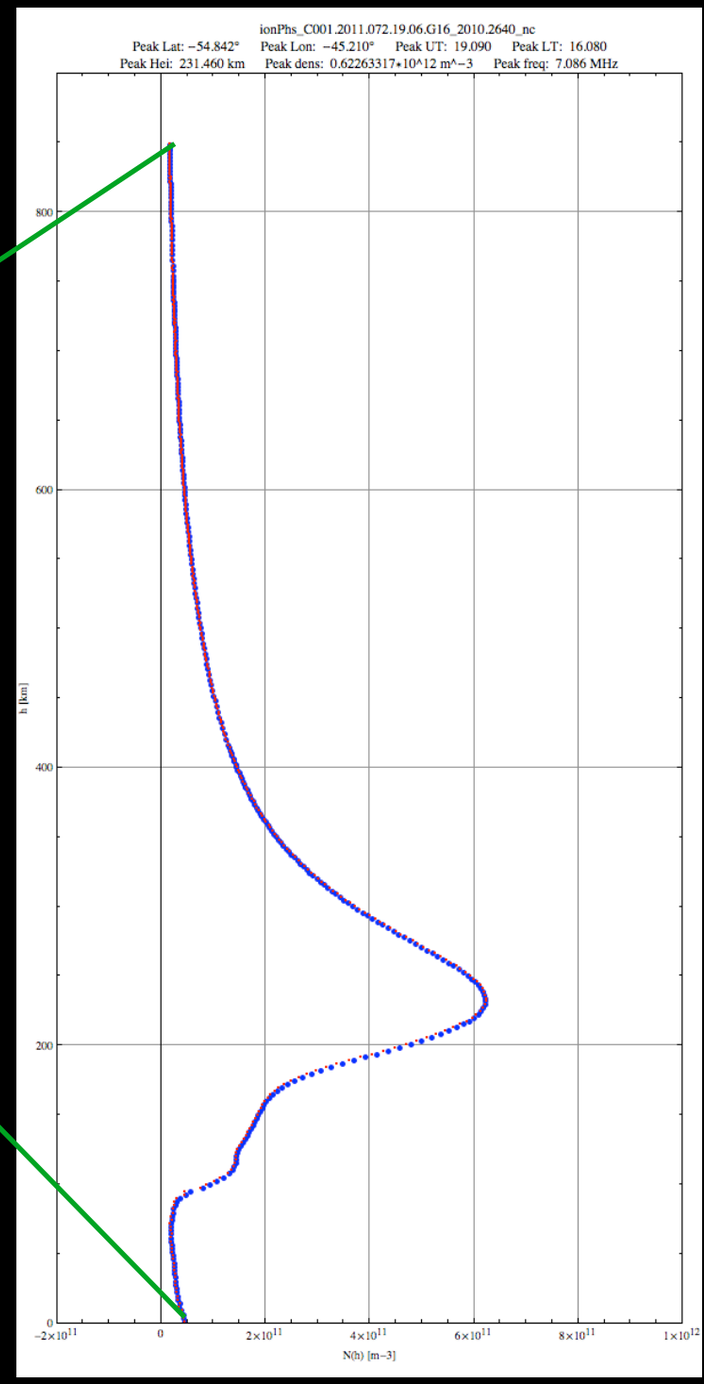

The Onion Peeling algorithm

- The “Onion Peeling” algorithm is a procedure that permits to compute a vertical electron density profile if the slant TEC from a LEO to a GPS satellite are available for an occultation event.

- Since the ray bending in the ionosphere is small enough, the straight-line propagation from GPS to LEO satellites is assumed for the GPS signals.

- As required by the inversion technique adopted, the spherical symmetry for the electron density of the ionosphere has been assumed.

- To compute the (calibrated) TEC in the shell determined by the LEO orbit, excess phase measurements at L1 and L2 GPS frequencies during one occultation event are used: uncalibrated_TEC[TECU] = 9.52*(delayL1[m] - delayL2[m]).

The Onion Peeling algorithm

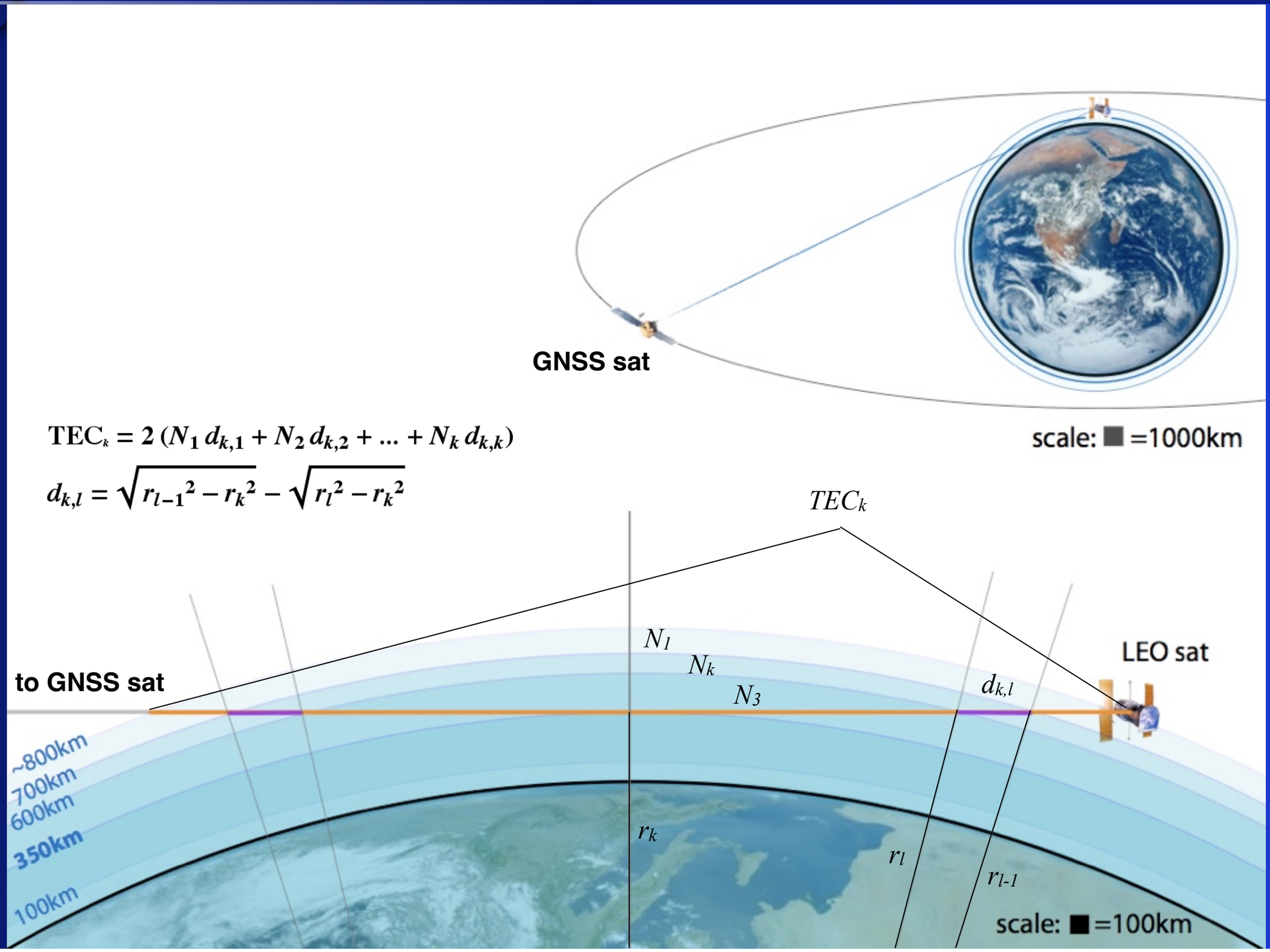

The Onion Peeling algorithm

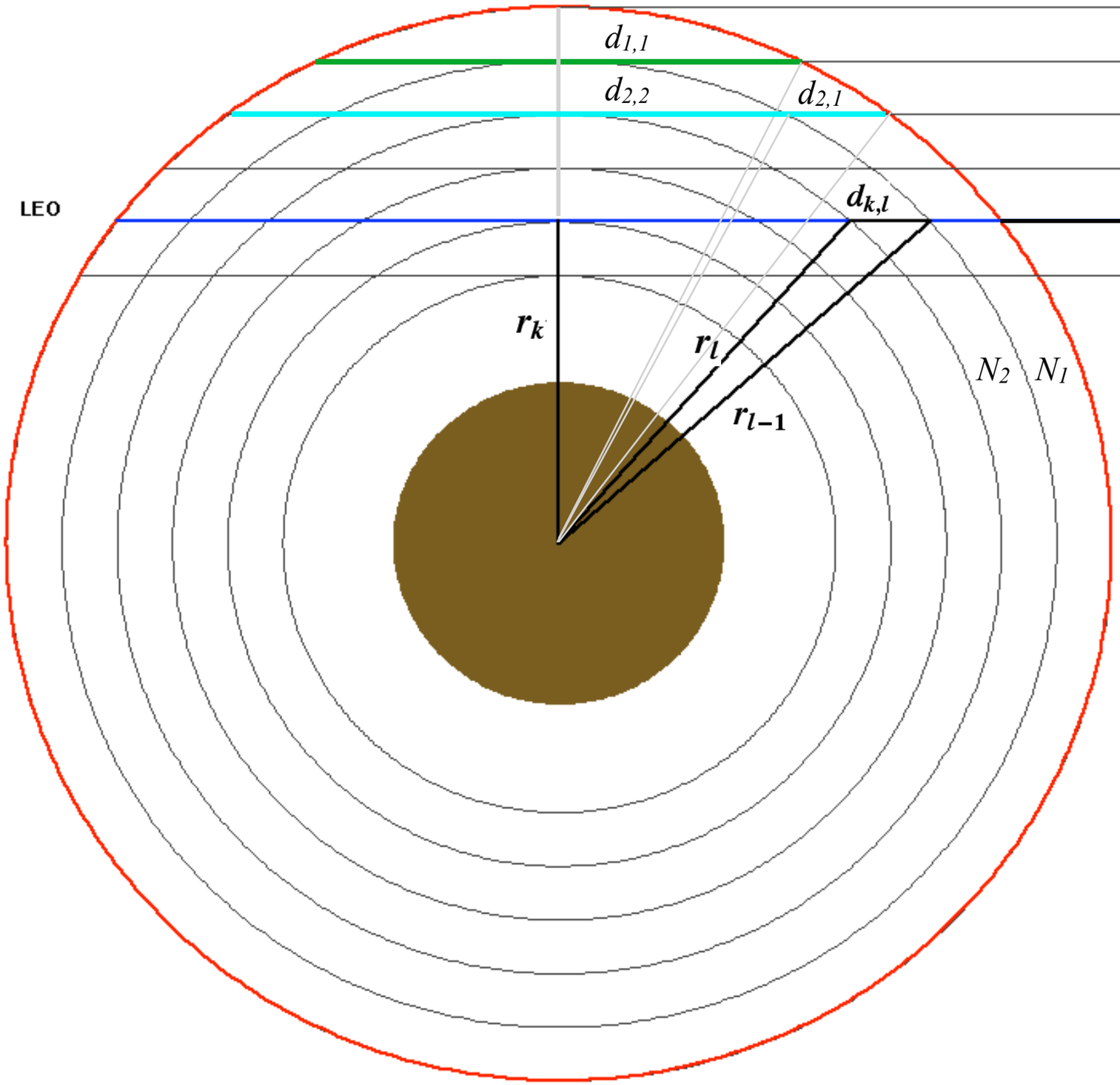

$TEC_1 = 2\, N_1\, d_{1,1}$

$TEC_2 = 2\, (N_1\, d_{2,1} + N_2\, d_{2,2})$

...

$TEC_k = 2\, (N_1\, d_{k,1} + N_2\, d_{k,2} + \ldots + N_k\, d_{k,k})$

$$d_{k,l} = \sqrt{r_{l-1}^2 - r_k^2} - \sqrt{r_l^2 - r_k^2}$$

TEC calibration

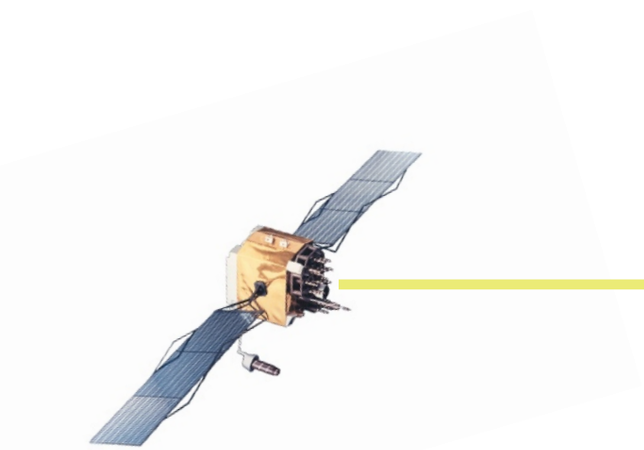

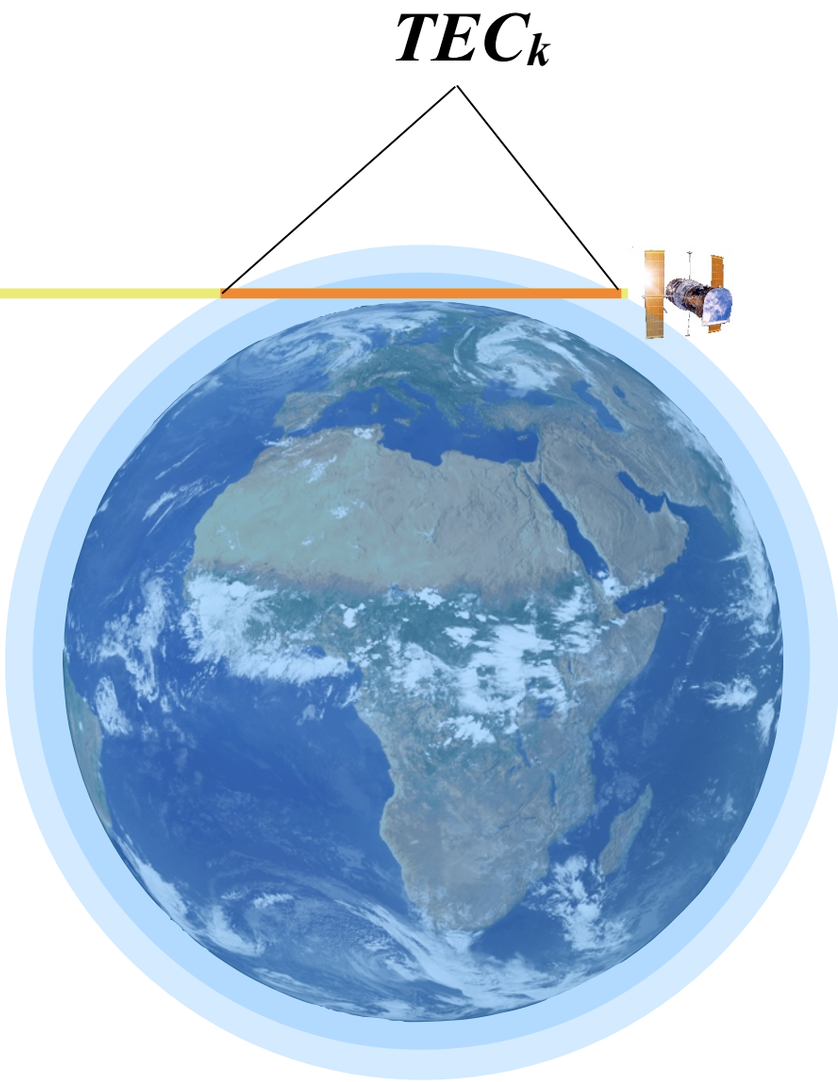

$$TEC_k =$$

TEC calibration

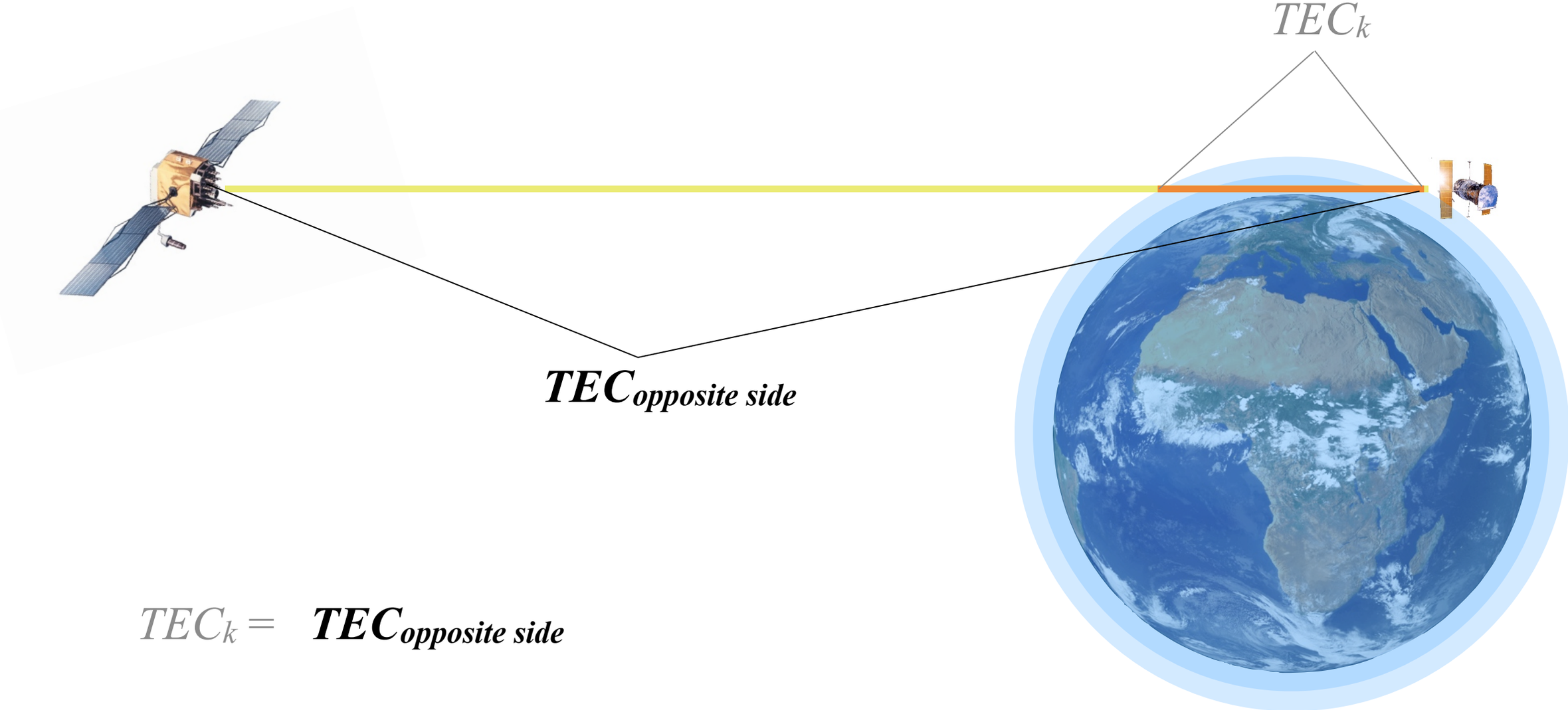

$$TEC_k = TEC_{opposite\ side}$$

TEC calibration

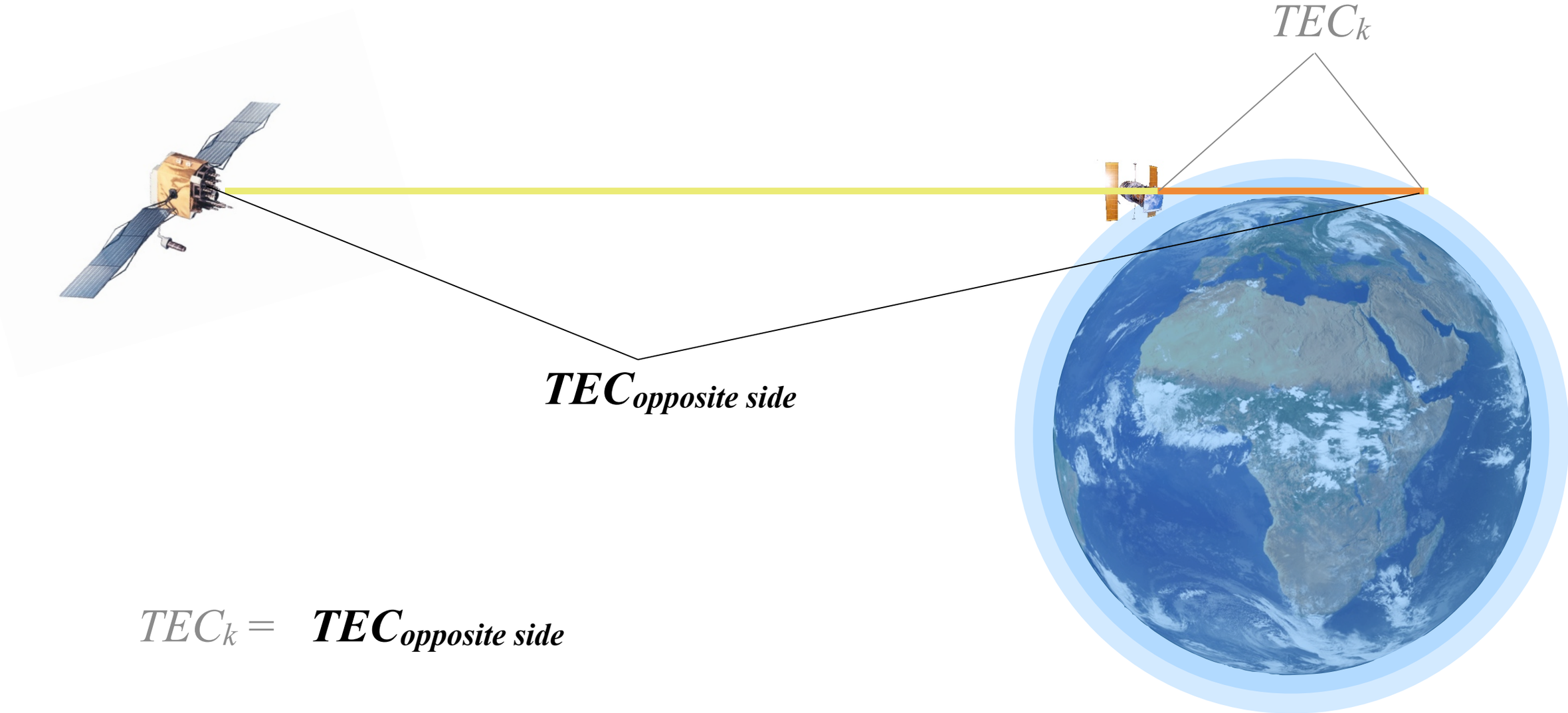

$$TEC_k = TEC_{opposite\ side}$$

TEC calibration

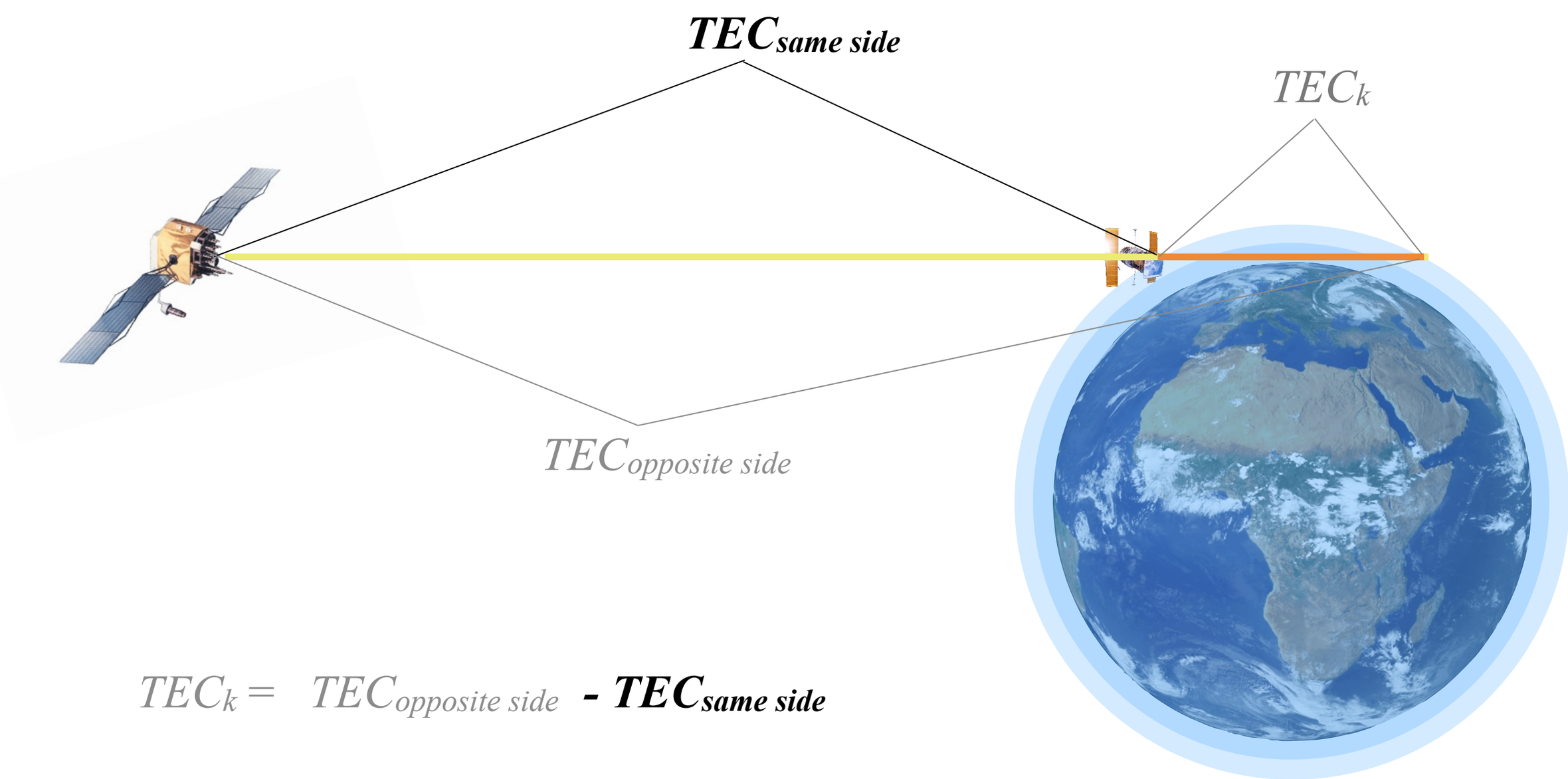

$$TEC_k = TEC_{opposite\ side} - \mathbf{TEC_{same\ side}}$$

TEC calibration

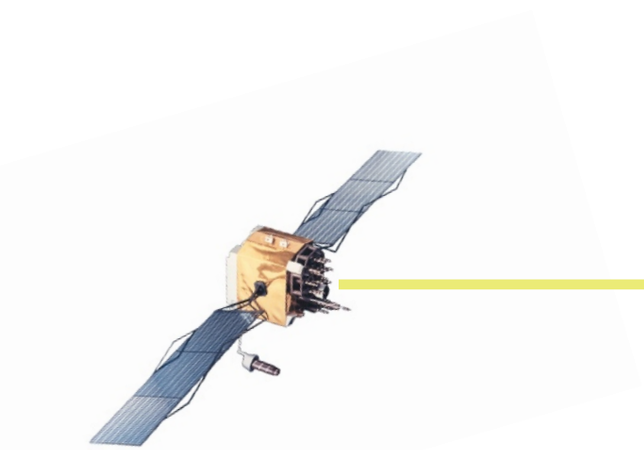

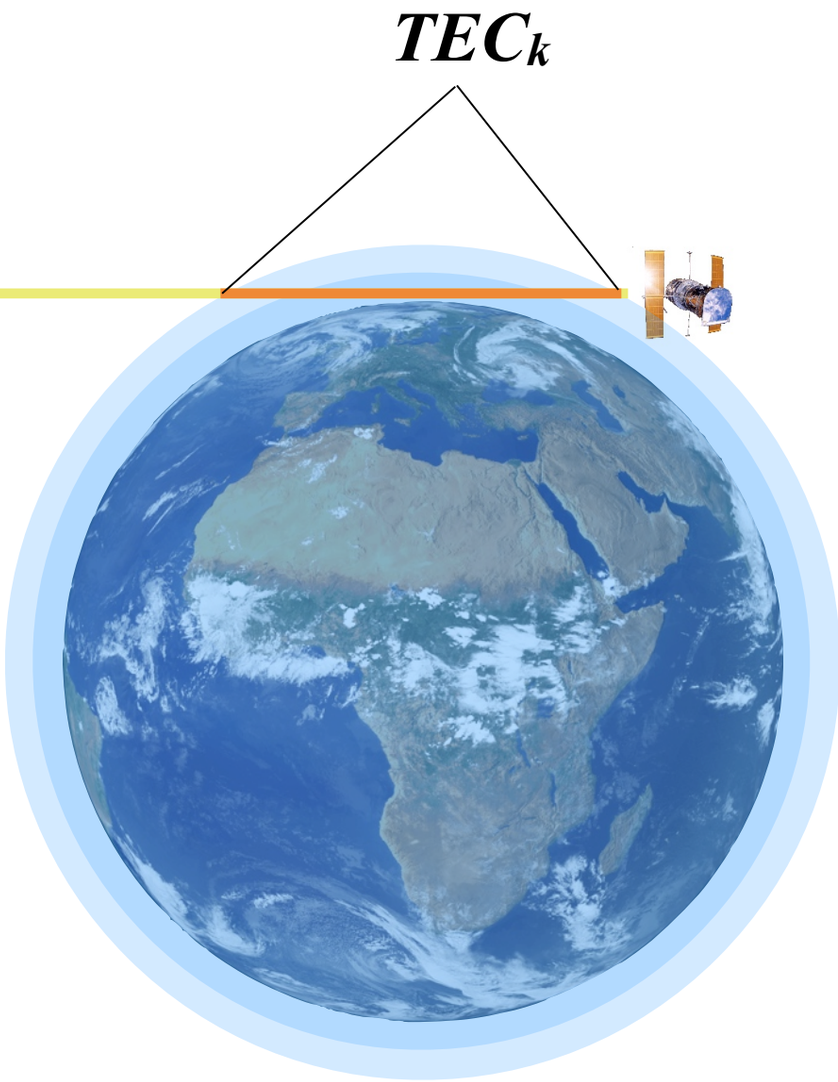

$$TEC_k =$$

TEC calibration

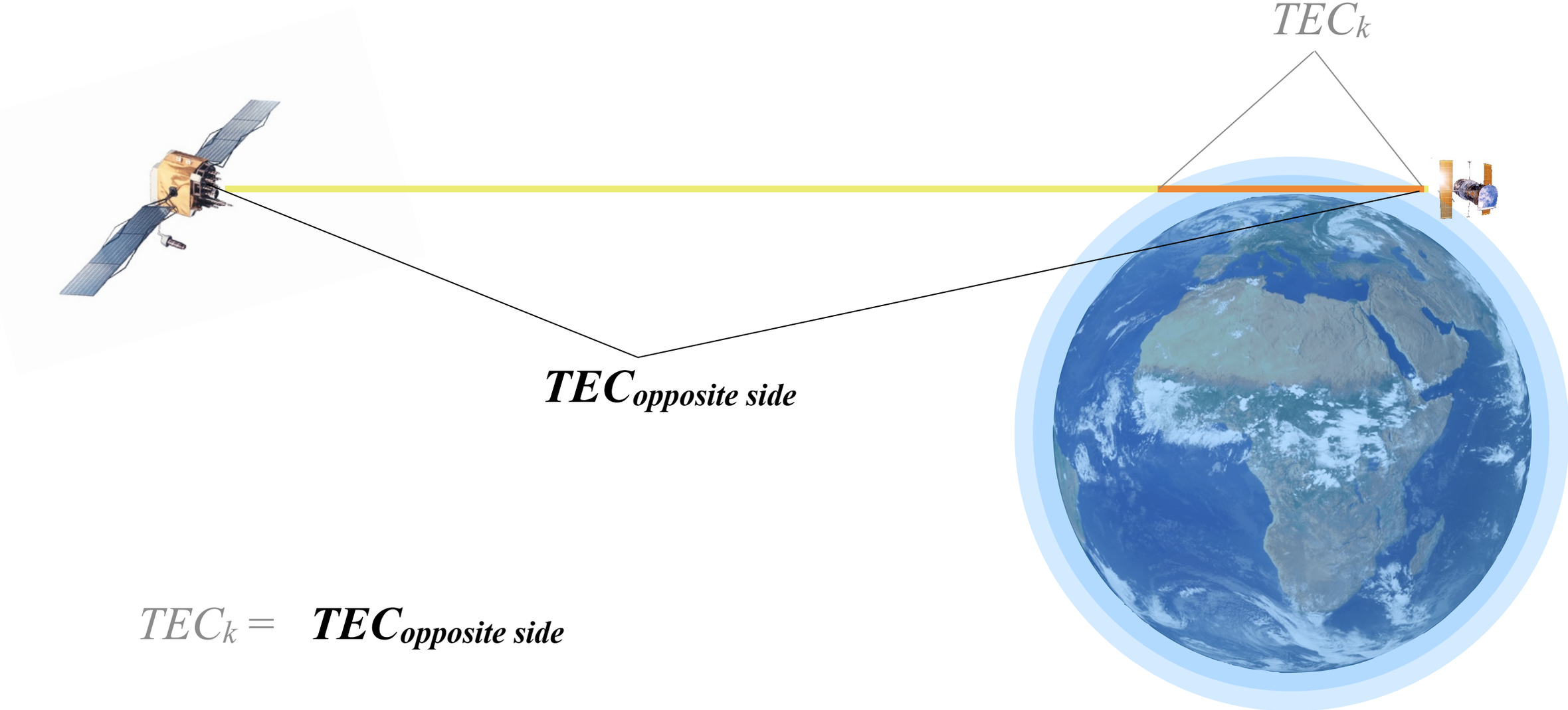

$$TEC_k = TEC_{opposite\ side}$$

TEC calibration

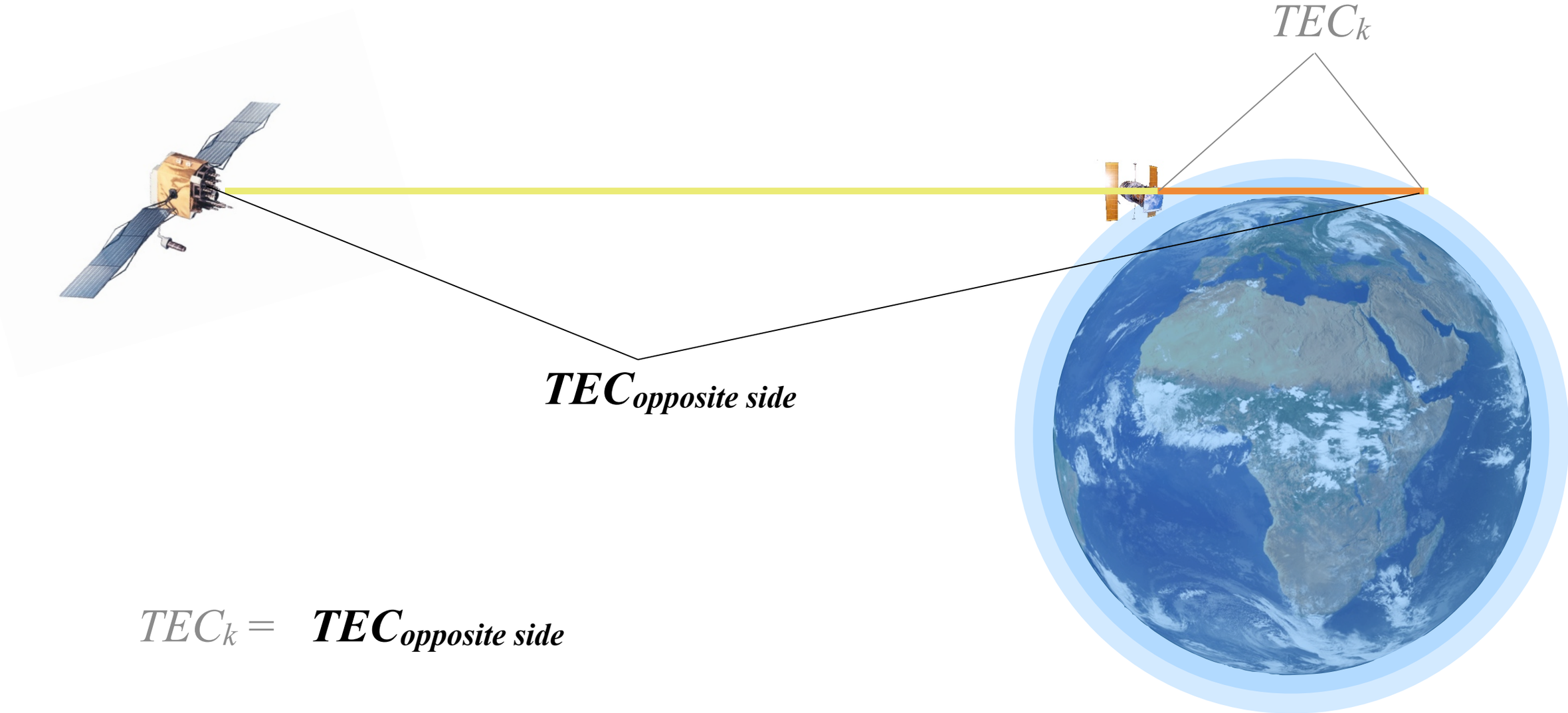

$$TEC_k = TEC_{opposite\ side}$$

TEC calibration

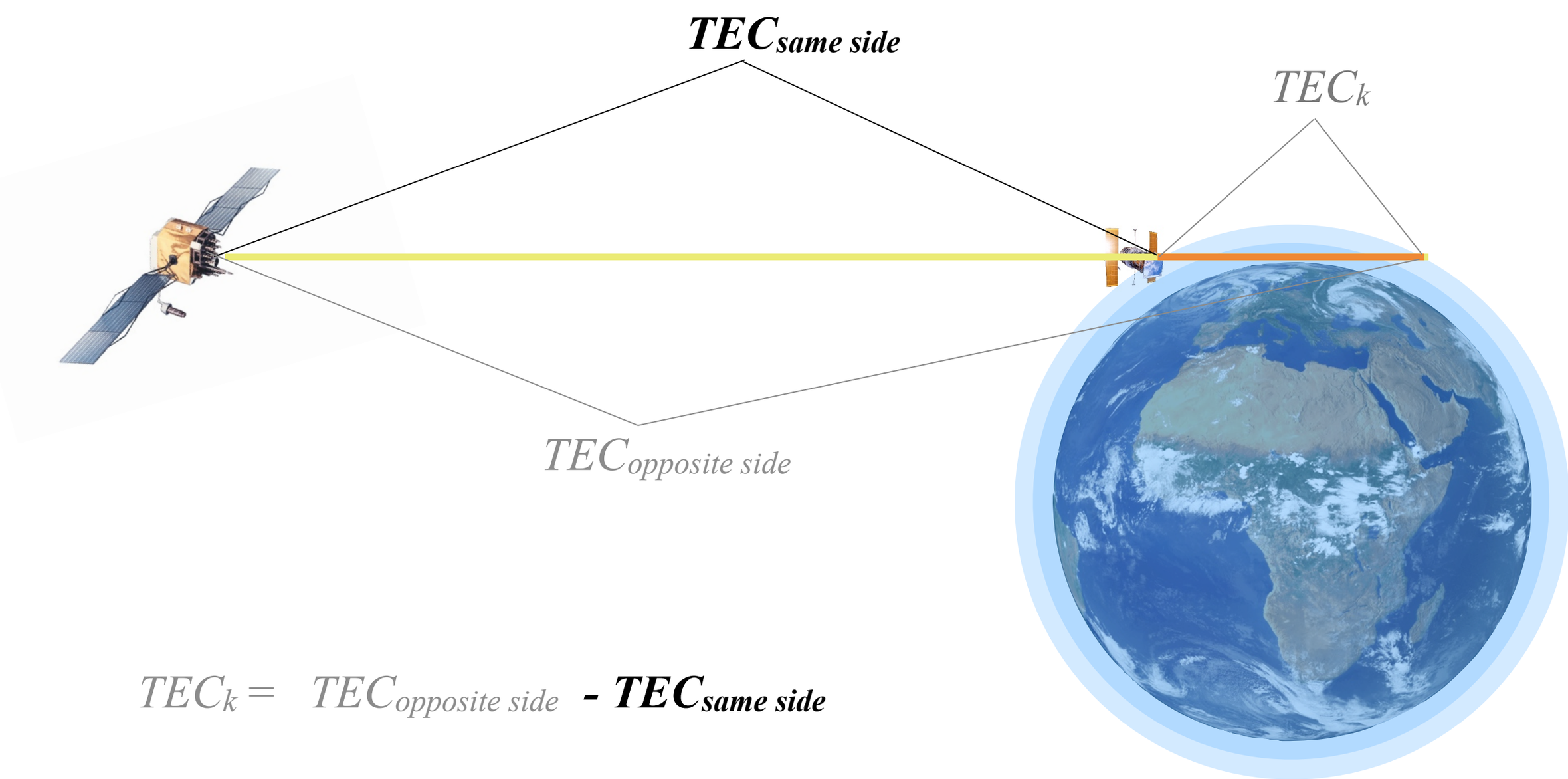

$$TEC_k = TEC_{opposite\ side} - \mathbf{TEC_{same\ side}}$$

The role of the “same side” (auxiliary) data in TEC calibration

SIMULATION RESULTS

TEC calibration (COSMIC like sat.)

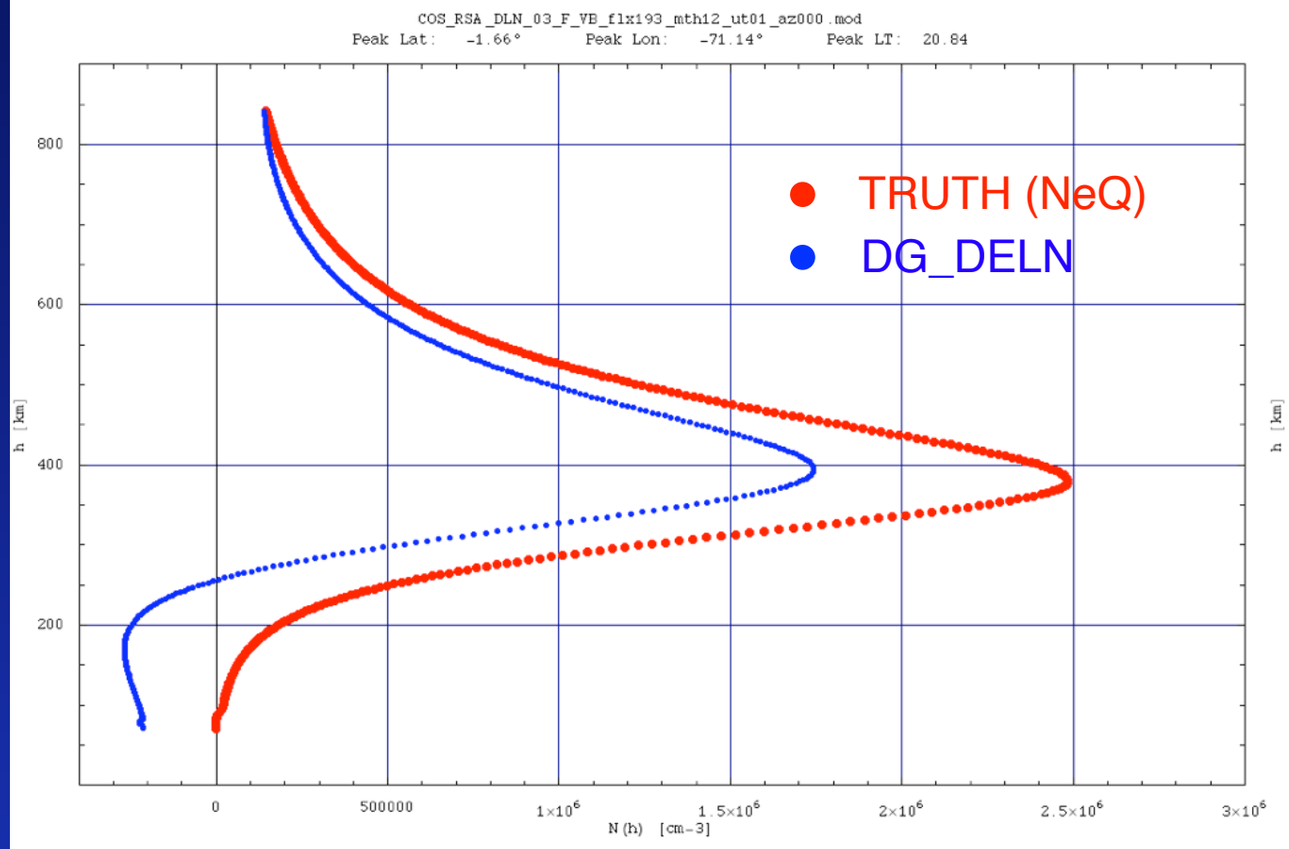

WITH auxiliary data

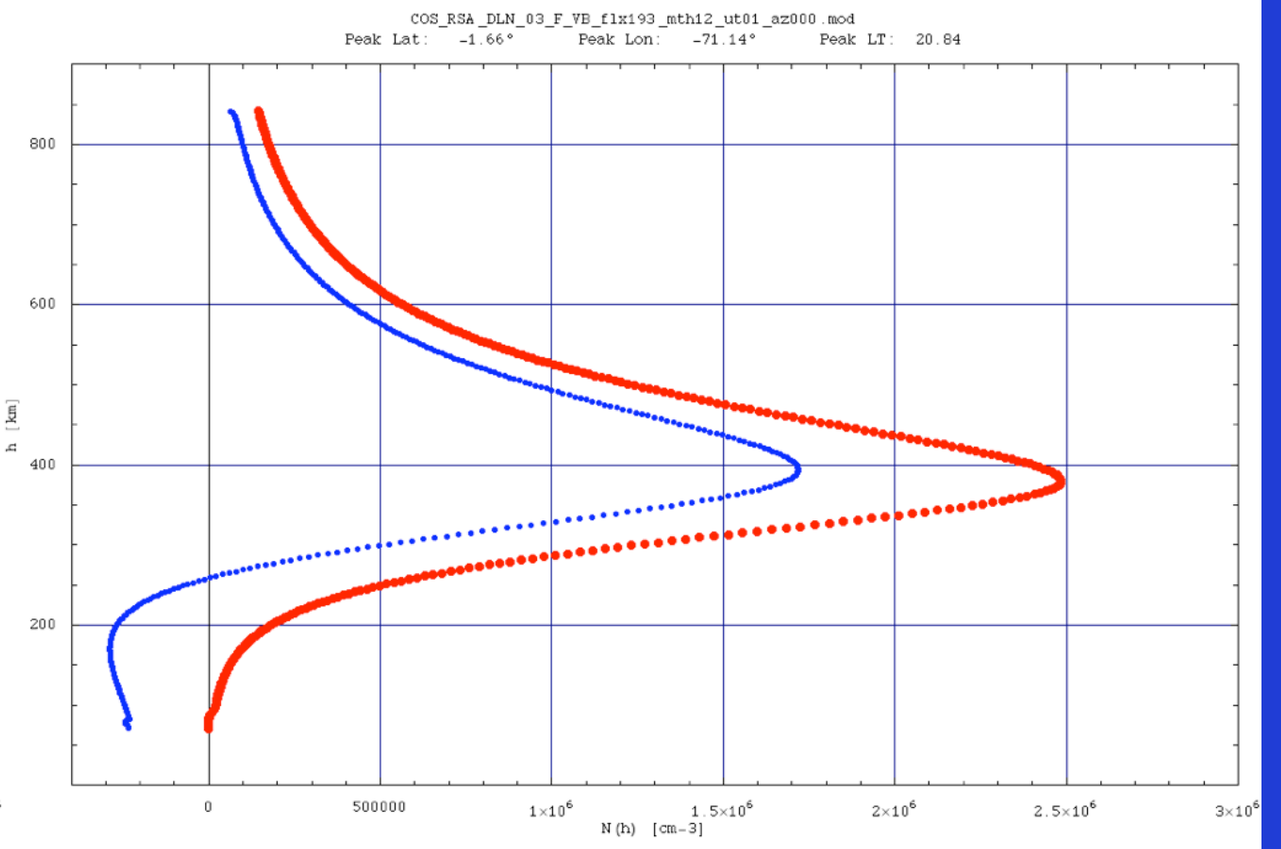

WITHOUT auxiliary data

TEC calibration (CHAMP like sat.)

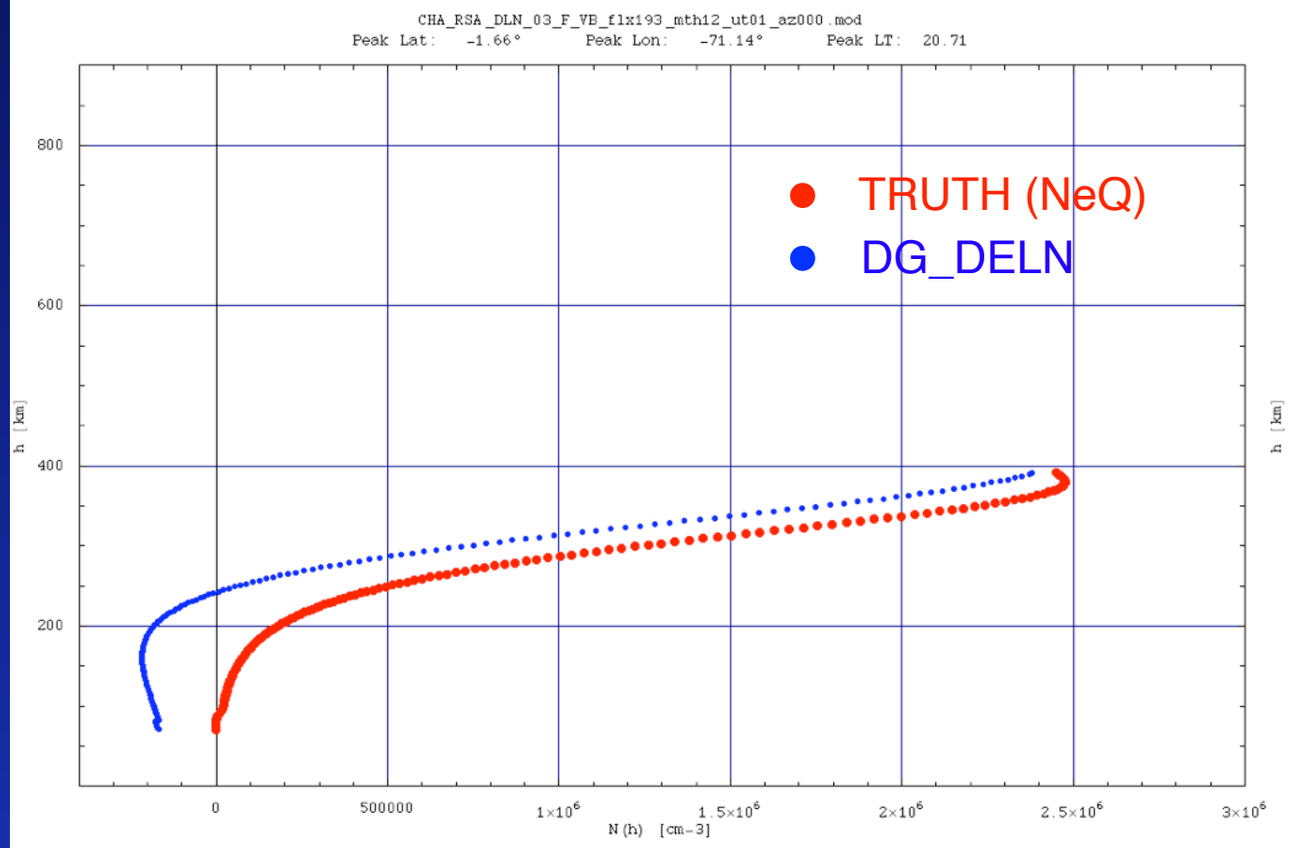

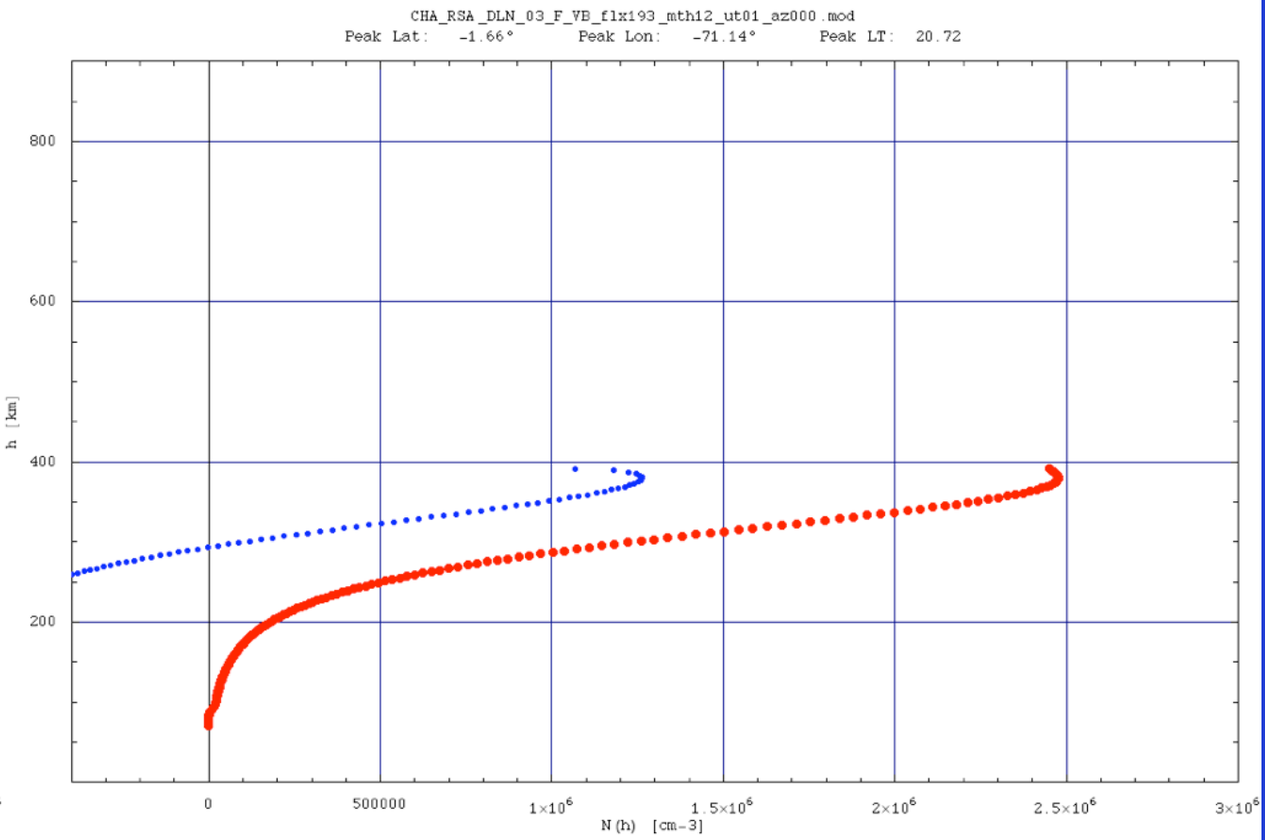

WITH auxiliary data

WITHOUT auxiliary data

The spherical symmetry assumption for the electron density of the ionosphere: effects on the reconstructed profiles.

SIMULATION RESULTS

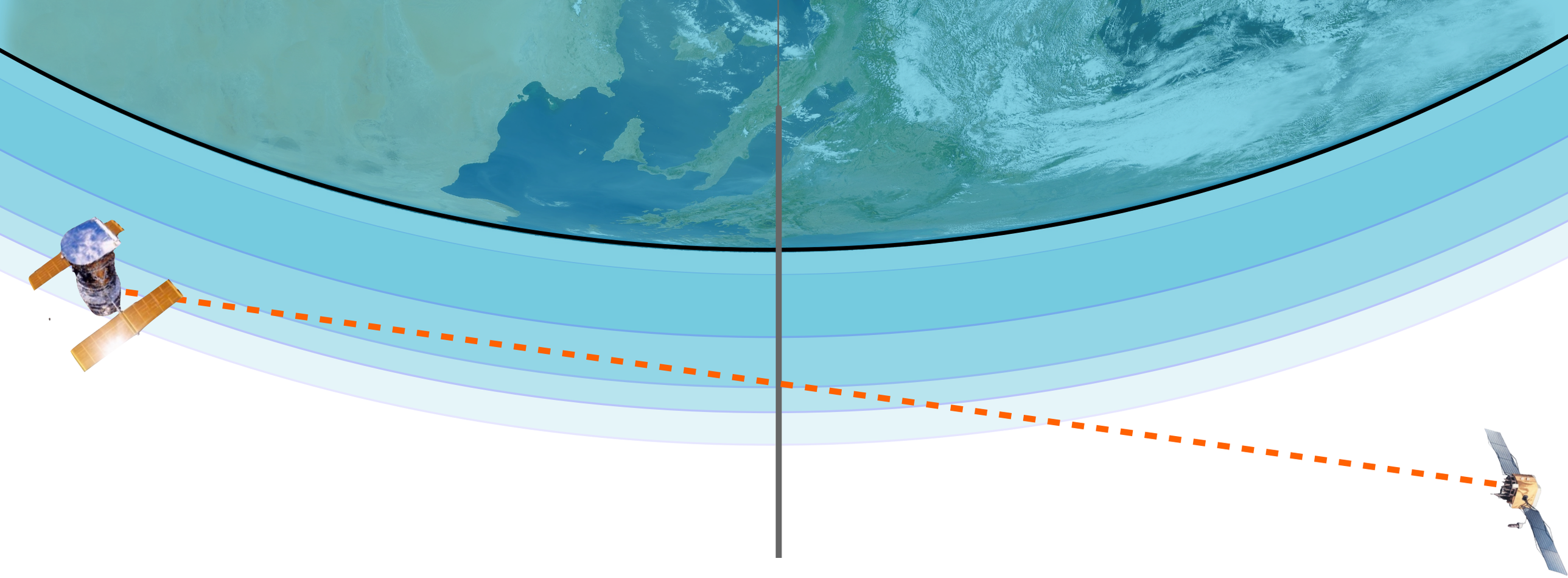

0°

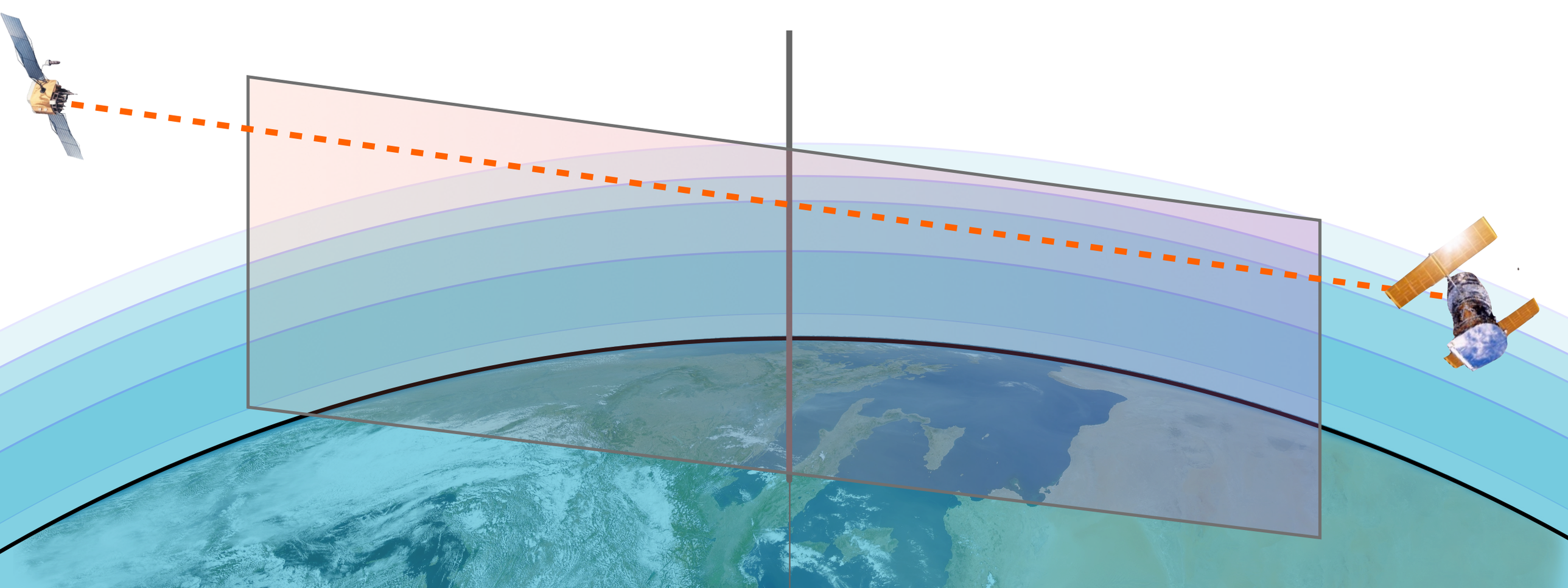

0°

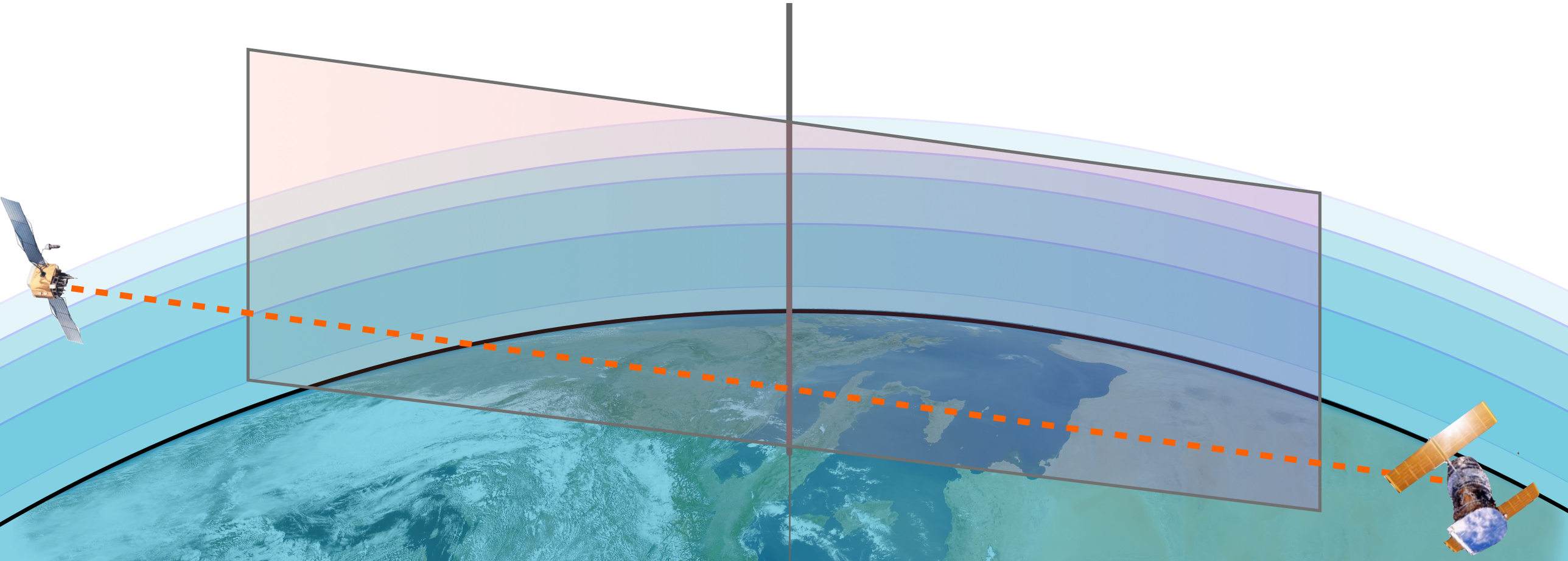

0°

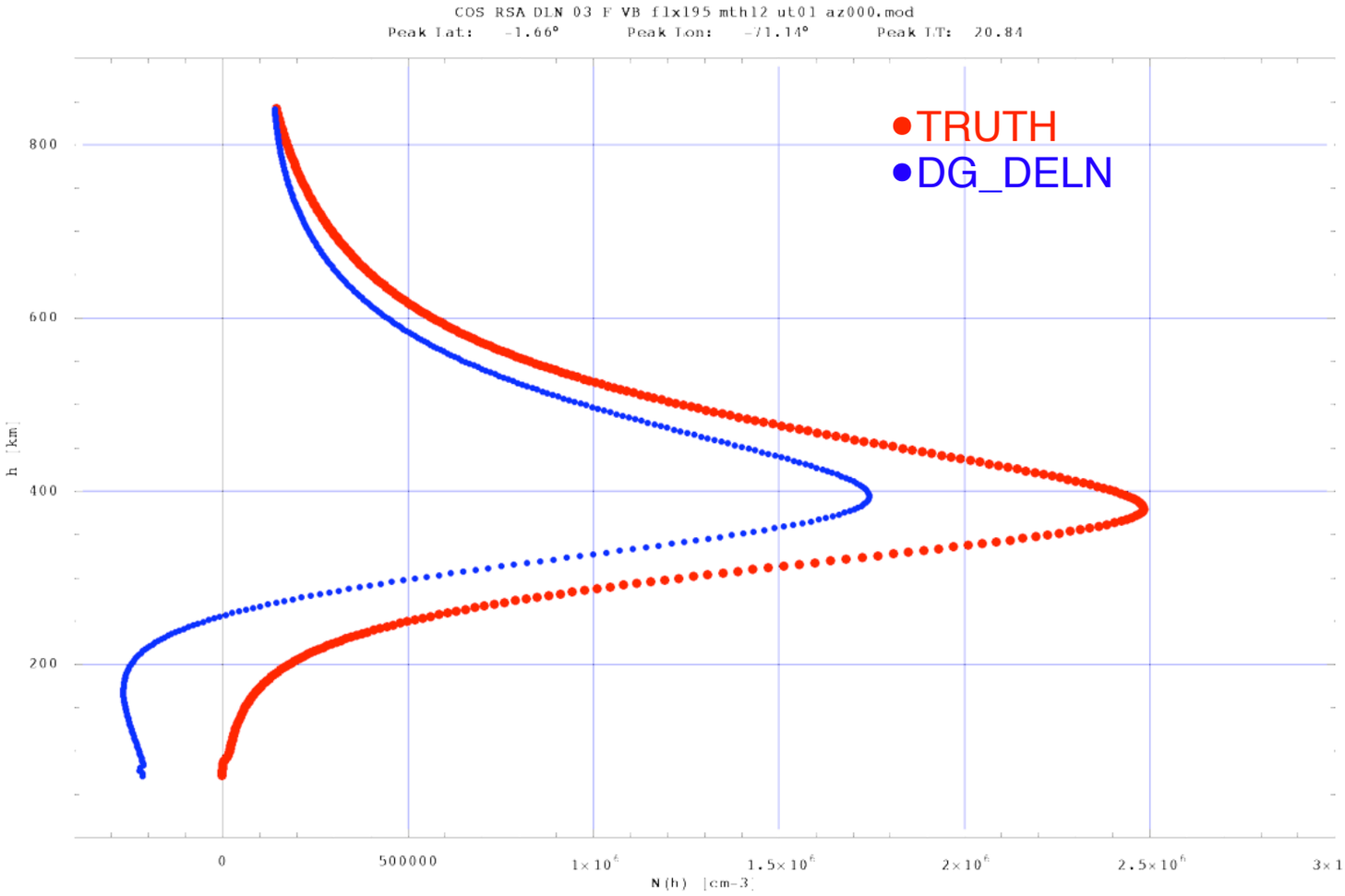
COS RSA DLN 03 F VB f1x195 mth12 ut01 az000.mod
Peak Lat: -1.66° Peak Lon: -71.14° Peak LT: 20.84
TRUTH
DG_DELN
800
600
400
200
h [km]
0
500000
1×10^6
1.5×10^6
2×10^6
2.5×10^6
3×10^6
N(h) [cm-3]

30°

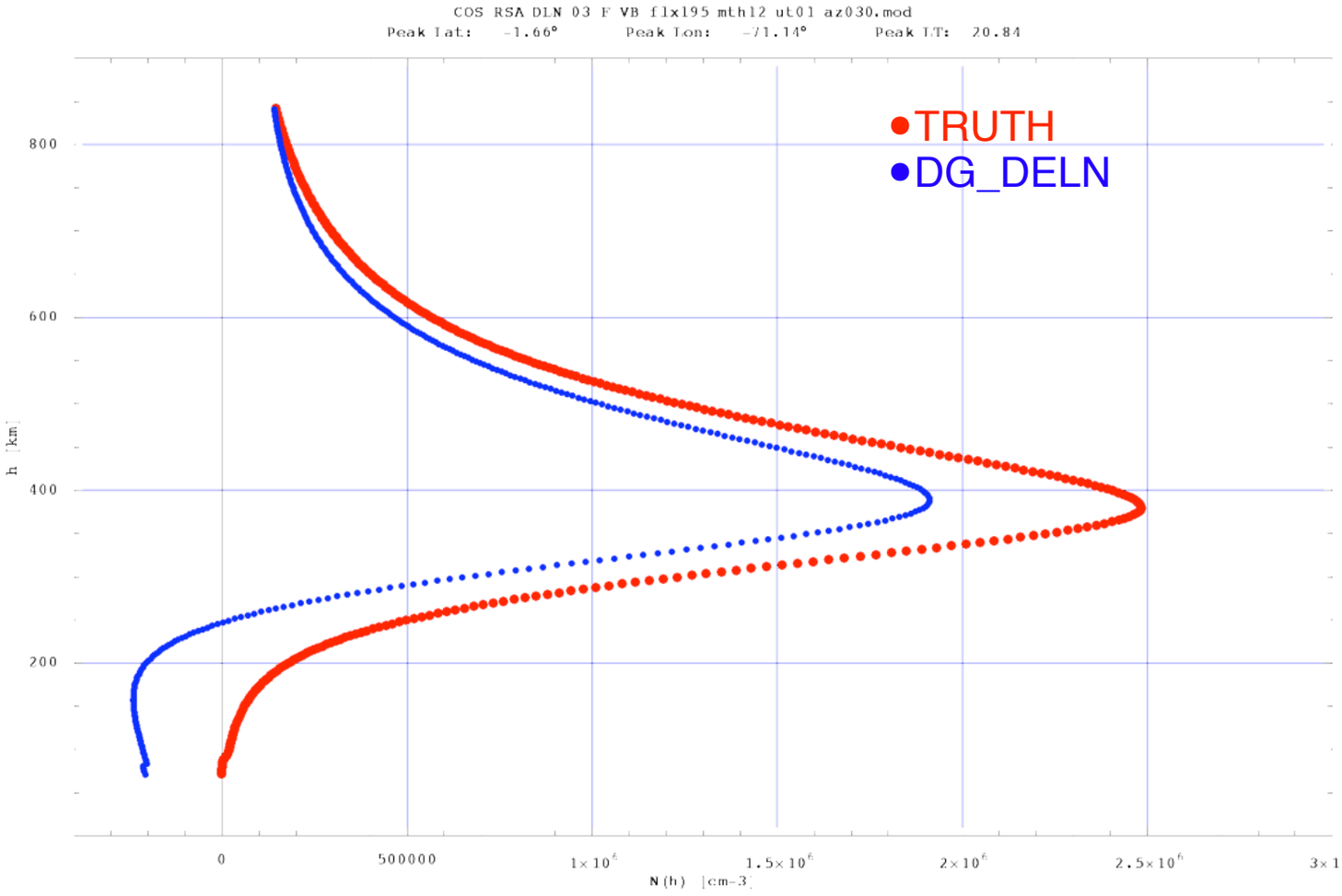
COS RSA DLN 03 F VB f1x195 mth12 ut01 az030.mod
Peak Lat: -1.66° Peak Lon: -71.14° Peak LT: 20.84
TRUTH
DG_DELN
800
600
400
200
h [km]
0
500000
1×10^6
1.5×10^6
2×10^6
2.5×10^6
3×10^6
N(h) [cm-3]

60°

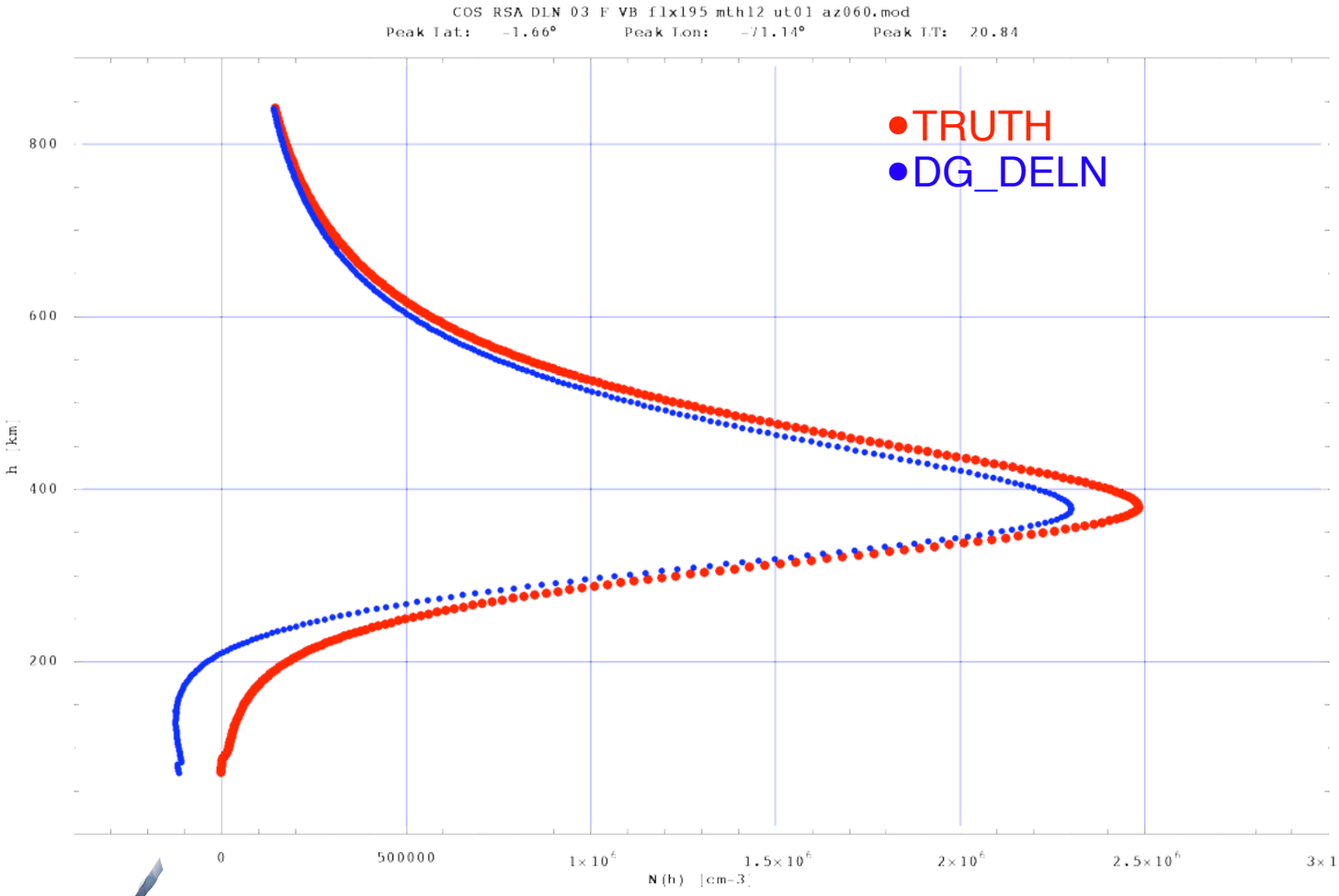
COS RSA DLN 03 F VB f1x195 mth12 ut01 az060.mod
Peak Lat: -1.66° Peak Lon: -71.14° Peak LT: 20.84
TRUTH
DG_DELN
800
600
400
200
h [km]
0
500000
1×10^6
1.5×10^6
2×10^6
2.5×10^6
3×10^6
N(h) [cm-3]

90°

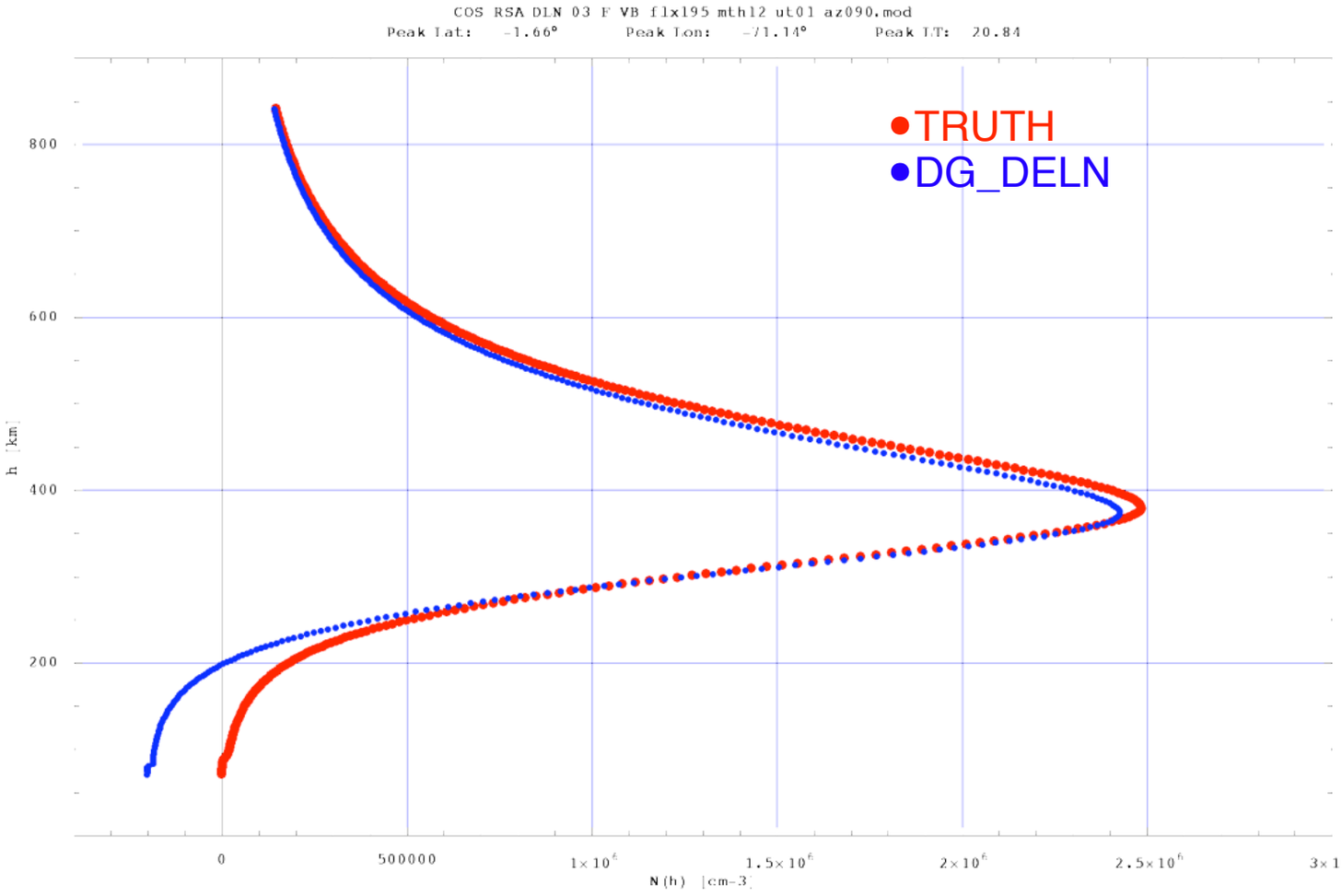
COS RSA DLN 03 F VB f1x195 mth12 ut01 az090.mod
Peak Lat: -1.66° Peak Lon: -71.14° Peak LT: 20.84
TRUTH
DG_DELN
800
600
400
200
h [km]
0
500000
1×10^6
1.5×10^6
2×10^6
2.5×10^6
3×10^6
N(h) [cm-3]

120°

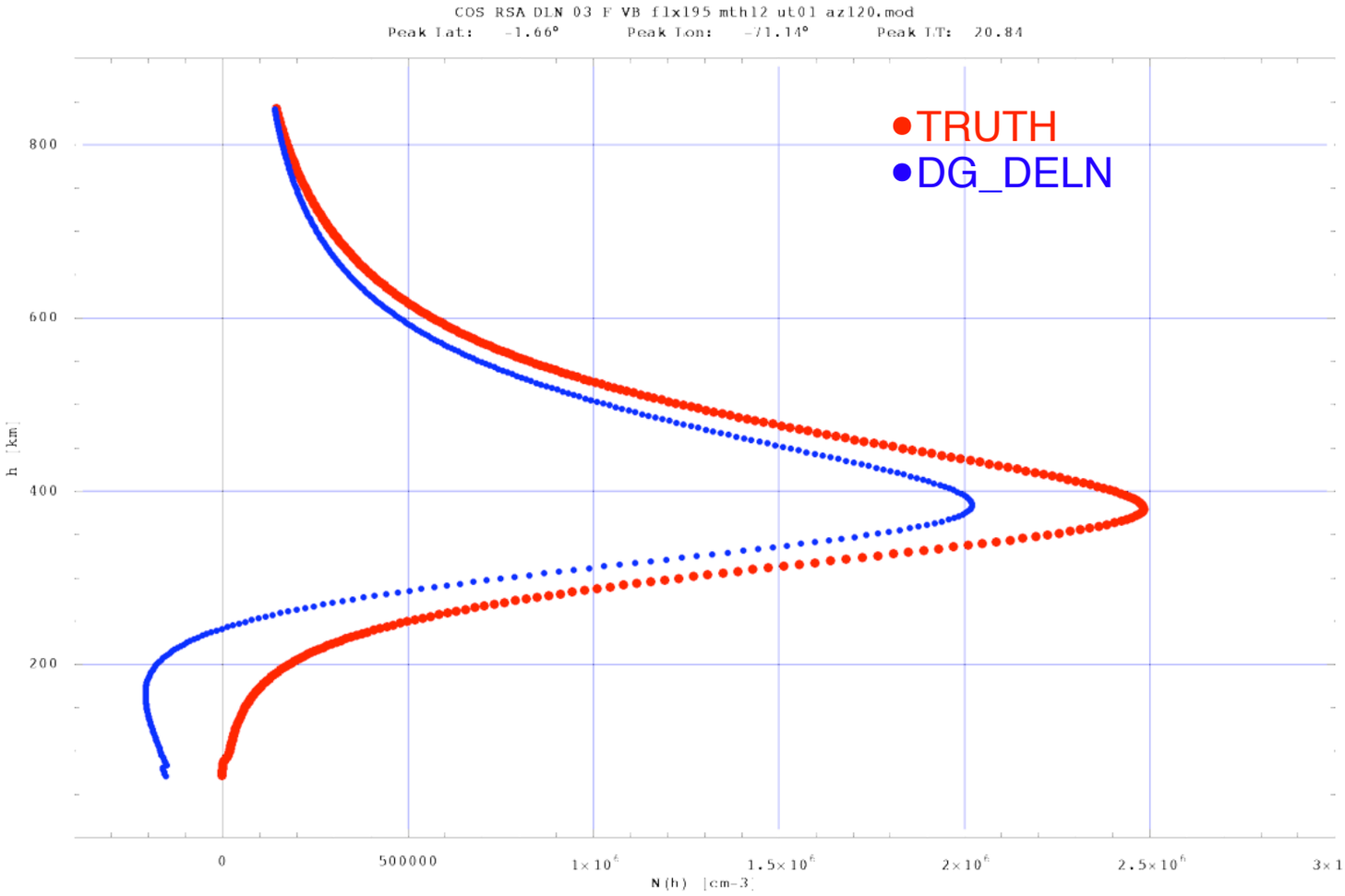
COS RSA DLN 03 F VB f1x195 mth12 ut01 az120.mod
Peak Lat: -1.66° Peak Lon: -71.14° Peak LT: 20.84
TRUTH
DG_DELN
800
600
400
200
h [km]
0
500000
1×10^6
1.5×10^6
2×10^6
2.5×10^6
3×10^6
N(h) [cm-3]

150°

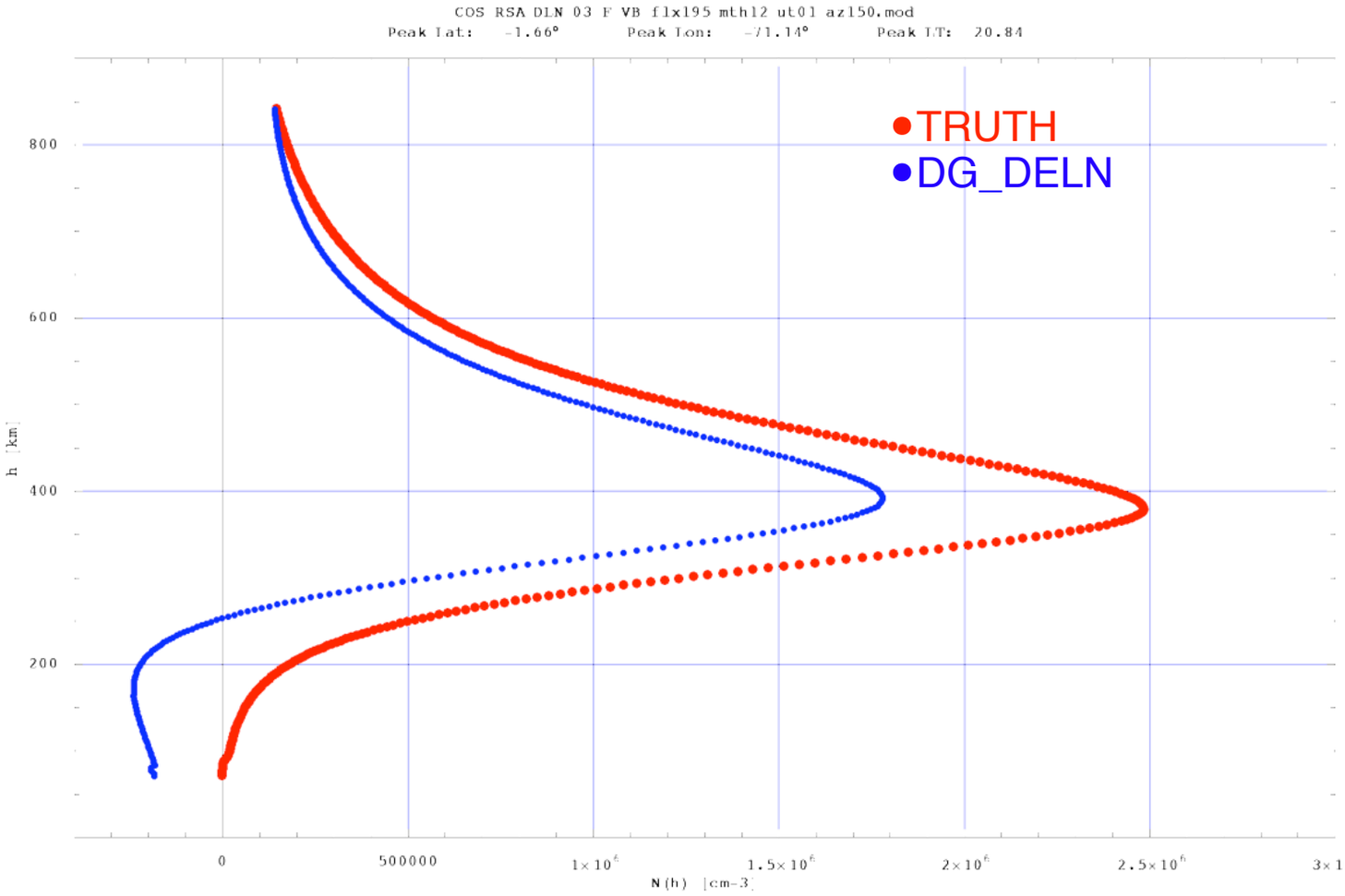
COS RSA DLN 03 F VB f1x195 mth12 ut01 az150.mod
Peak Lat: -1.66° Peak Lon: -71.14° Peak LT: 20.84
TRUTH
DG_DELN
800
600
400
200
h [km]
0
500000
1×10^6
1.5×10^6
2×10^6
2.5×10^6
3×10^6
N(h) [cm-3]

180°

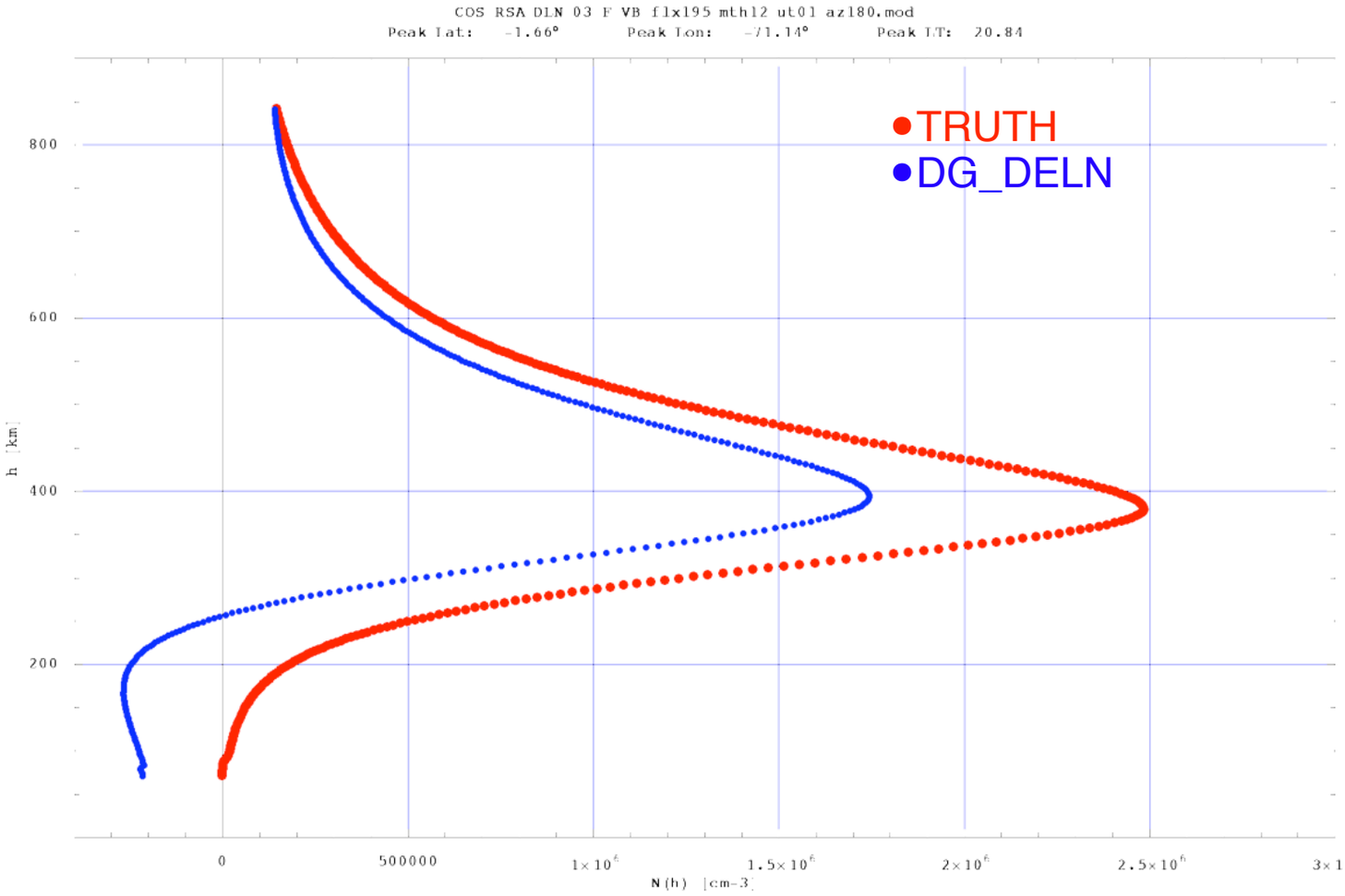
COS RSA DLN 03 F VB f1x195 mth12 ut01 az180.mod
Peak Lat: -1.66° Peak Lon: -71.14° Peak LT: 20.84
TRUTH
DG_DELN
800
600
400
200
h [km]
0
500000
1×10^6
1.5×10^6
2×10^6
2.5×10^6
3×10^6
N(h) [cm-3]

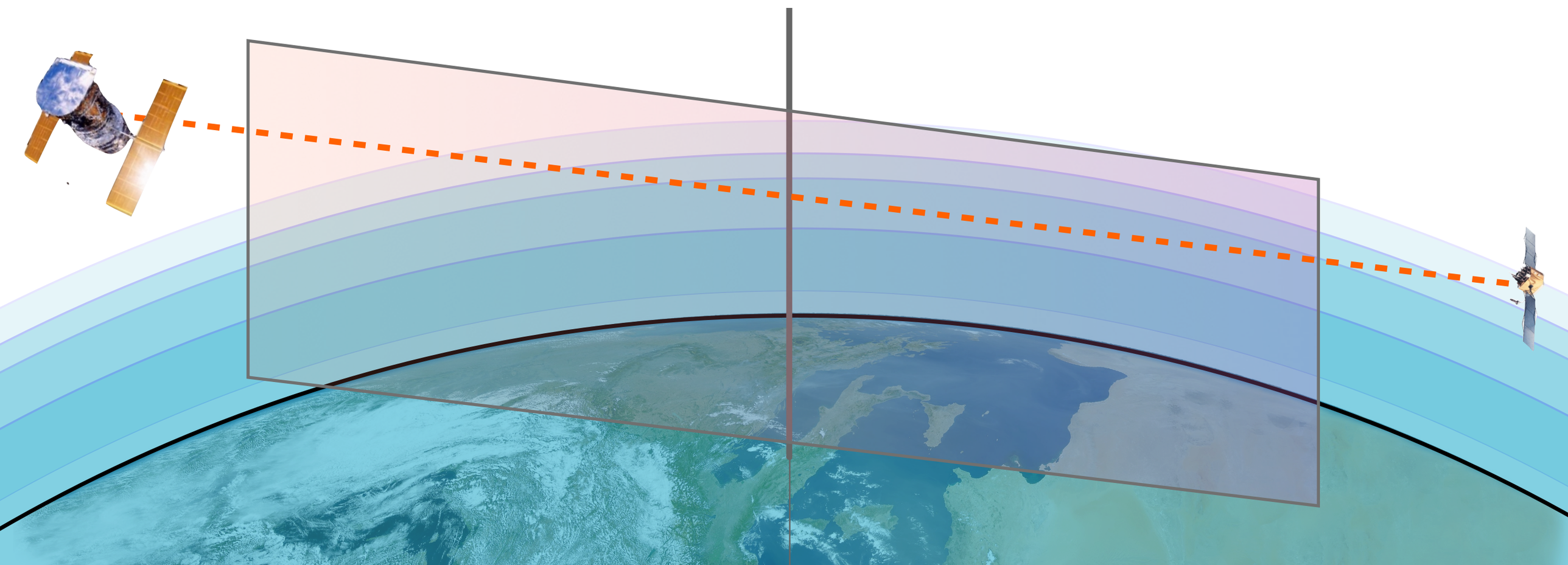

Plasma “caves”

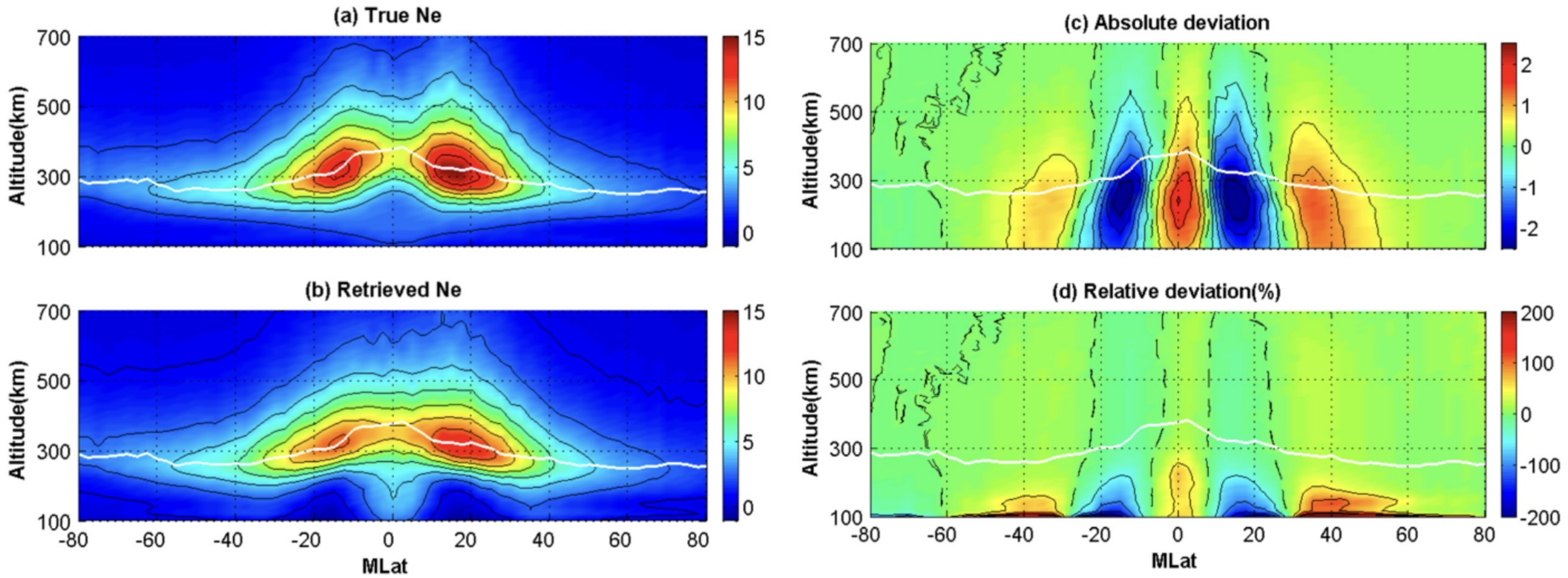

Geomagnetic latitudinal and altitudinal variations of true (NeQuick) electron density (a), retrieved electron density (b), absolute deviation (c) and relative deviation (d) between retrieved and true electron density during 12:00–14:00LT. The unit in panels (a–c) is 10^11 m^–3 and in panel (d) is percentage. The intervals between the contour lines in (c) and (d) are 0.5×10^11 m^–3 and 50%, respectively (from Yue, et al., 2010).

Plasma “caves”

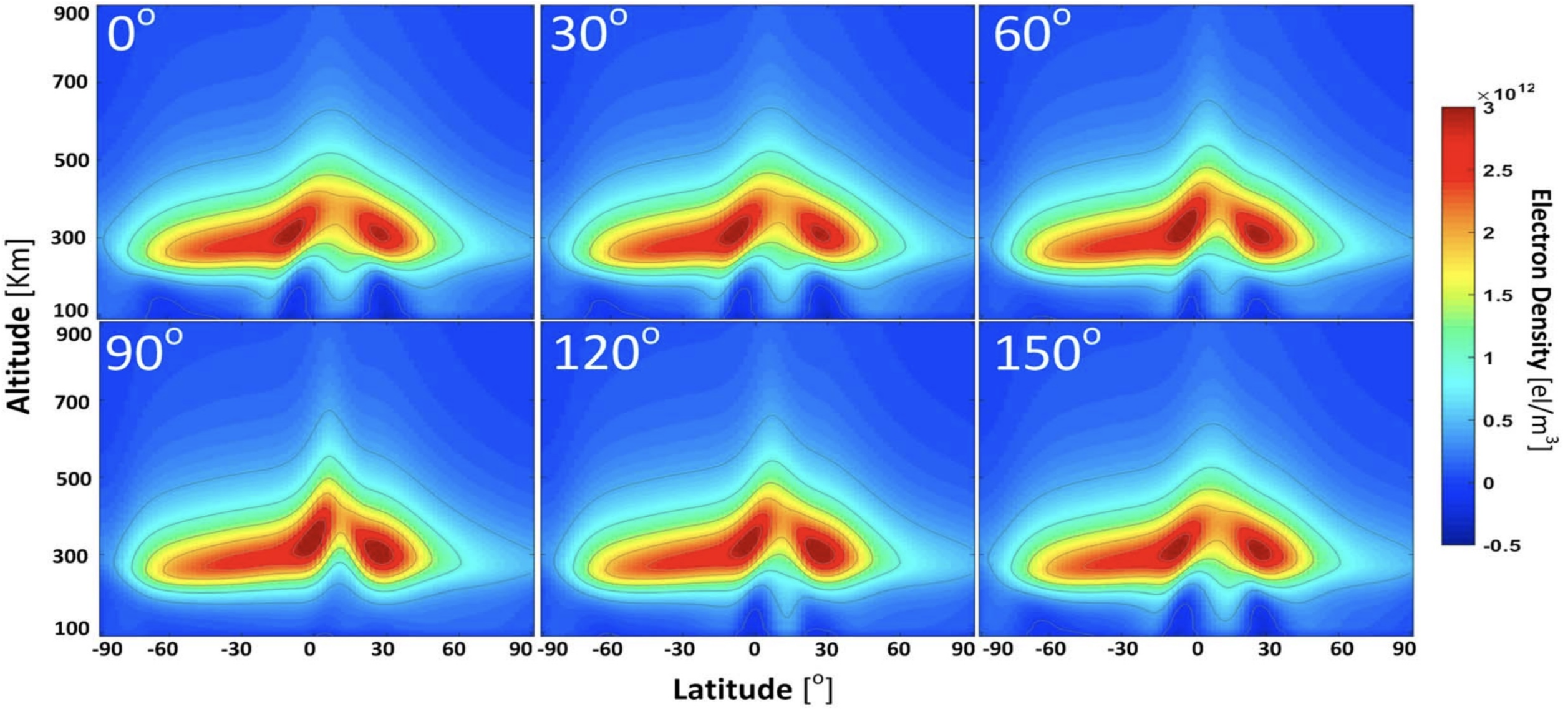

NeQuick-based simulation: Ne from Abel inversion for April, 1400 UT, high solar activity conditions. Each of the six plots shows the RO-derived vertical Ne profiles as a function of latitude along the 0°E longitude meridian for a given azimuth of the occultation plane (indicated at the top left corner of the plot). (From Shaikh et. al, 2018).

Plasma “caves”

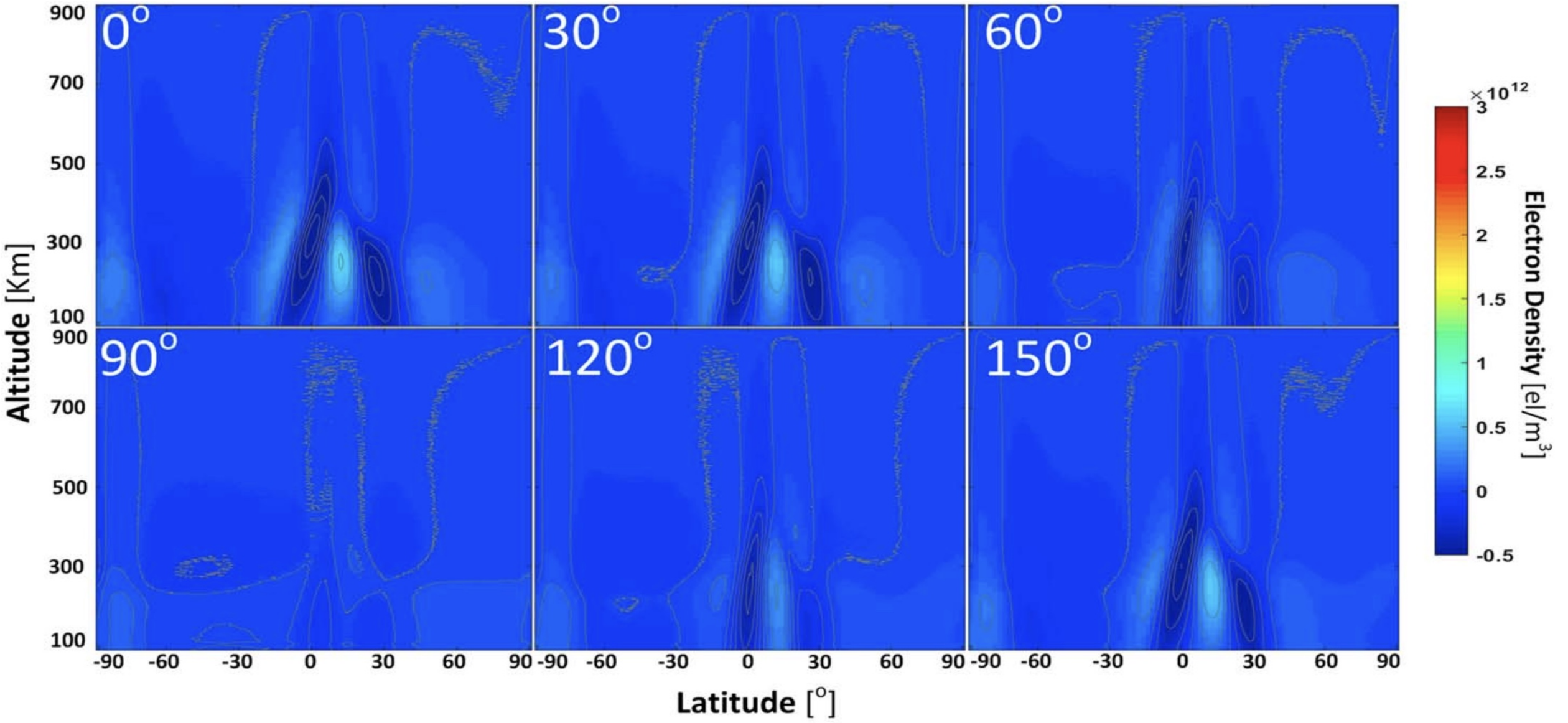

NeQuick-based simulation: Ne difference Abel inversion - “experimental” for the same conditions as in previous slide. (From Shaikh et. al, 2018).

Model assisted RO data inversion

A model assisted inversion technique based on the adaption of the NeQuick to RO-derived TEC data has been proposed by Shaikh et al. (2018) to mitigate the spherical symmetry assumption effects on RO data inversion, without using external data (such as for example global ionospheric VTEC maps).

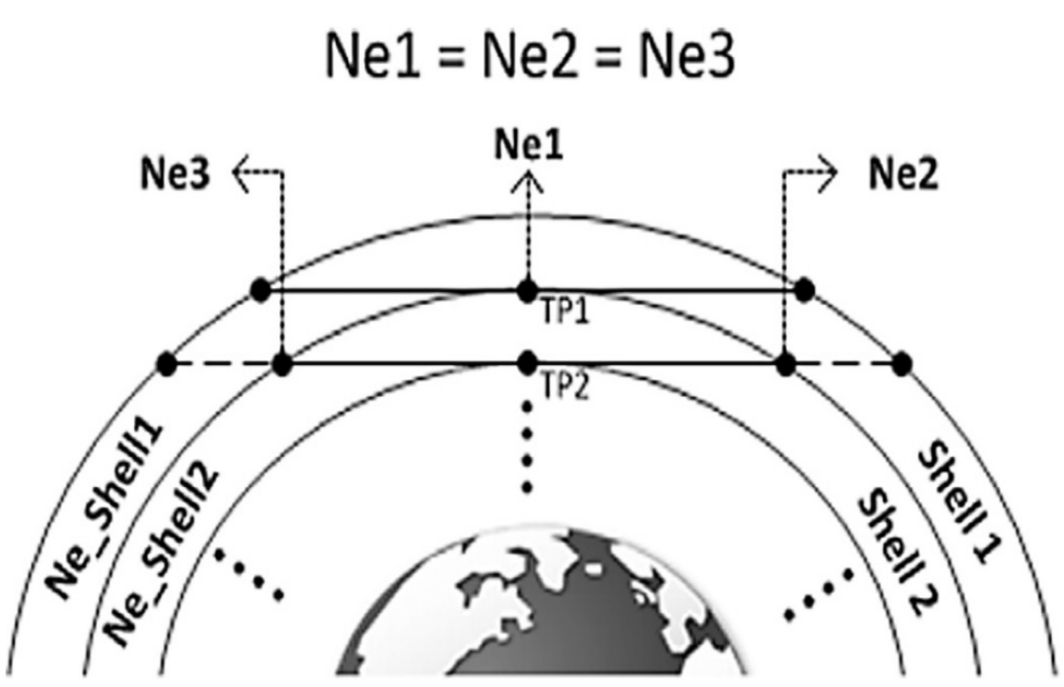

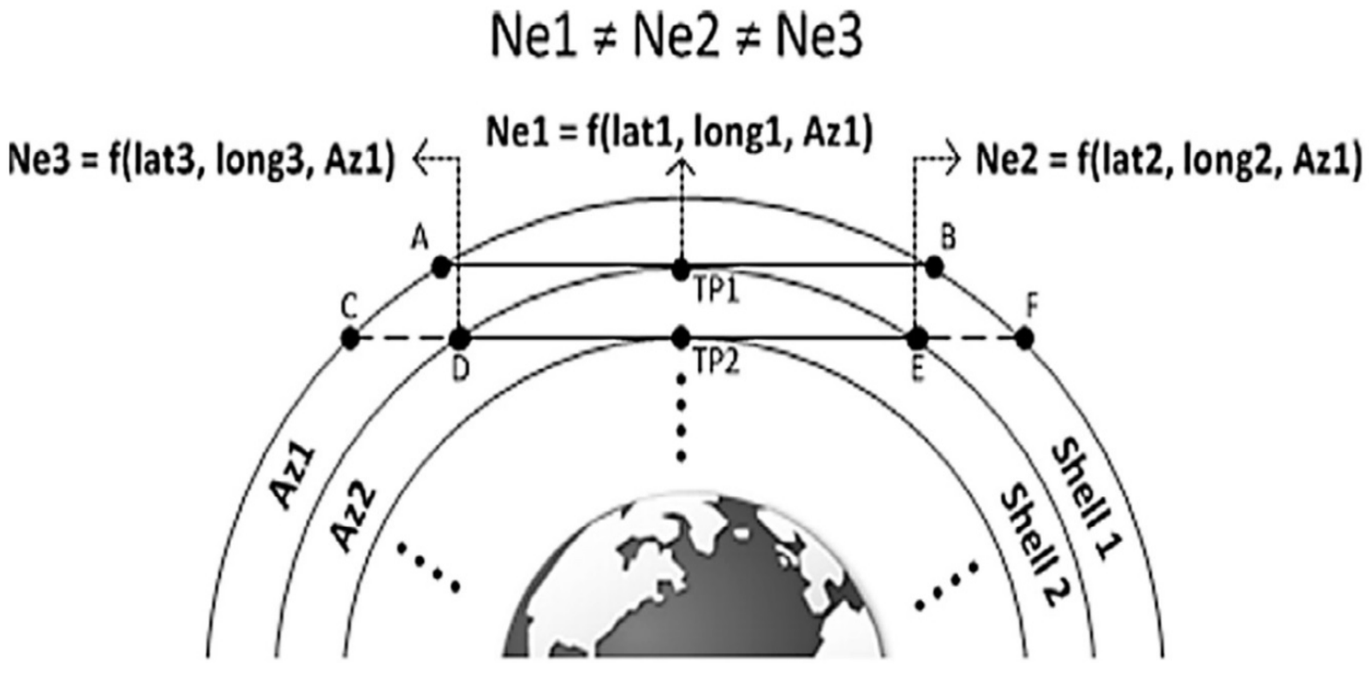

Illustration of spherical symmetry hypothesis for the electron density (left) in contrast to the spherical symmetry assumption of the NeQuick effective parameter Az1 (effective F10.7) used to apply the model-assisted inversion (right).

Model assisted RO data inversion

The effectiveness of the method has been quantified utilising the relative frequency distribution of the relative NmF2 errors (period: 01/2007 to 09/2015).

All stations, global

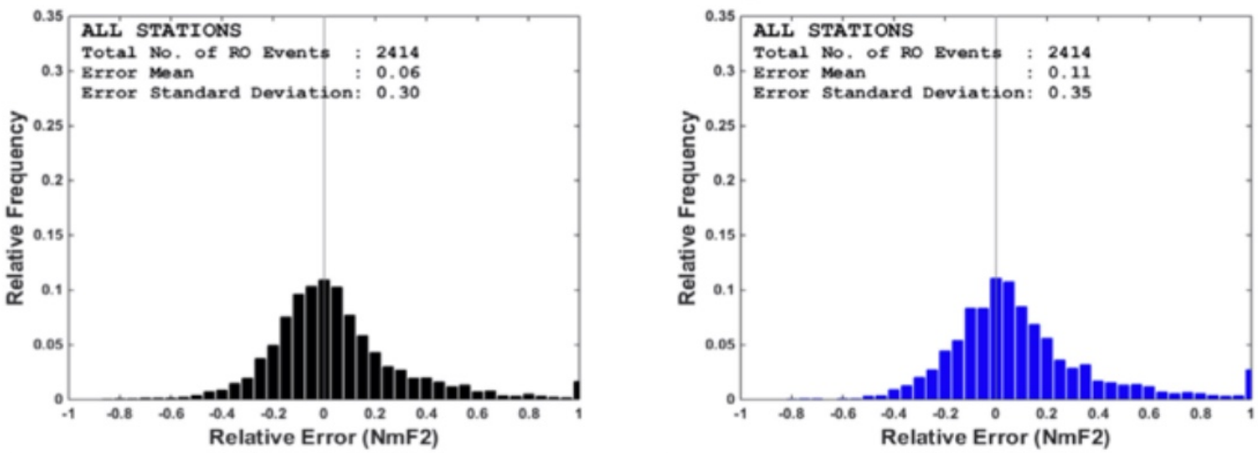

All stations, day

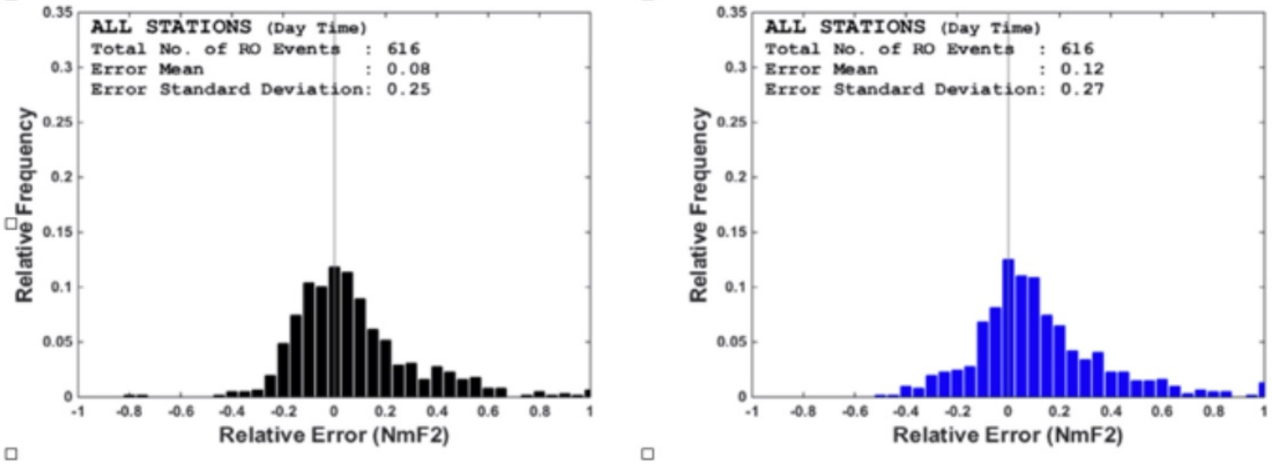

All stations, HSA

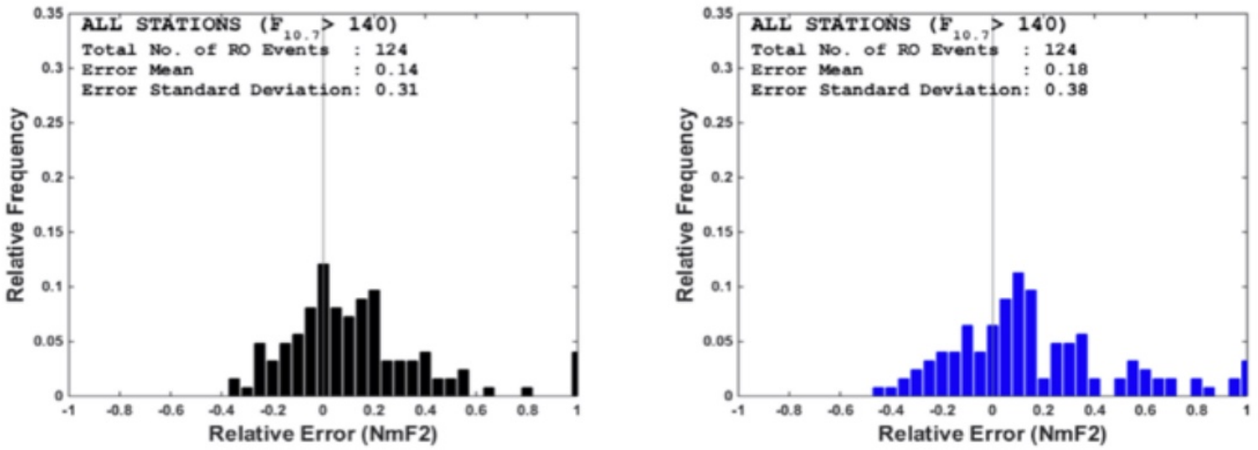

All stations, night

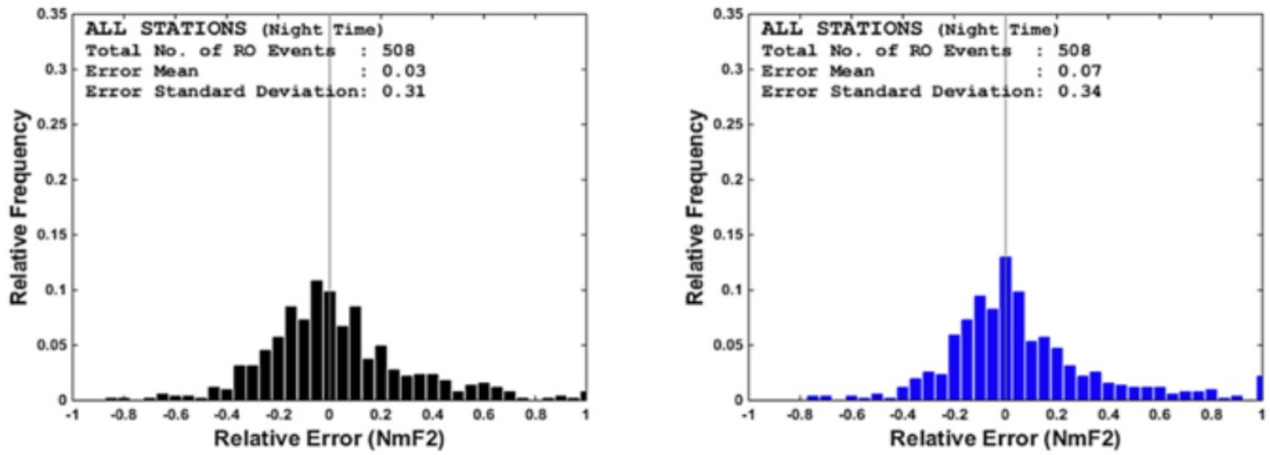

■ Model-assisted RO data inversion ■ Abel inversion

Relative NmF2 error for 13 ionosondes (a), during high solar activity (b), day-time (c), night-time (d). Model-assisted inversion (black); (b) Standard Abel inversion

Test Cases

A test case

Day: 31 Dec. 2007

True satellite orbits (GPS + COSMIC)

Synthetic ionosphere
(TEC from 3D electron density)

Onion Peeling
vs
True profile
(NeQuick)

High & Low solar activity

True ionosphere
(excess phase @ L1,L2)

Onion Peeling
vs
True profile
(Ionosonde)

Onion Peeling performance analyzed in
terms of foF2 & hmF2 error statistics

Simulation results (HSA)

foF2 and hmF2 errors statistics

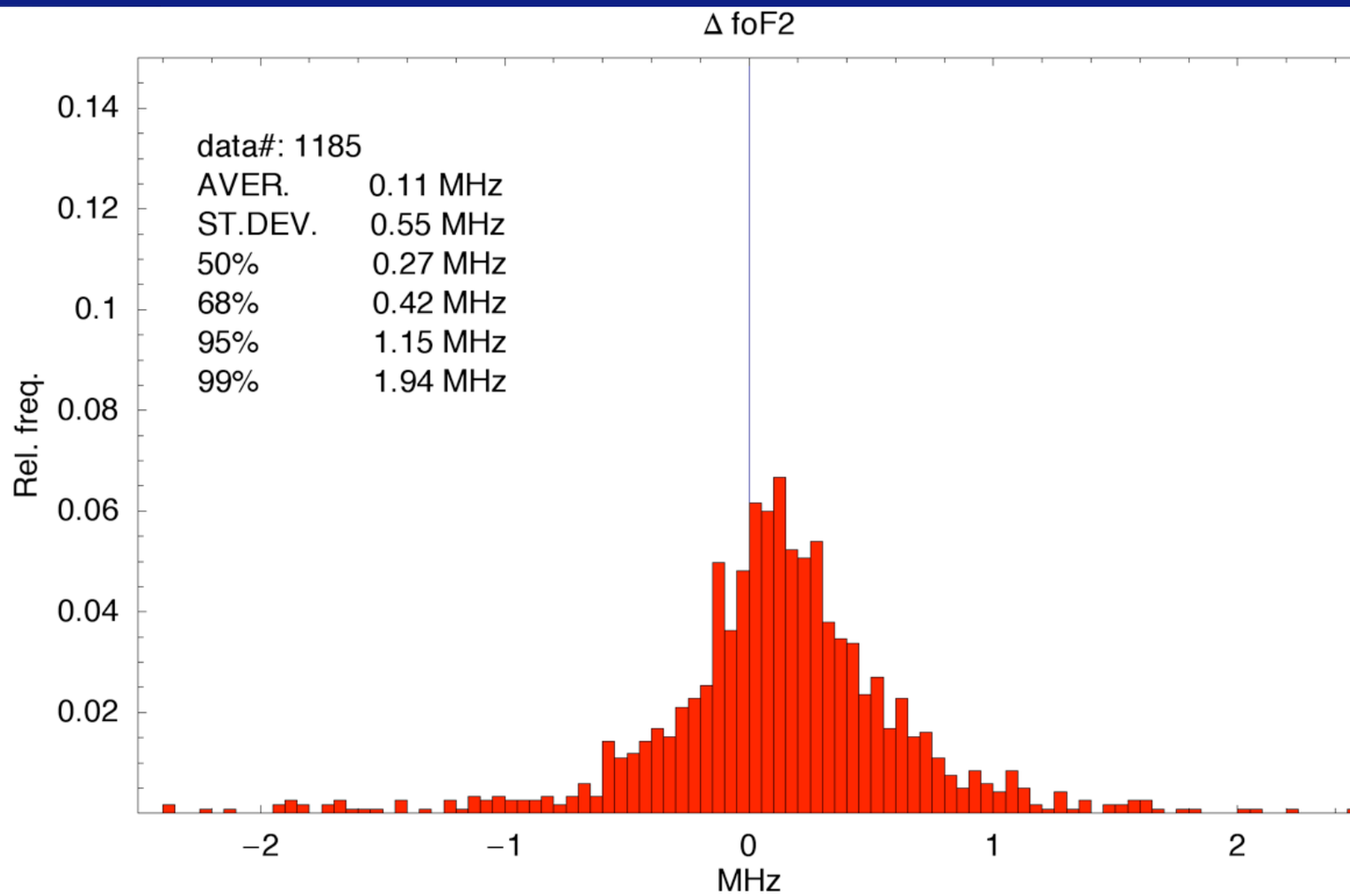

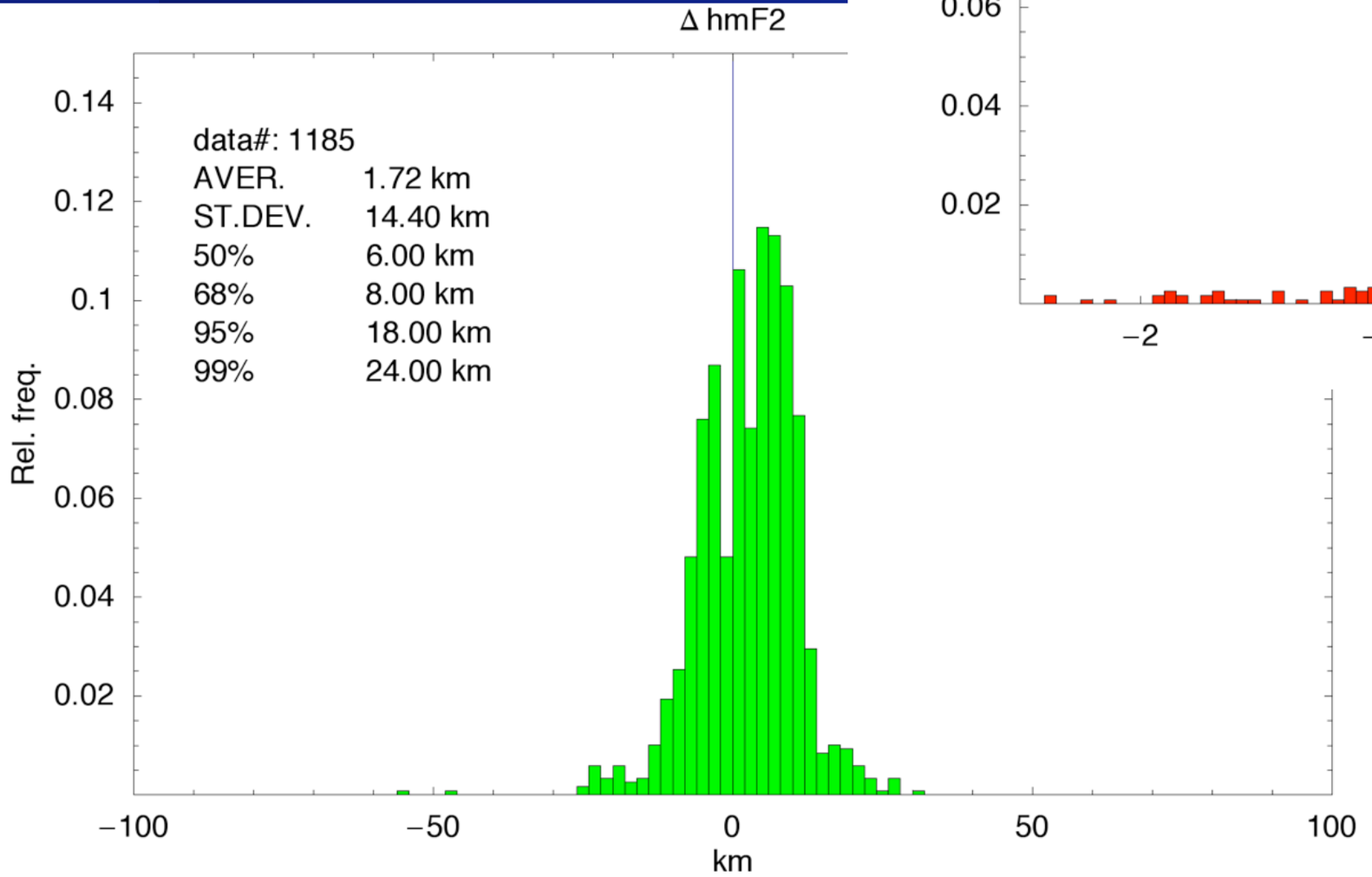

Co-location criteria for true profile and Onion Peeling derived profile

↓

exact matching

Simulation results (LSA)

foF2 and hmF2 errors statistics

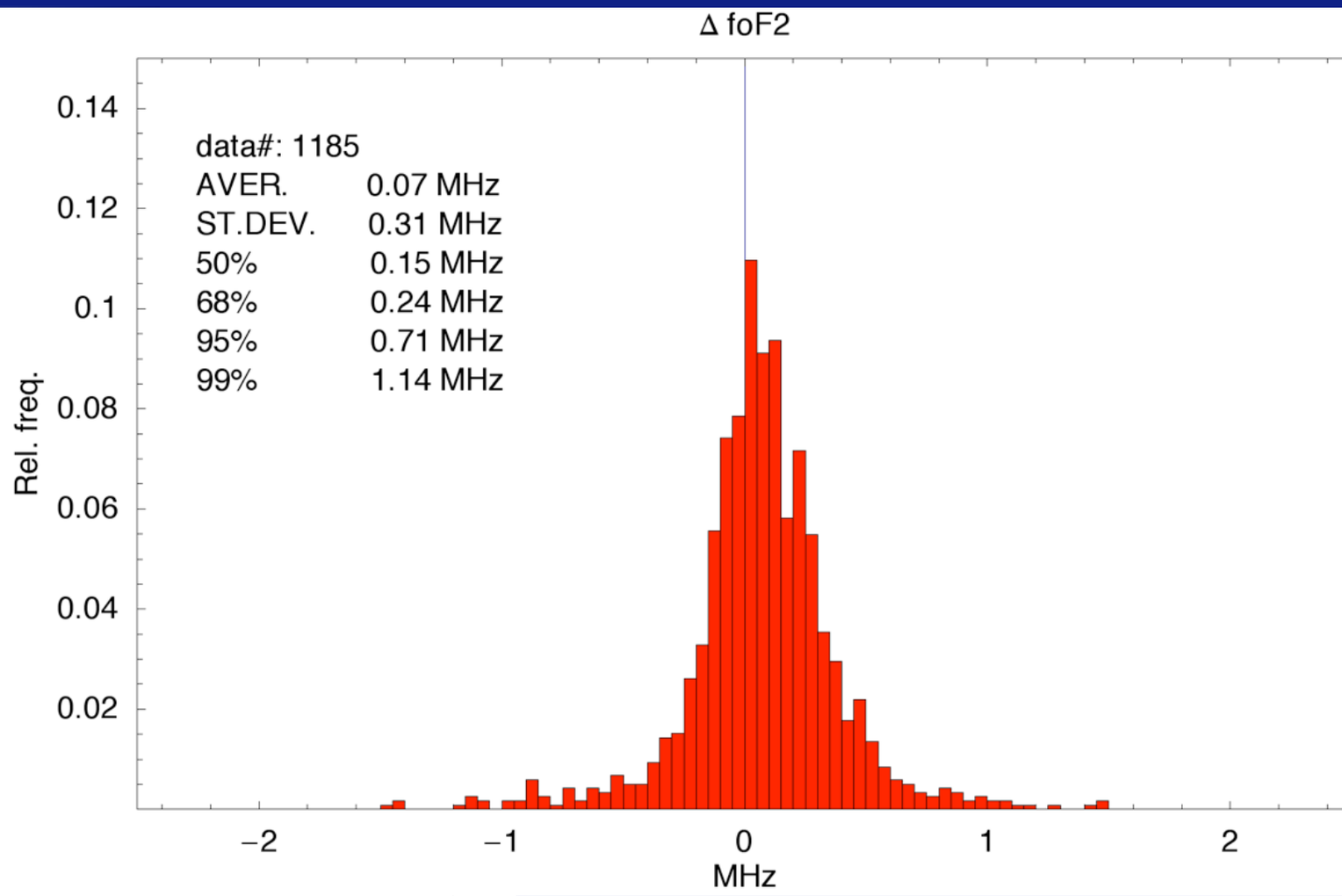

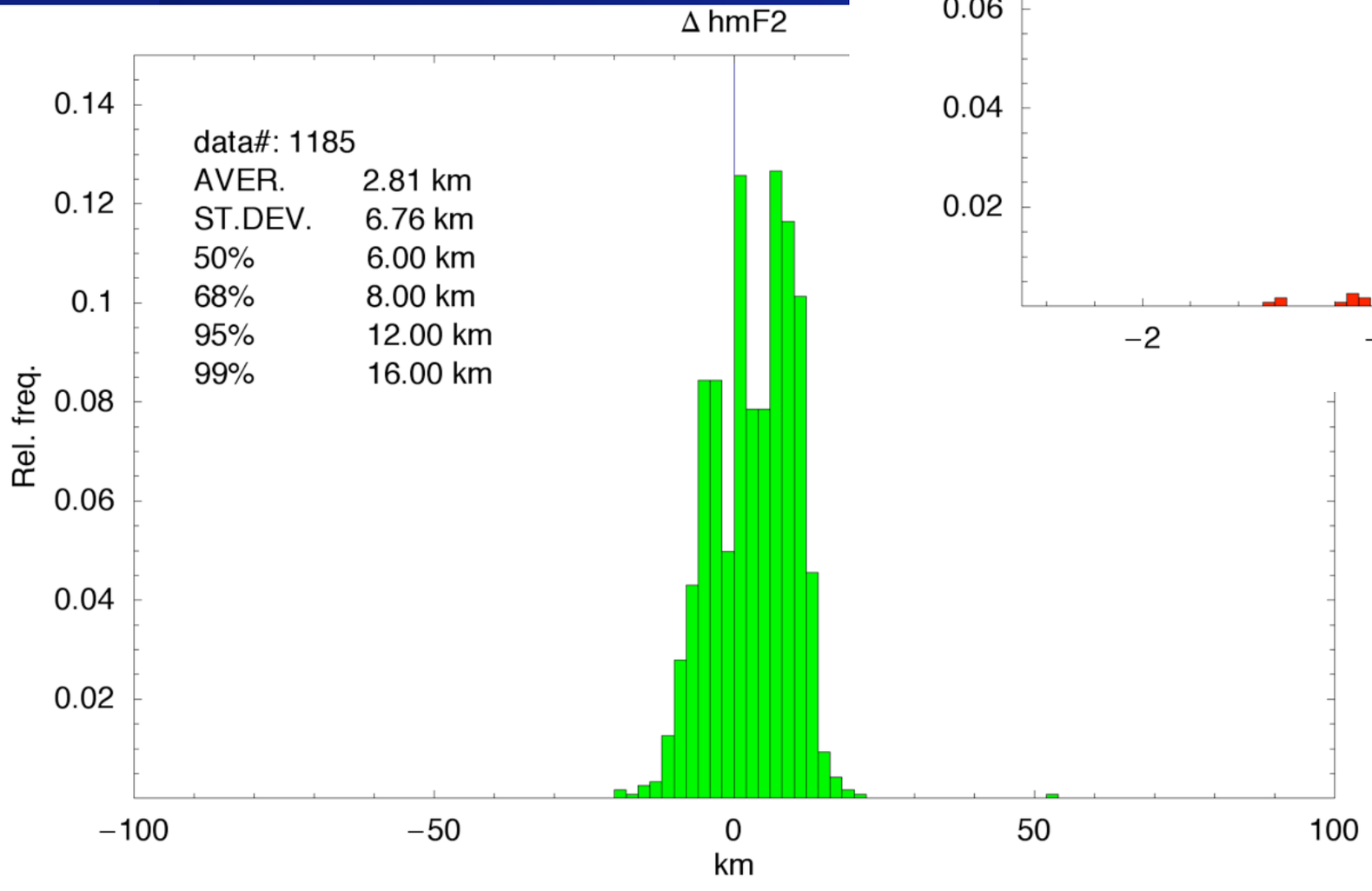

Co-location criteria for true profile and Onion Peeling derived profile

↓

exact matching

Experimental data (LSA)

foF2 and hmF2 errors statistics

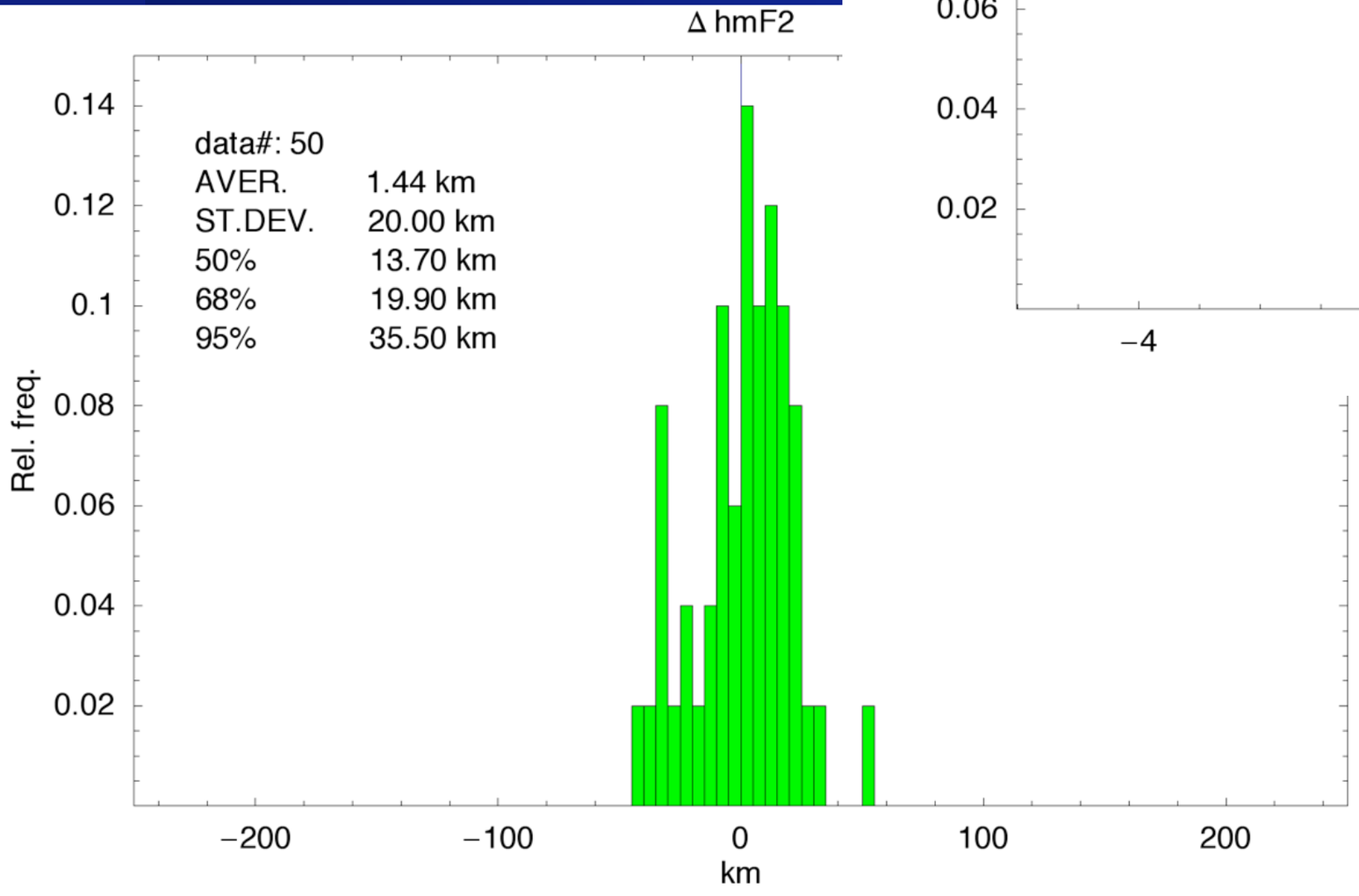

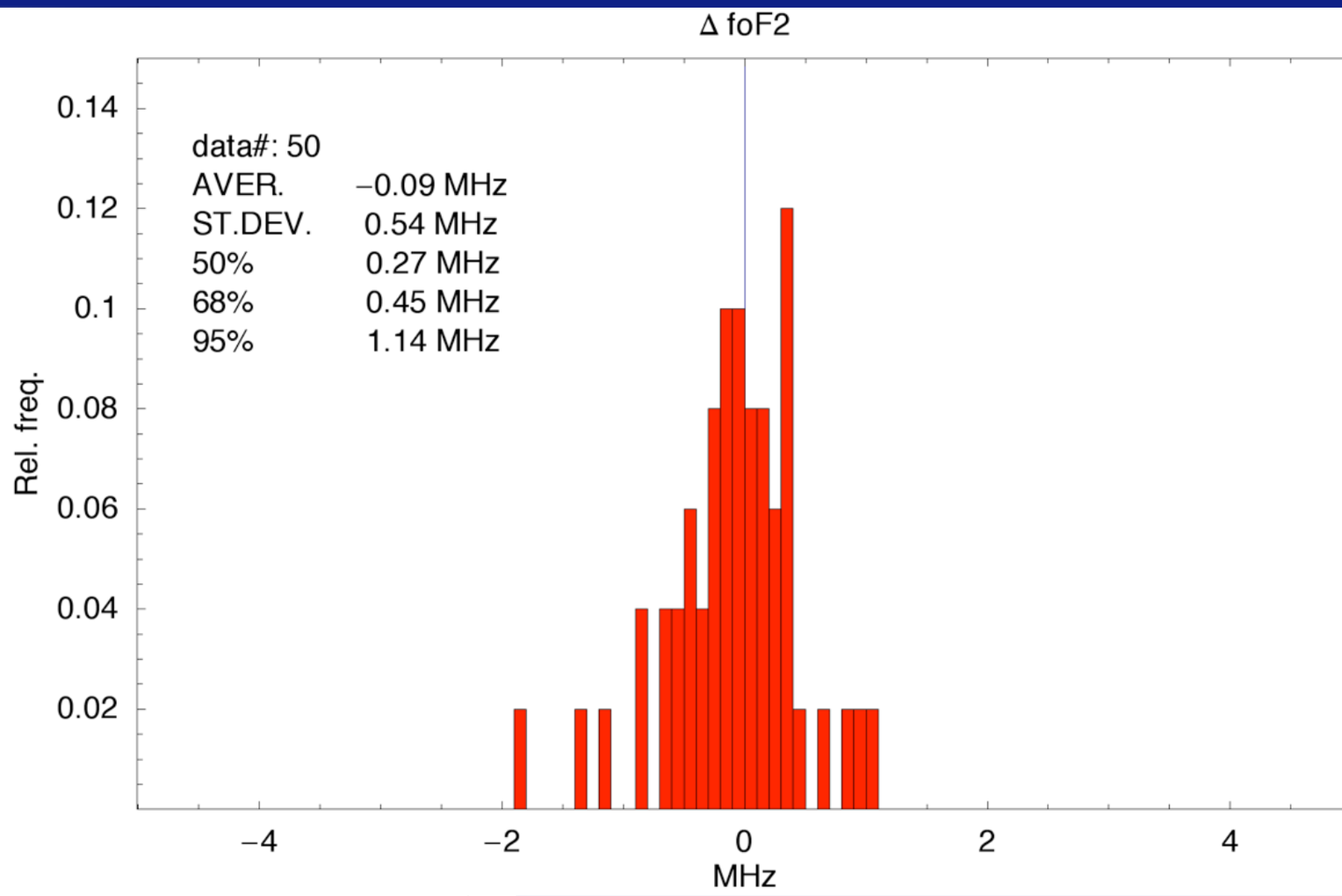

Co-location criteria for true profile and Onion Peeling derived profile

↓

Delta Time < 15 min
Delta Lat < 5°
Delta Lon < 10°

Experimental data (01/2007 -> 09/2015)

foF2 errors statistics (13 ionosondes)

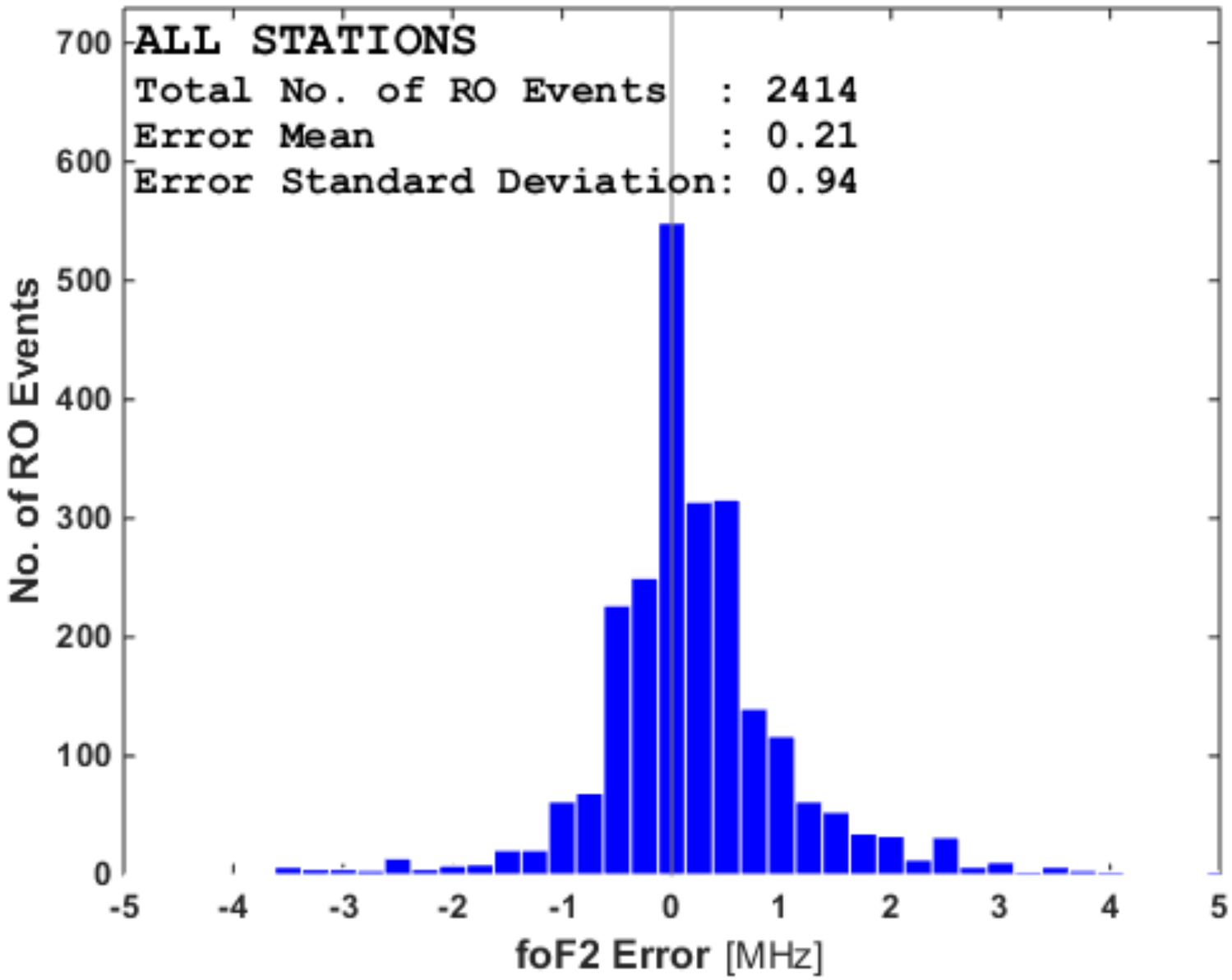

Quiet geomagnetic period
Dst > -50 nT

Co-location criteria for true profile and Onion Peeling derived profile

↓

| Delta Time | < 15 min
| Delta Lat | < 1.5°
| Delta Lon | < 3.0°

Experimental data (01-02 / 2020)

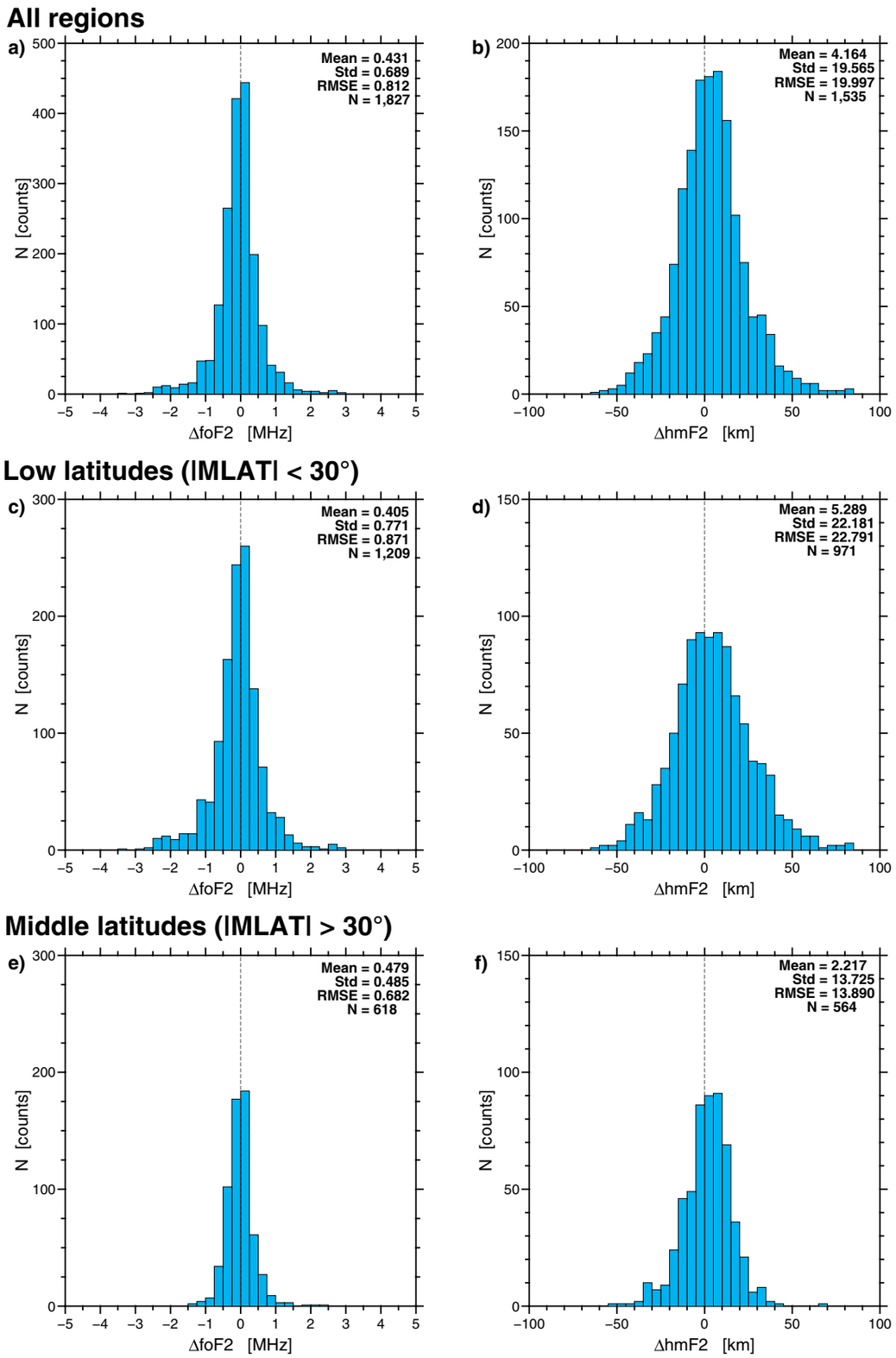

Peak values from ~2200 COSMIC-2 Ne profiles

foF2 and hmF2 errors statistics using 29 ionosondes globally distributed

Colocation criteria:
| Delta Time | < 15 min
| Ang dist | < 5°

Histograms of the F2 peak parameters residuals ΔfoF2 (ΔfoF2 = foF2RO – foF2ionosonde) and ΔhmF2 (ΔhmF2 = hmF2RO – hmF2ionosonde) between collocated COSMIC-2 and ionosonde measurements.

Each plot contains information about the mean, standard deviation, RMS error, and total number of matches (from: Cherniak et al., 2021).

Some electron density profiles obtained applying the “onion peeling” algorithm*

*implemented as DG_DELN SW

Onion peeling derived profile

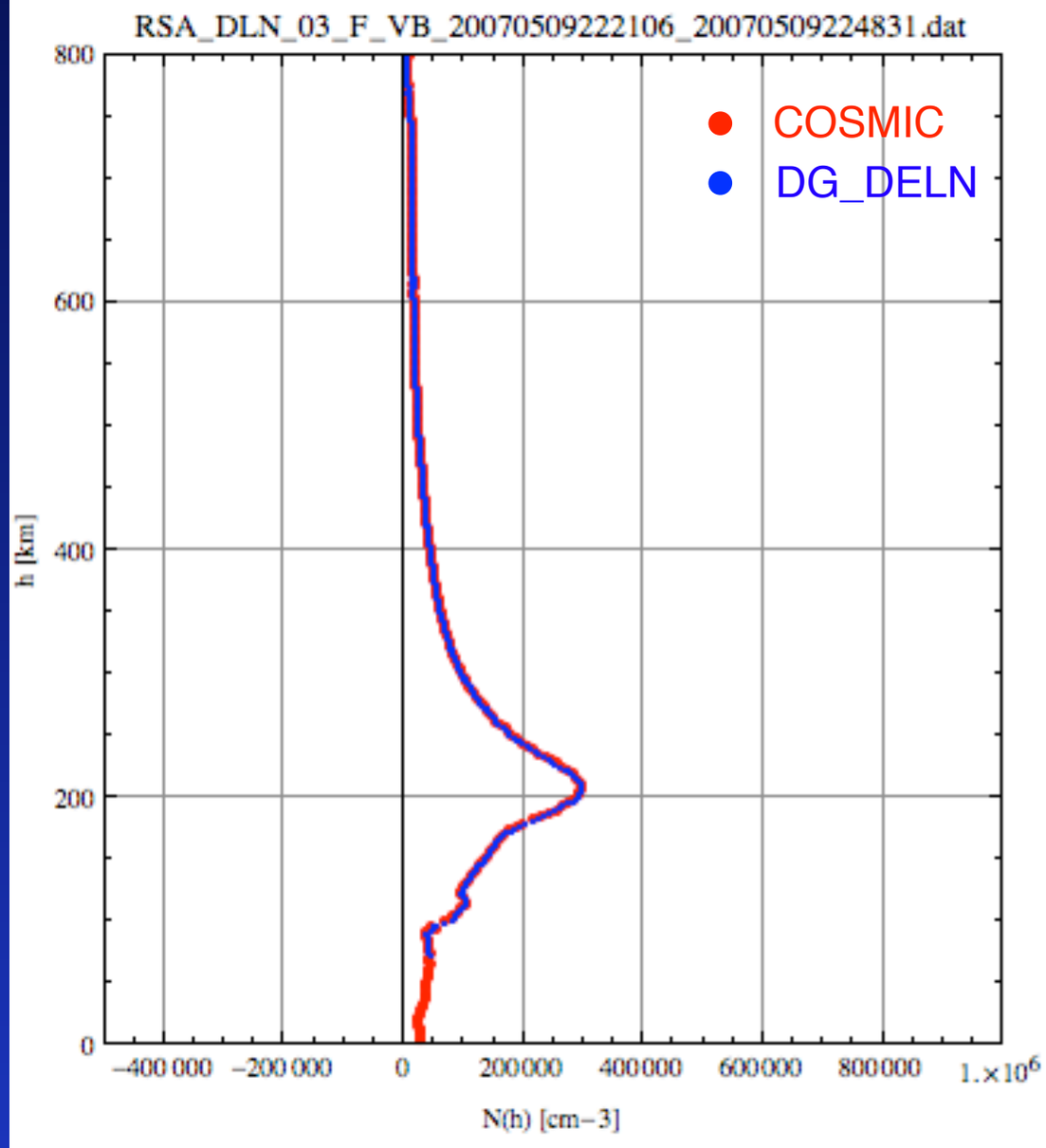

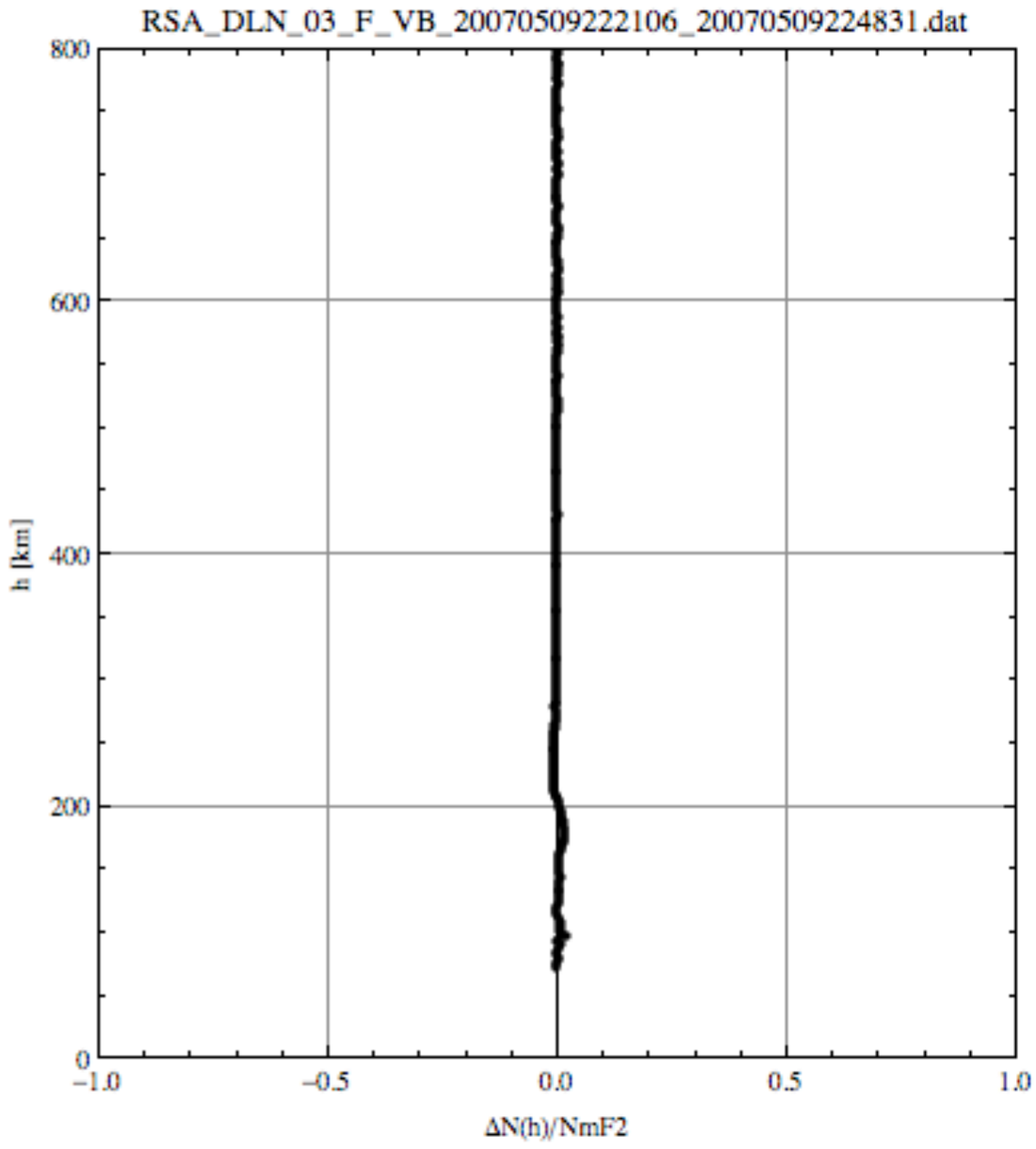

COSMIC data are used

Profile example 1

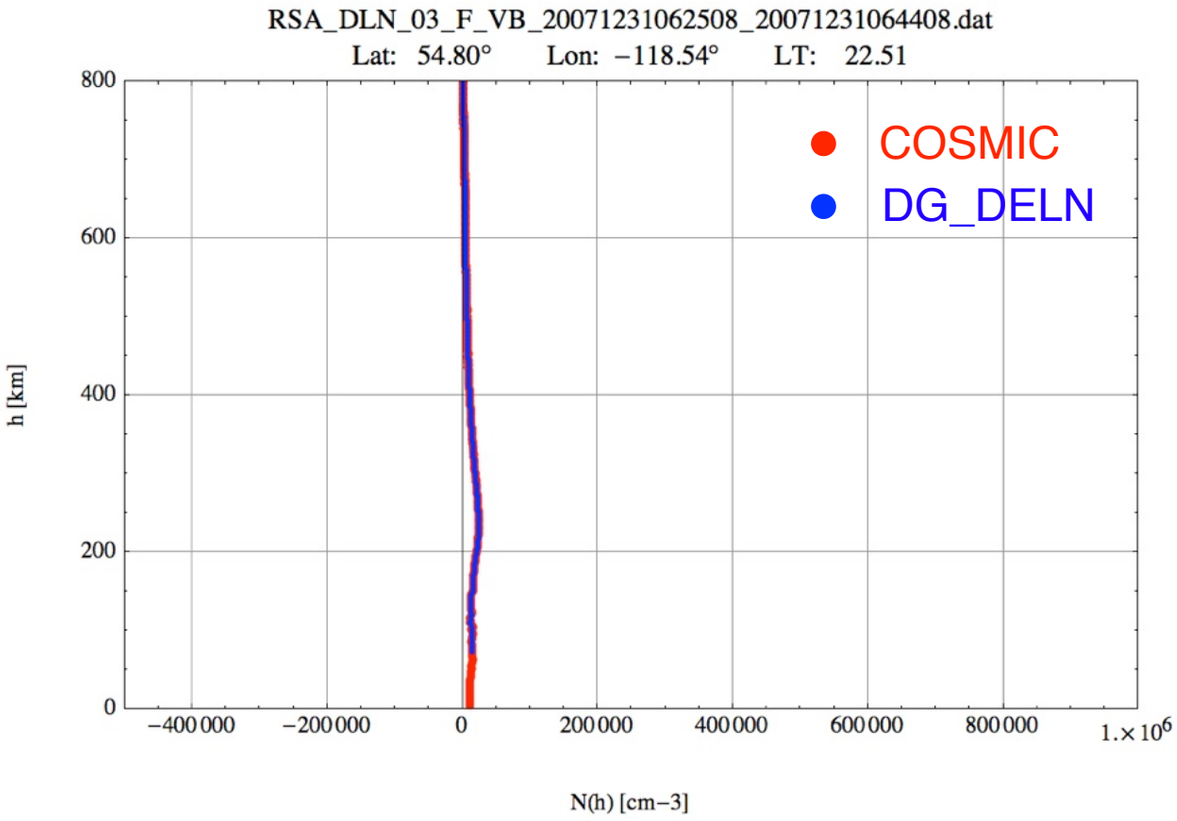

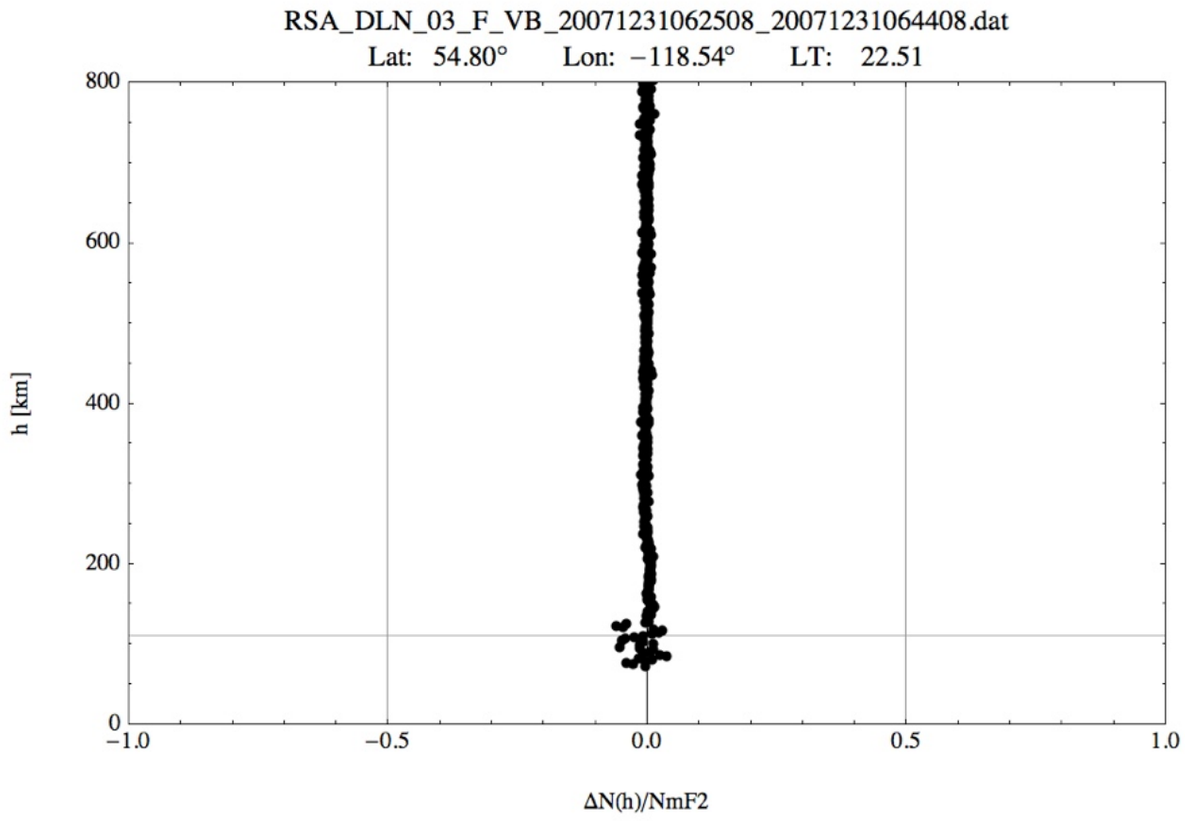

COSMIC data are used

Profile example 2

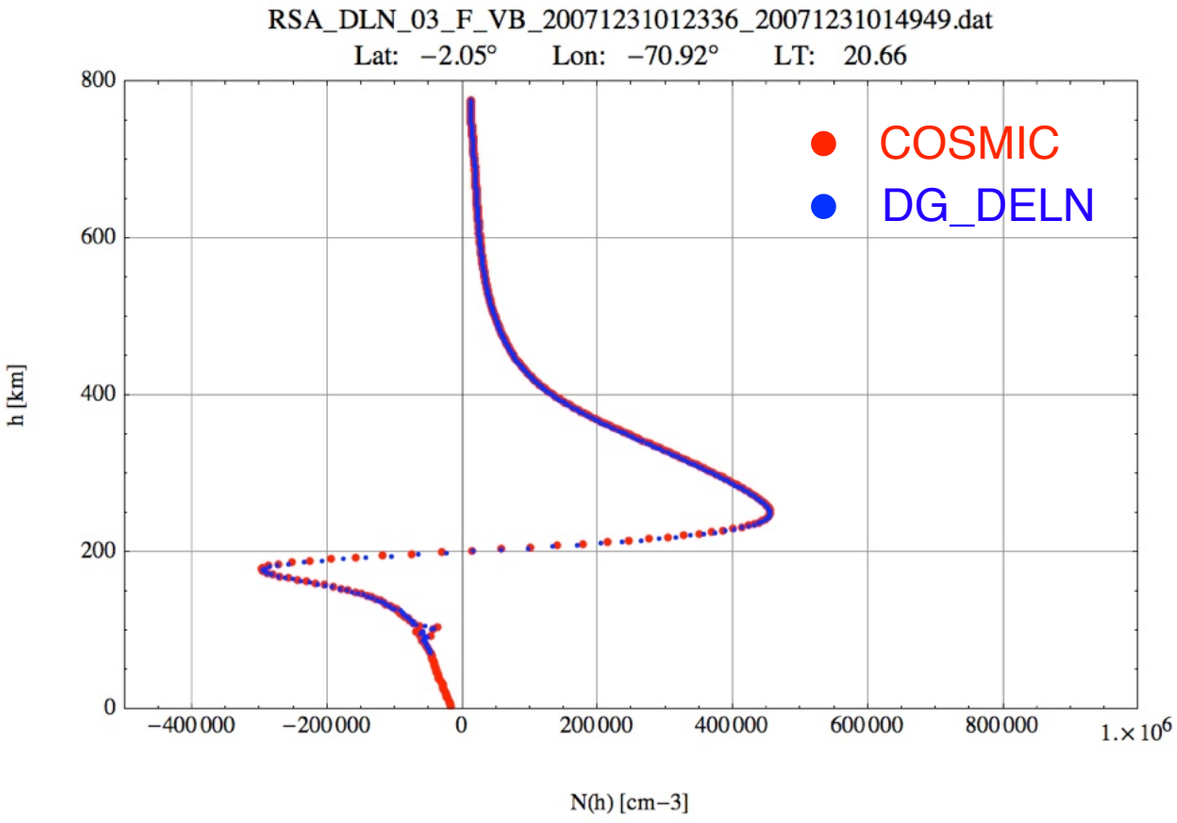

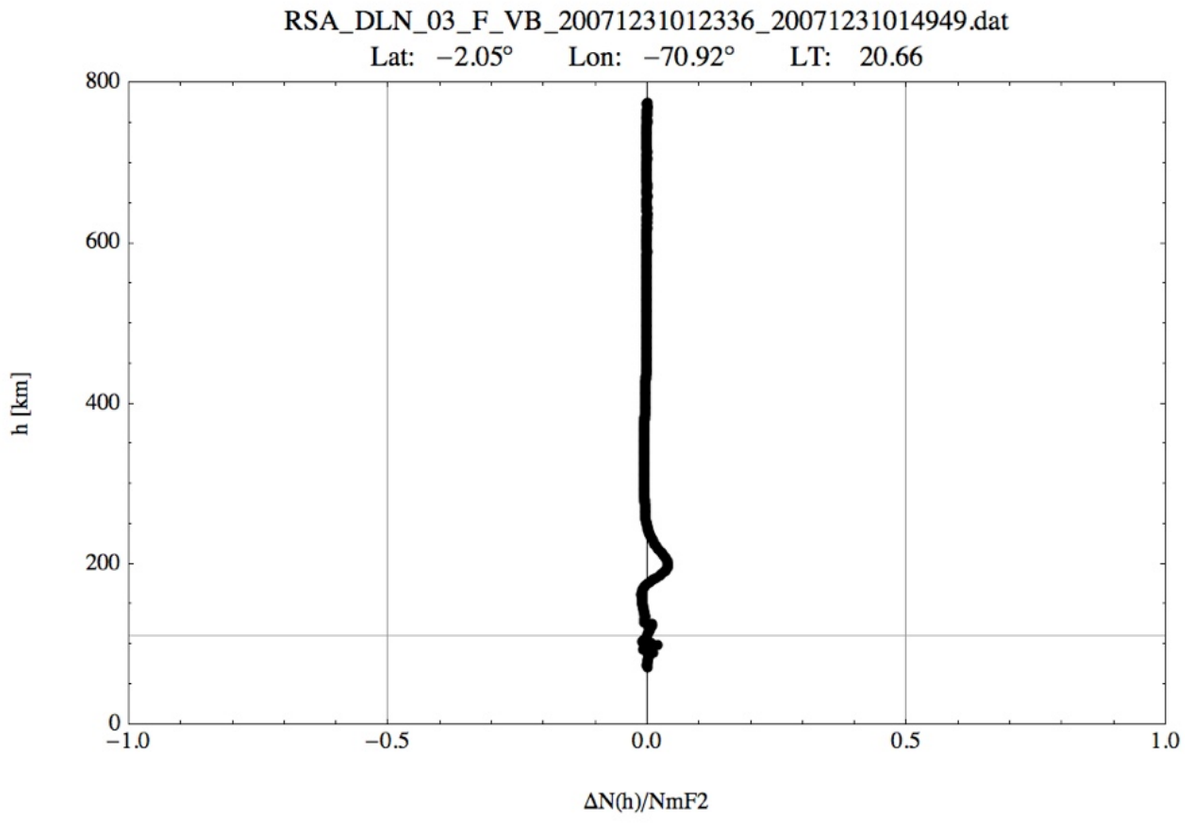

COSMIC data are used

Profile example 3

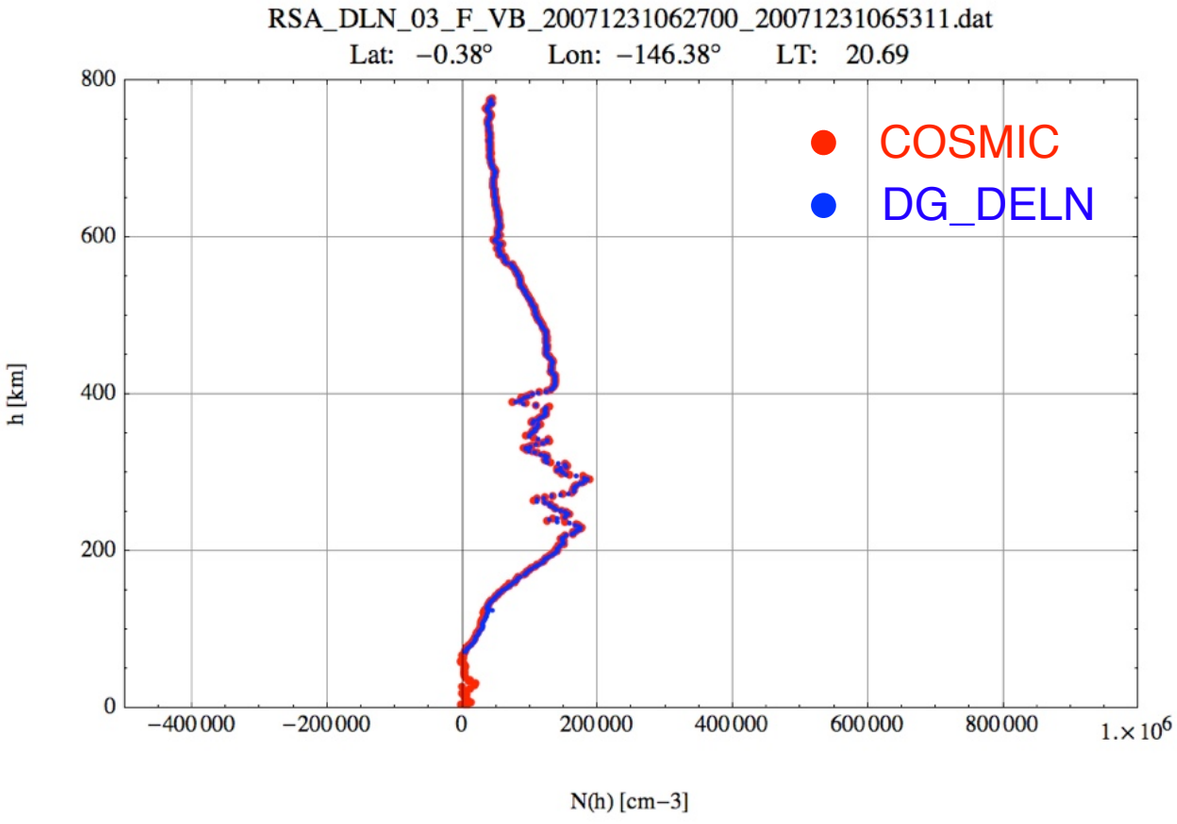

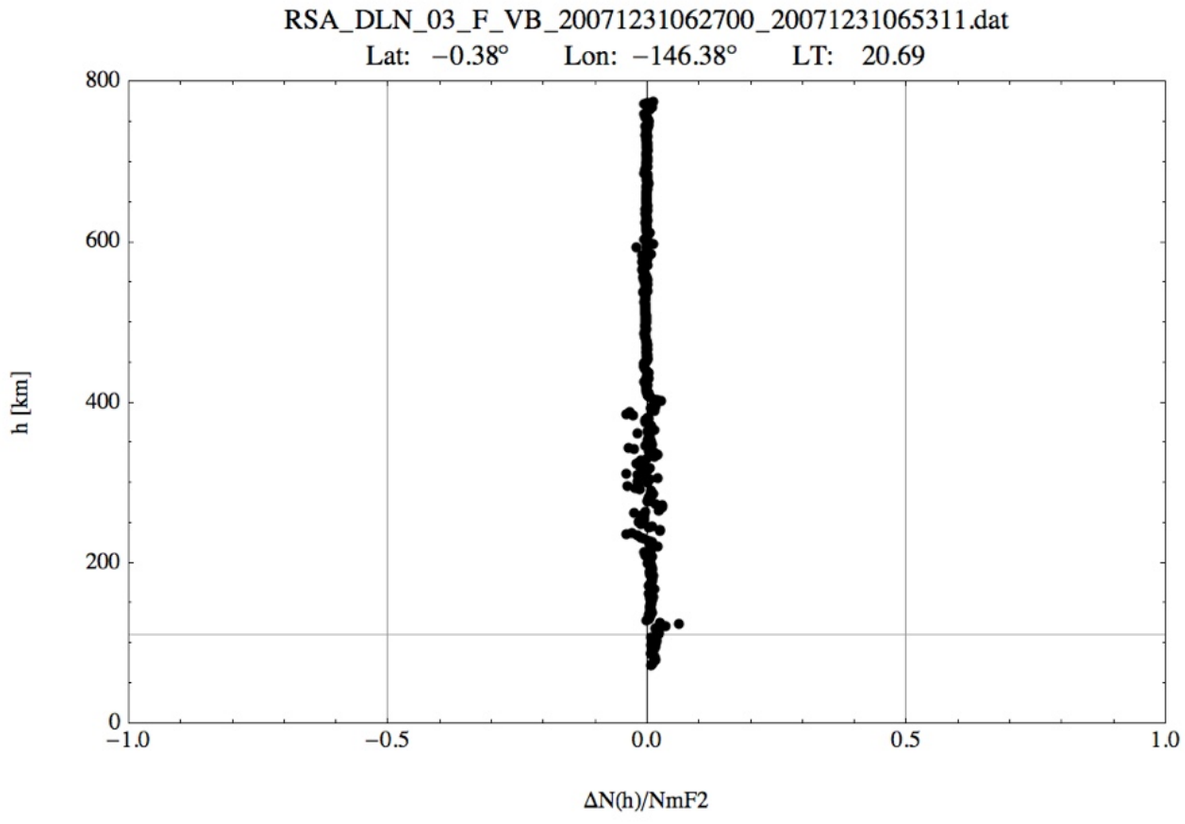

COSMIC data are used

Depletion signatures in RO data

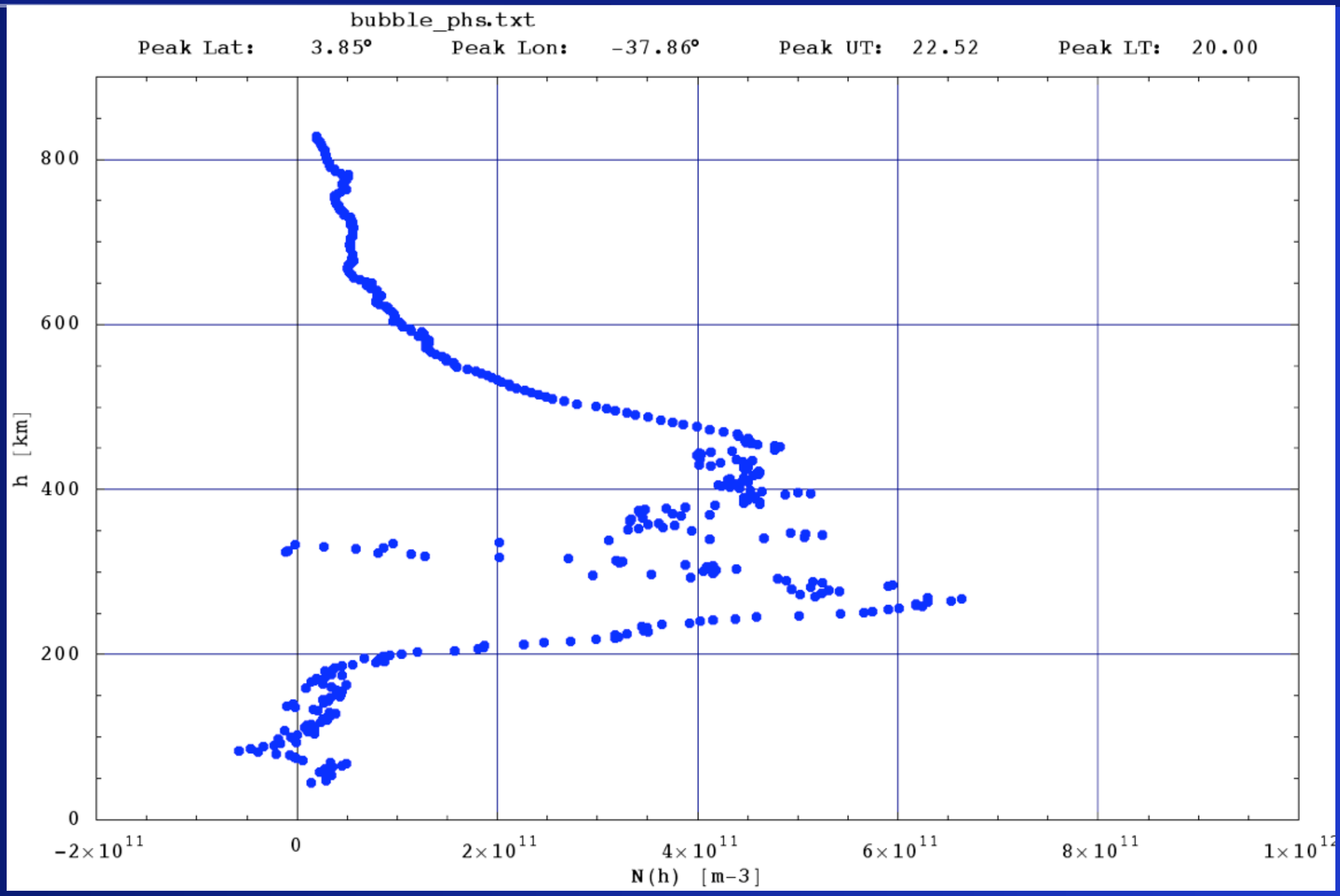

"Vertical" electron density profile obtained inverting RO data using the Onion Peeling algorithm

Profile1

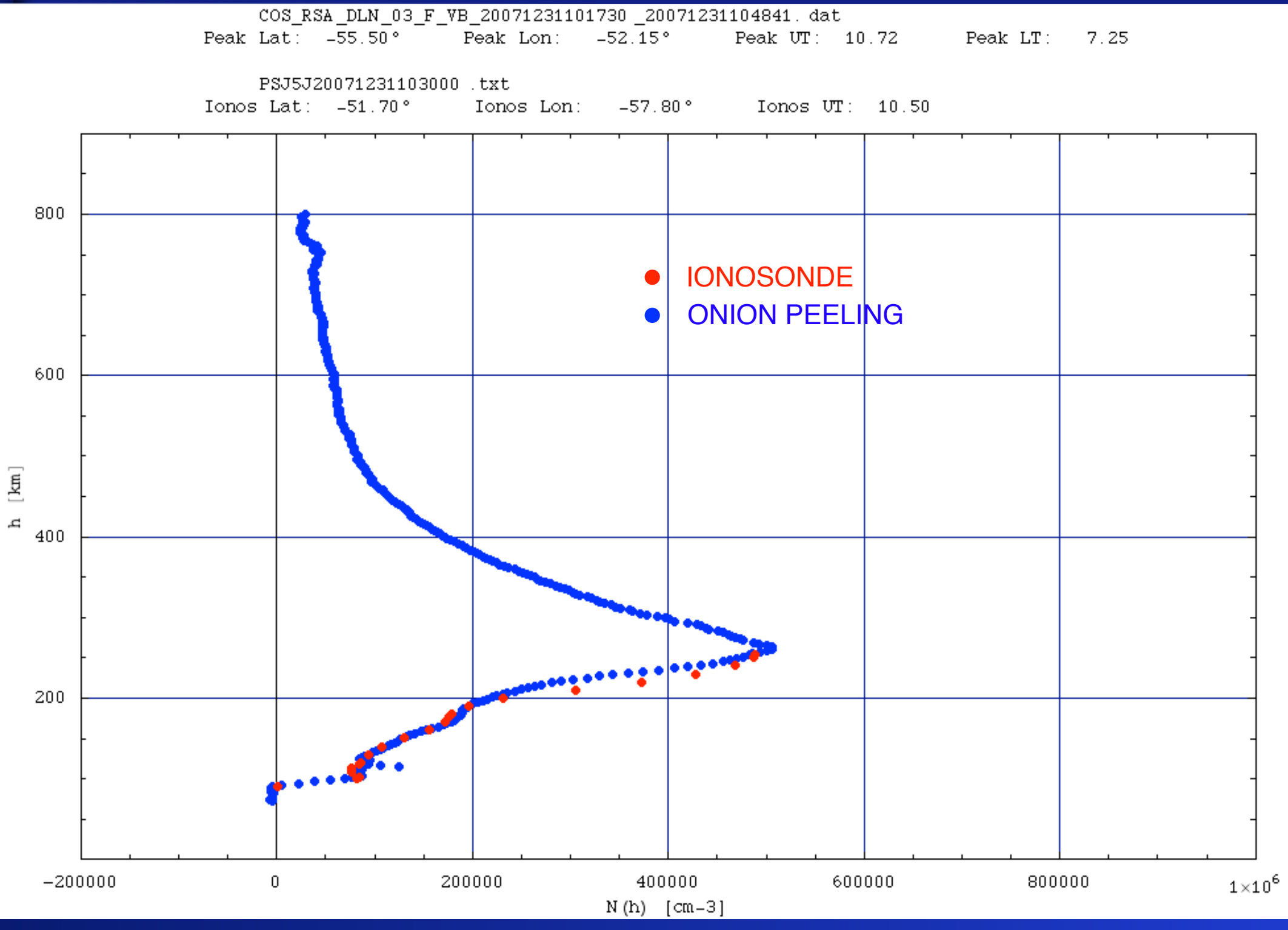
COS_RSA_DLN_03_F_VB_20071231101730 _20071231104841. dat
Peak Lat: -55.50° Peak Lon: -52.15° Peak UT: 10.72 Peak LT: 7.25
PSJ5J20071231103000 .txt
Ionos Lat: -51.70° Ionos Lon: -57.80° Ionos UT: 10.50
IONOSONDE
ONION PEELING
800
600
400
200
h [km]
-200000
0
200000
400000
600000
800000
1×10^6
N(h) [cm-3]

VTEC map 1

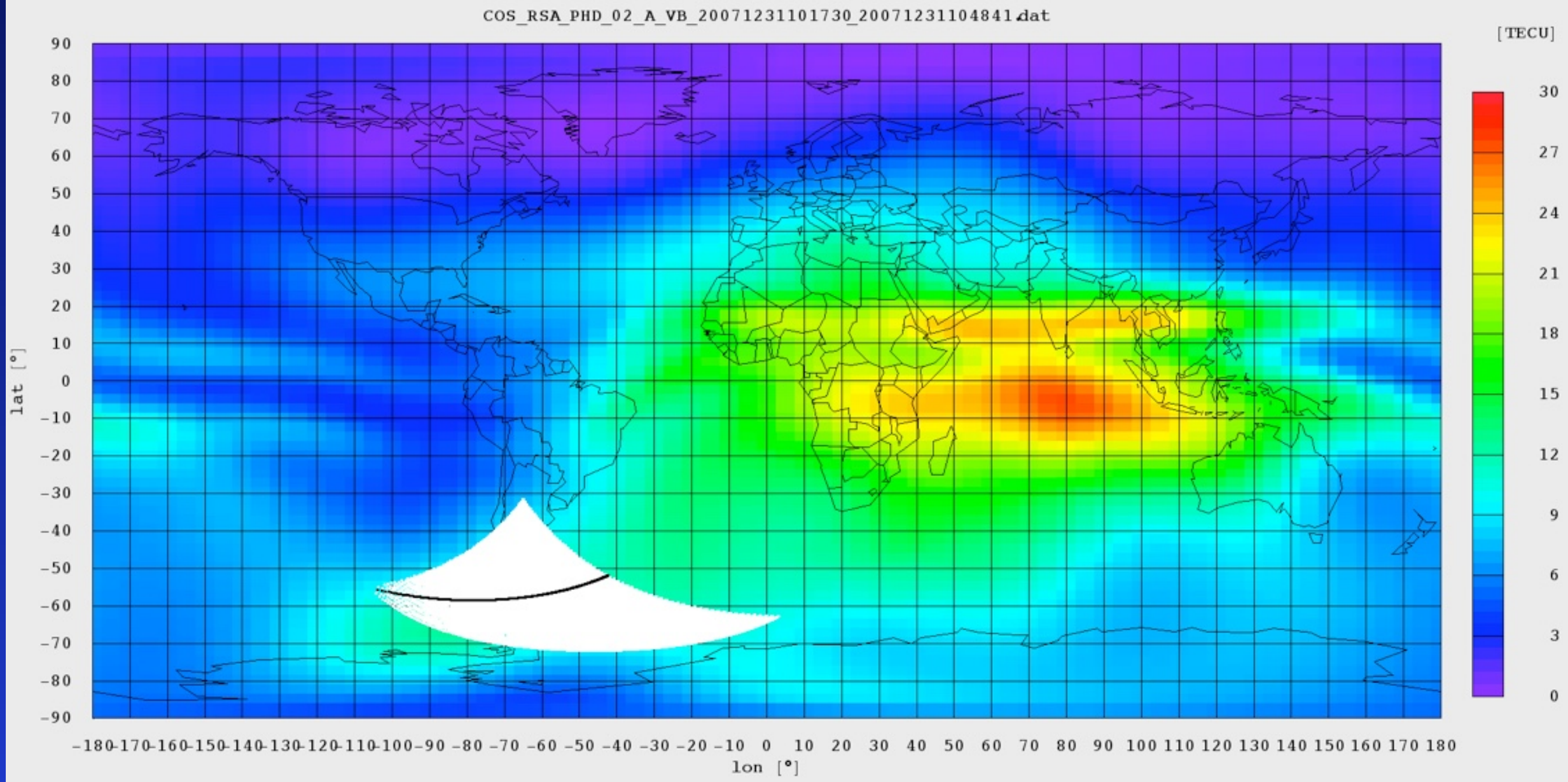
COS_RSA_PHD_02_A_VB_20071231101730_20071231104841.dat
[TECU]
30
27
24
21
18
15
12
9
6
3
0
90
80
70
60
50
40
30
20
10
0
−10
−20
−30
−40
−50
−60
−70
−80
−90
lat [°]
−180 −170 −160 −150 −140 −130 −120 −110 −100 −90 −80 −70 −60 −50 −40 −30 −20 −10 0 10 20 30 40 50 60 70 80 90 100 110 120 130 140 150 160 170 180
lon [°]

Profile 2

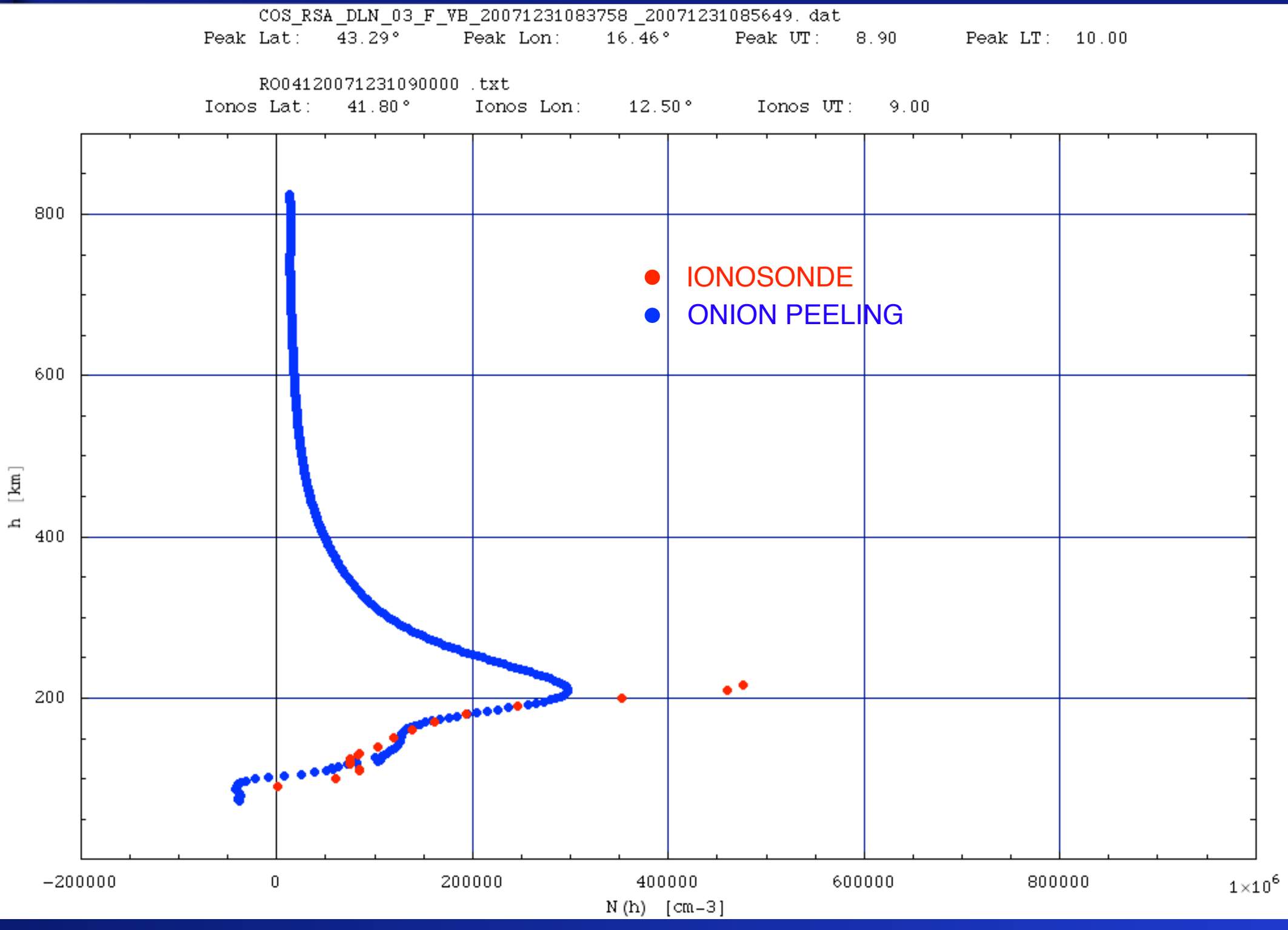
COS_RSA_DLN_03_F_VB_20071231083758 _20071231085649. dat
Peak Lat: 43.29° Peak Lon: 16.46° Peak UT: 8.90 Peak LT: 10.00
RO04120071231090000 .txt
Ionos Lat: 41.80° Ionos Lon: 12.50° Ionos UT: 9.00
IONOSONDE
ONION PEELING
800
600
400
200
h [km]
-200000
0
200000
400000
600000
800000
1×10^6
N(h) [cm-3]

VTEC map 2

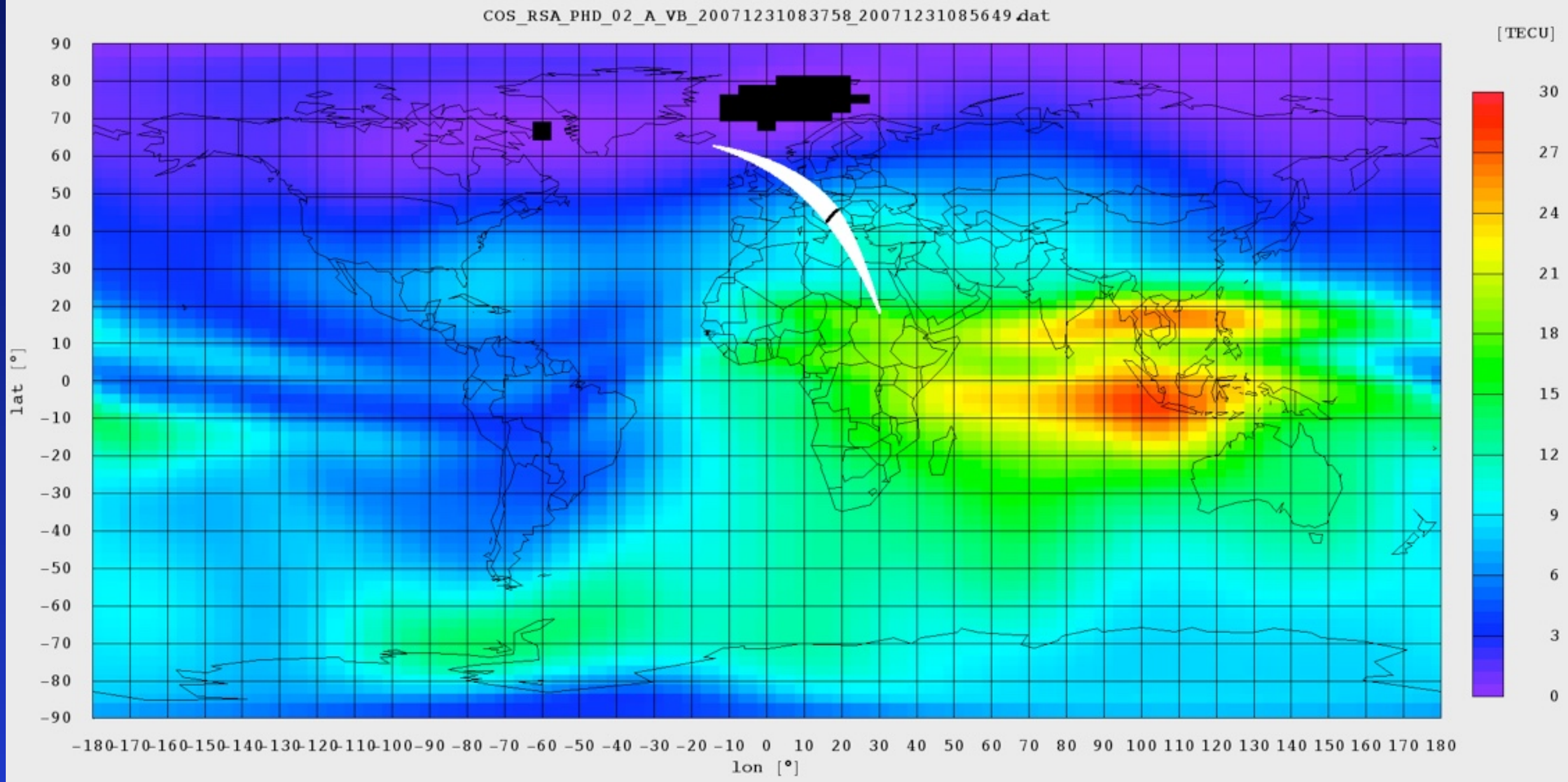
COS_RSA_PHD_02_A_VB_20071231083758_20071231085649.dat
[TECU]
30
27
24
21
18
15
12
9
6
3
0
lat [°]
90
80
70
60
50
40
30
20
10
0
−10
−20
−30
−40
−50
−60
−70
−80
−90
−180 −170 −160 −150 −140 −130 −120 −110 −100 −90 −80 −70 −60 −50 −40 −30 −20 −10 0 10 20 30 40 50 60 70 80 90 100 110 120 130 140 150 160 170 180
lon [°]

NeQuick adaptation to foF2, hmF2 (and Tau_{top})

Matching the first 200 km above the peak

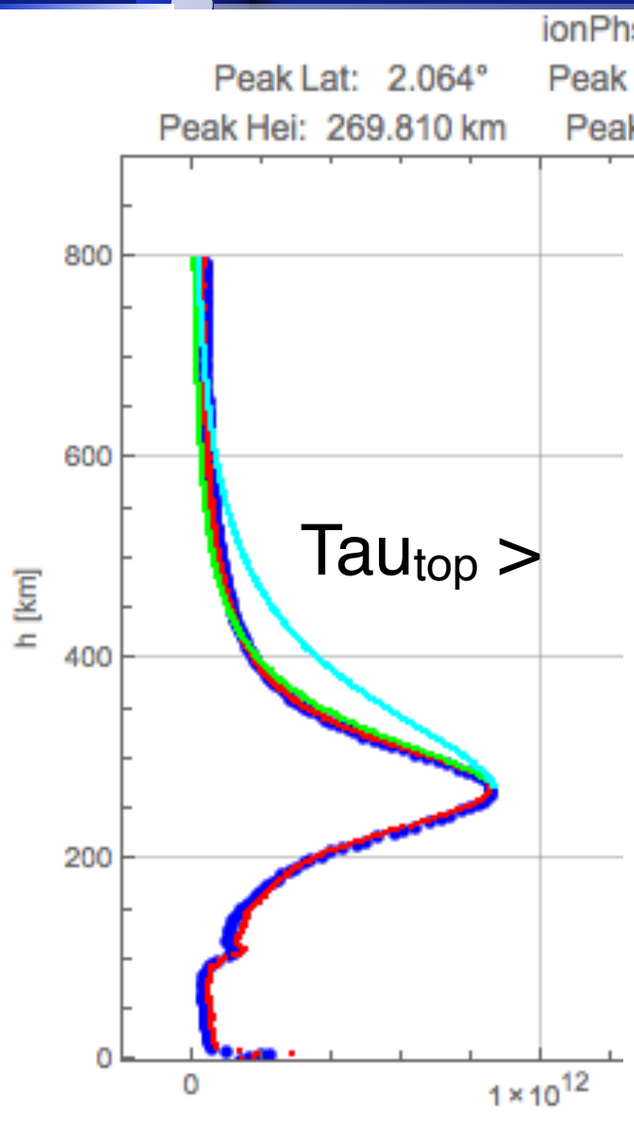

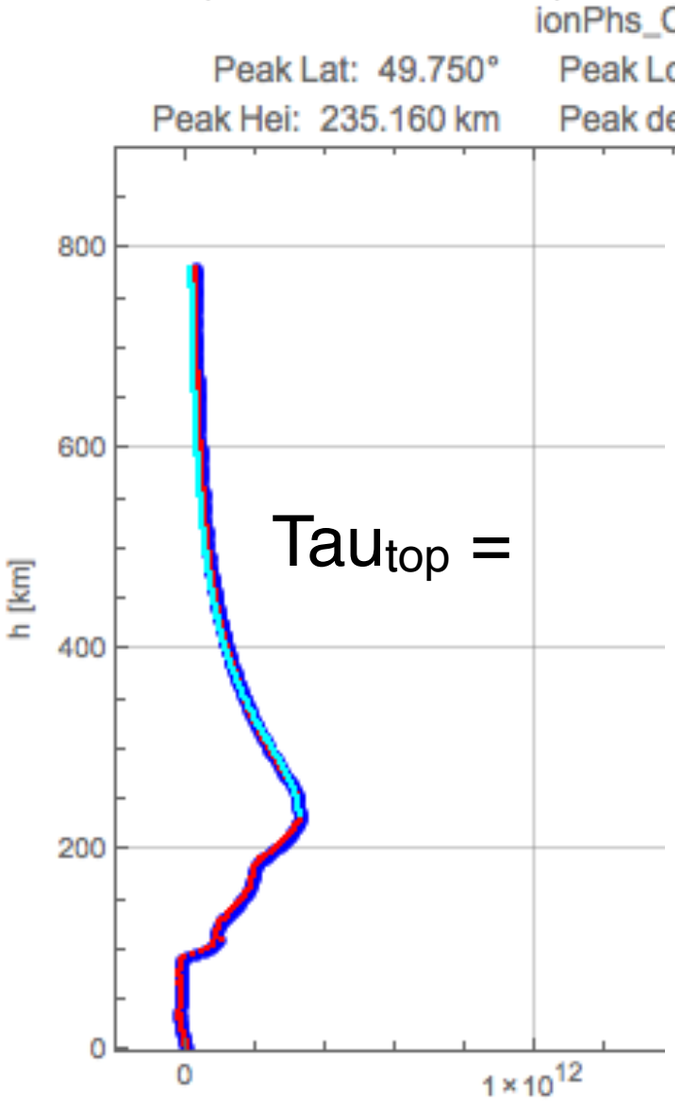

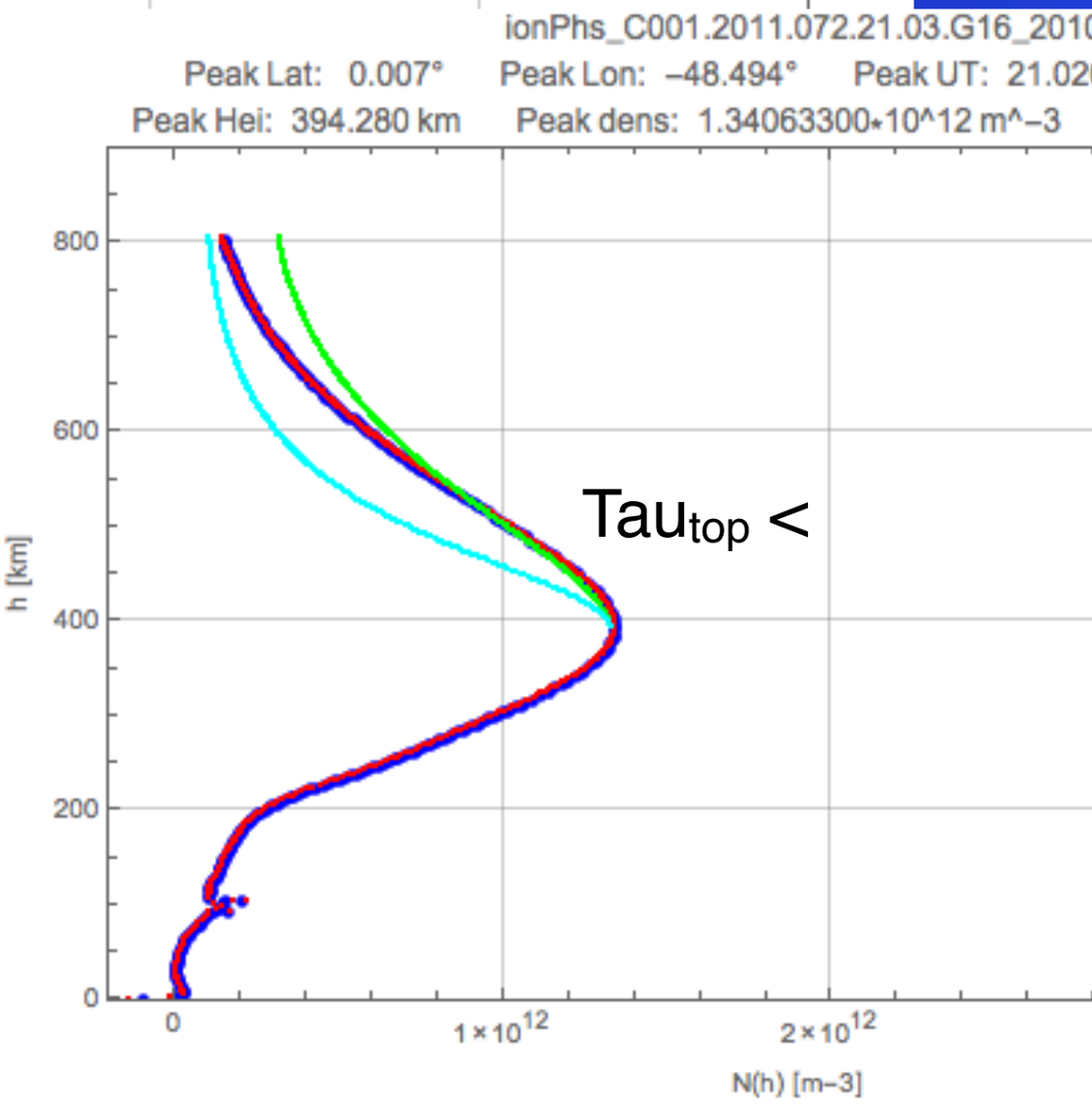

- COSMIC
- ICTP
- NeQuick (ing. hmF2, foF2)
- NeQuick (ing. hmF2, foF2, Tau)

GNSS TEC DA

- For the assimilation
  - Ground-based GPS-derived slant TEC data provided by the Low Latitude Ionospheric Sensor Network (LISN)
  - Radio-Occultation-derived TEC data obtained by COSMIC (calibrated TEC values along the LEO-to-GPS link below the LEO orbit)

- For the validation
  - Manually scaled foF2 data obtained from the Tucuman Ionosonde
  - JRO electron density profiles

- The data correspond the period 11-13 March 2011

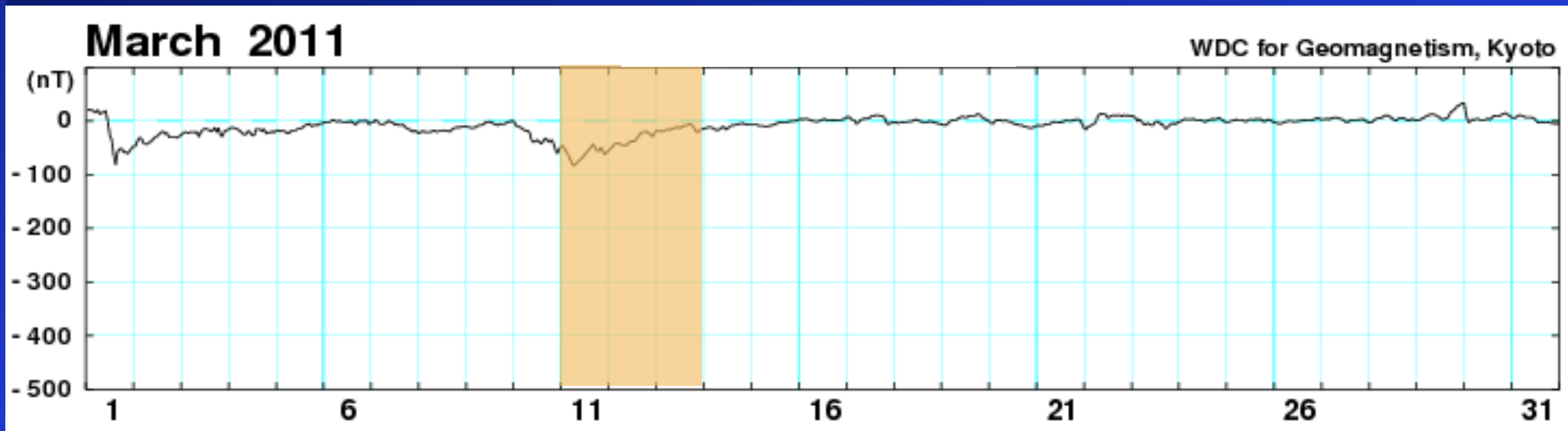

TEC DA (example)

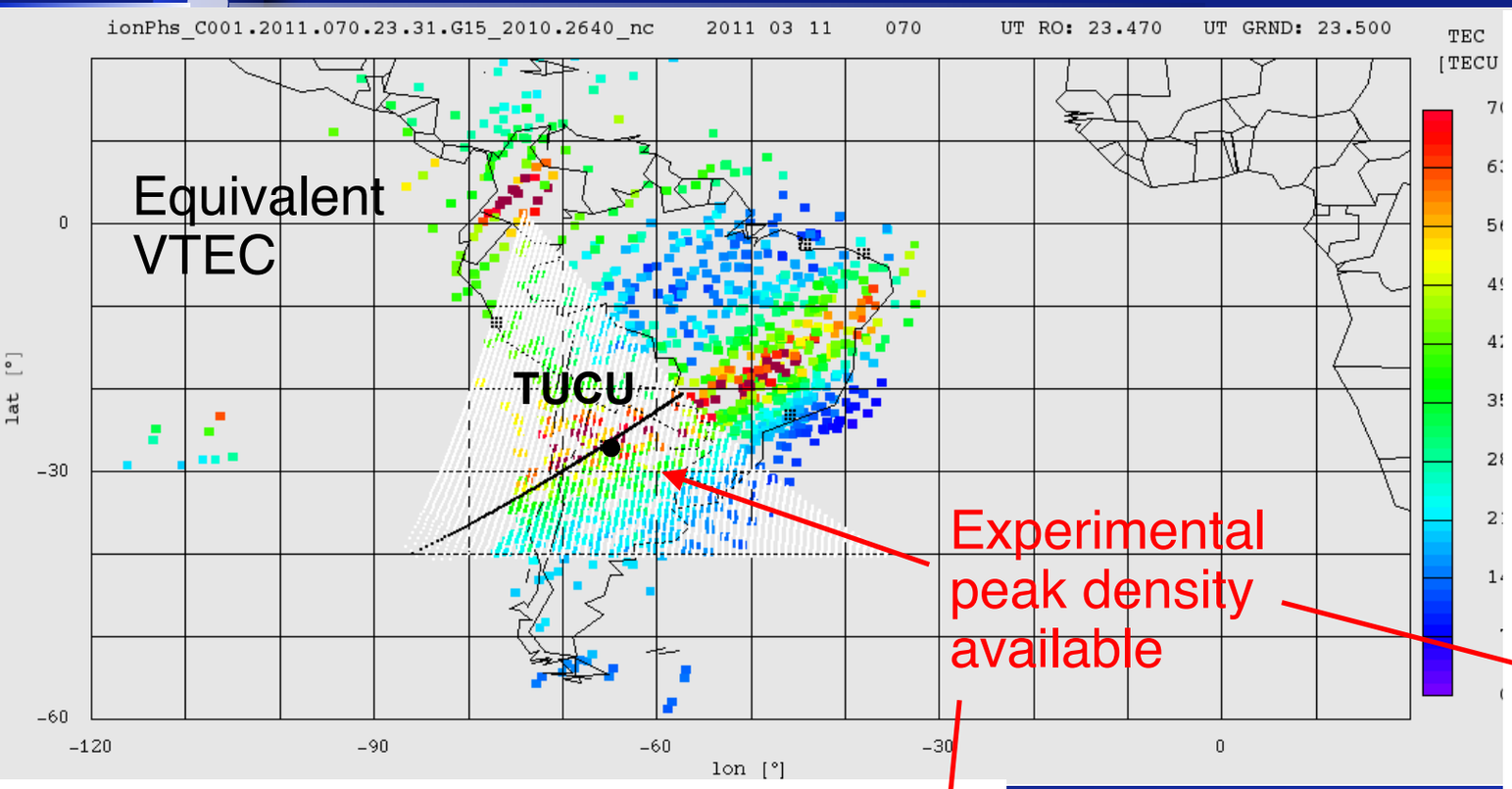

Experimental peak density available

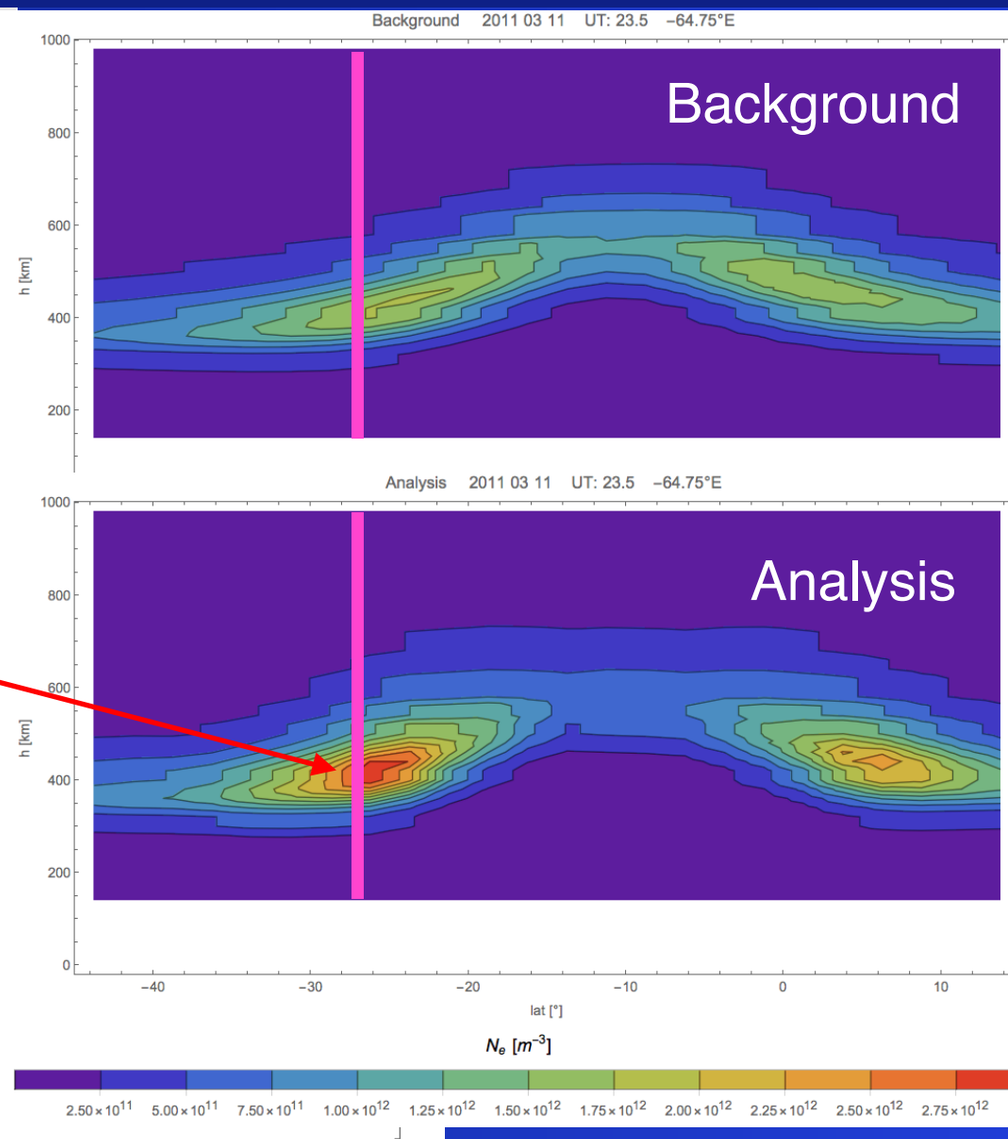

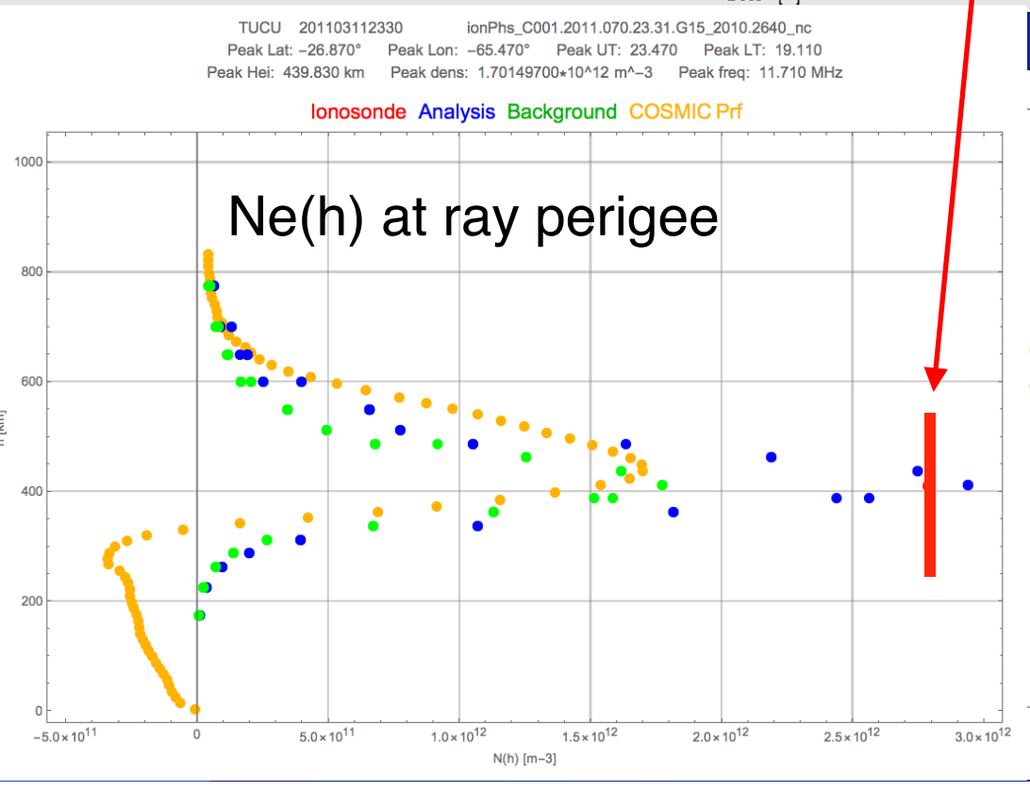

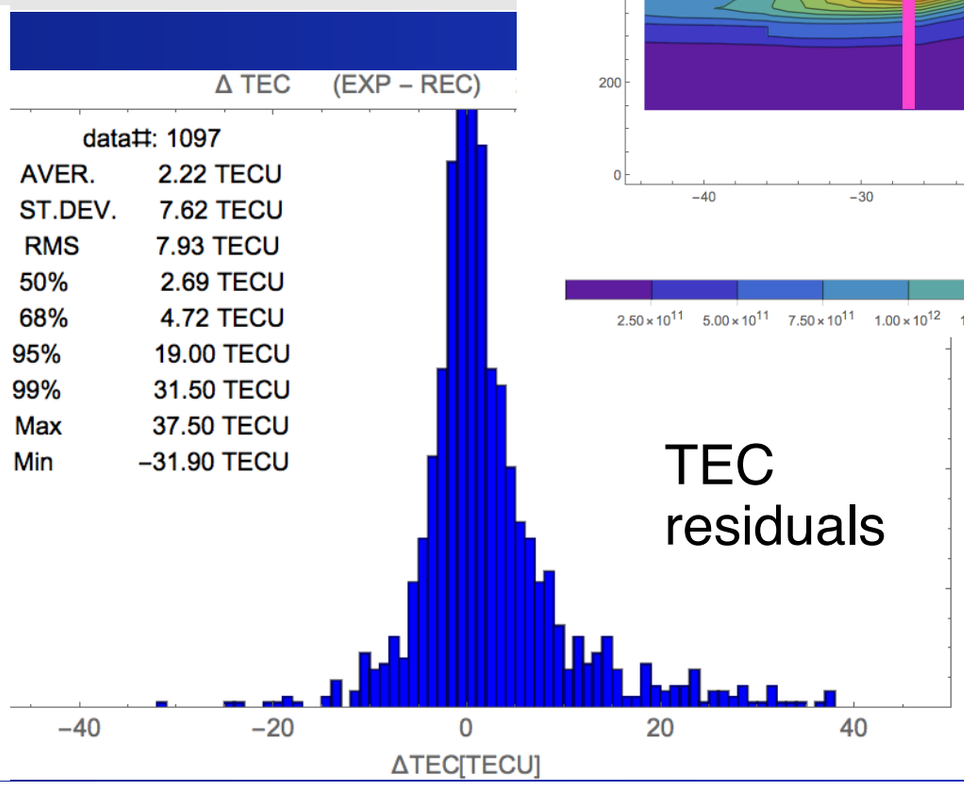

TEC residuals

Electron density cross sections at ionosonde longitude

Thank you for your attention

References

- Angling M, Nogués-Correig O, Nguyen V, Vetra-Carvalho S, Bocquet F, et al. 2021. Sensing the ionosphere with the Spire radio occultation constellation. J. Space Weather Space Clim. 11, 56. https://doi.org/10.1051/swsc/2021040.
- Hernández-Pajares, M., J. M. Juan, and J. Sanz. "Improving the Abel inversion by adding ground GPS data to LEO radio occultations in ionospheric sounding." Geophysical research letters 27.16 (2000): 2473-2476.
- Lee, I. T., W. Wang, J. Y. Liu, C. Y. Chen, and C. H. Lin (2011), The ionospheric midlatitude trough observed by FORMOSAT-3/COSMIC during solar minimum, J. Geophys. Res., 116, A06311, doi:10.1029/2010JA015544.
- Liu, L., H. Le, Y. Chen, M. He, W. Wan, and X. Yue (2011), Features of the middle- and low-latitude ionosphere during solar minimum as revealed from COSMIC radio occultation measurements, J. Geophys. Res., 116, A09307, doi:10.1029/2011JA016691.
- Liu, J.-Y.; Lin, C.-H.; Rajesh, P.K.; Lin, C.-Y.; Chang, F.-Y.; Lee, I.-T.; Fang, T.-W.; Fuller-Rowell, D.; Chen, S.-P. Advances in Ionospheric Space Weather by Using FORMOSAT-7 COSMIC-2 GNSS Radio Occultations. Atmosphere 2022, 13,858. https://doi.org/10.3390/ atmos13060858
- Nava, B., P. Coïsson, S. M. Radicella (2008). A new version of the NeQuick ionosphere electron density model. Journal of Atmospheric and Solar-Terrestrial Physics, doi:10.1016/j.jastp.2008.01.015.
- Shaikh, M. M., Nava, B., Kashcheyev, A., (2017). A model-assisted radio occultation data inversion method based on data ingestion into NeQuick. Adv. Space Res. 59 (1), 326-336. http://dx.doi.org/10.1016/j.asr.2016.09.006.
- Shaikh, M. M., Nava, B., & Haralambous, H. (2018). On the use of topside RO-derived electron density for model validation. Journal of Geophysical Research: Space Physics, 123. https://doi.org/10.1029/2017JA025132.
- Tulasi Ram, S., S.-Y. Su, and C. H. Liu (2009), FORMOSAT-3/COSMIC observations of seasonal and longitudinal variations of equatorial ionization anomaly and its interhemispheric asymmetry during the solar minimum period, J. Geophys. Res., 114, A06311, doi:10.1029/2008JA013880.
- Yue, X., W. S. Schreiner, J. Lei, S. V. Sokolovskiy, C. Rocken, D. C. Hunt, and Y.-H. Kuo (2010), Error analysis of Abel retrieved electron density profiles from radio occultation measurements, Ann. Geophys., 28(1), 217–222.